AD NUMBER
AD822424
LIMITATION CHANGES
TO: **Approved for public release; distribution is unlimited.**
FROM: **Distribution authorized to U.S. Gov't. agencies and their contractors; Critical Technology; SEP 1967. Other requests shall be referred to Air Force Technical Applications Center, Attn: VELA Seismological Center, Washington, DC 20333. This document contains export-controlled technical data.**
AUTHORITY
usaf ltr, 25 jan 1972

TR67-59

AD822424

TECHNICAL REPORT NO. 67-59

MULTICOMPONENT STRAIN SEISMOGRAPH

Quarterly Report No.9, Project VT/5081

1 July to 30 September 1967

STATEMENT #2 UNCLASSIFIED

This document is subject to special export controls and each transmittal to foreign governments or foreign nationals may be made only with prior approval of AIR FORCE TECHNICAL APPLICATIONS CENTER, Attn: VELA Seismological Center, Washington, D.C. 20333.

GEOTECH
A TELEDYNE COMPANY

TECHNICAL REPORT NO. 67-59

MULTICOMPONENT STRAIN SEISMOGRAPH

Quarterly Report No. 9, Project VT/5081
1 July to 30 September 1967

Sponsored by

Advanced Research Projects Agency
Nuclear Test Detection Office
ARPA Order No. 624

Availability

Qualified users may request copies of this document from:
Defense Documentation Center
Cameron Station
Alexandria, Virginia 22341

Acknowledgement

This research was supported by the Advanced Research Projects Agency, Nuclear Test Detection Office, and was monitored by the Air Force Technical Applications Center under Contract No. AF 33(657)-15288.

GEOTECH
A TELEDYNE COMPANY
3401 Shiloh Road
Garland, Texas

16 October 1967

IDENTIFICATION

AFTAC Project No.	VELA T/5081
Project Title:	Multicomponent Strain Seismograph
ARPA Order No.	624
ARPA Code No.	8100
Contractor:	The Geotechnical Corporation Garland, Texas
Date of Contract:	1 July 1965
Amount of Contract:	$393, 361
Contract No.	AF 33(657)-15288
Contract Expiration Date	31 December 1967
Project Manager	R.C. Shopland, BR 1-2561

CONTENTS

CONTENTS, Continued

ILLUSTRATIONS

ABSTRACT

Earthquake data and phase and amplitude responses measured at both the fixed and free ends of the horizontal strain seismometer show no discrepancies that would explain the apparent loss of motion between the ends during calibration. The capability of the long-period horizontal strain and inertial seismographs to operate as a matched pair has been demonstrated. The ability of the long-period strain directional array to discriminate between surface waves arriving simultaneously from different epicenters was also successfully demonstrated. A comparison of data from vertical strain seismometers interchanged in the steel-cased and plastic-cased boreholes indicates the problem of low coherence of strain signals between the two boreholes is caused by one of the strain instruments rather than differences in the boreholes. A seismic model for Wichita Mountains Seismological Observatory (WMSO) was hypothesized for the longitudinal wave velocity and for the shear wave velocity from the surface to below the Mohorovicic discontinuity. An evaluation is given of the variable-capacitance transducer as a calibration monitor and as a transducer for recording seismic data.

1. INTRODUCTION

This report discusses technical findings and accomplishments in a program of strain seismology performed under Contract AF 33(657)-15288, S/A No. 2, in the period 1 July to 30 September 1967. The work reported herein primarily covers development of a system of 3-component strain and 3-component short-period inertial seismographs having matched amplitude and phase responses in the frequency range 0.01 - 10 Hz.

This report is submitted in compliance with Item A002 of Contract Data Requirements List, Contract AF 33(657)-15288, S/A No. 2. The report is presented in the same sequence as the tasks in the Statement of Work. The Statement of Work is included as appendix 1.

During the reporting period, the following objectives received emphasis:

a. Evaluation of the variable-capacitance transducer;

b. Amplitude and phase measurements at the fixed and free ends of the strain seismometers, to investigate apparent loss of motion in the strain rod;

c. Evaluation of the long-period strain directional array;

d. Comparison of the steel-cased and plastic-cased boreholes;

e. Formulation of a seismic velocity model for WMSO.

Major accomplishments were as follows:

a. Specifications and drawing package of the variable-capacitance transducer were completed;

b. Phase and amplitude responses were measured at both the fixed and free ends of the horizontal strain seismometer and found to show no anomalies explaining the apparent loss of motion between these points during calibration. Measurements from earthquake data also fail to support the existence of a loss;

as a matched pair has been demonstrated;

d. The ability of the long-period strain directional array to enhance earthquake waves arriving from one direction in the presence of surface waves of an earthquake from another direction was successfully demonstrated;

e. Data from seismometers interchanged in the steel-cased and plastic-cased boreholes indicate the problem of low coherence of strain signals between the two boreholes is caused by the seismometer in the plastic-cased borehole rather than by differences in the borehole;

f. A seismic model for WMSO was constructed.

2. INSTRUMENTATION DEVELOPMENT

2.1 VARIABLE CAPACITANCE TRANSDUCER

2.1.1 General

The variable-capacitance transducer (VCT) is a device used to measure displacements of millimicron magnitude which are normally associated with strain seismometers. Figure 1 shows the vertical strain, VCT package installed in a test jig. In operation, displacement causes a change in capacitance between two plates. This change, in turn, causes a voltage change across an LC tank circuit tuned near resonance at approximately 5 MHz. After rectification and filtering, a dc output voltage is obtained which is proportional to displacement. Calibration is accomplished by using a micrometer driven, 100:1 linear motion reducer which displaces the capacitor plates a known amount.

2.1.2 Transducer Characteristics

2.1.2.1 Long Term Drift and Reliability

During early 1967, electronic long-term drift and reliability tests were performed on a VCT with a fixed capacitor in both tank circuits. The unit was operated in a borehole at a depth of eight meters to minimize noise-producing temperature changes in the laboratory and to approximate operational conditions in an underground vault. The unit was operated continuously for two months with no electronic failure. Figure 2 shows the electronic drift over a period of six weeks. Note that initial stabilization required approximately one week. After two weeks, the transducer exhibited near linear drift rate of six millivolts per day. Based on outside temperature

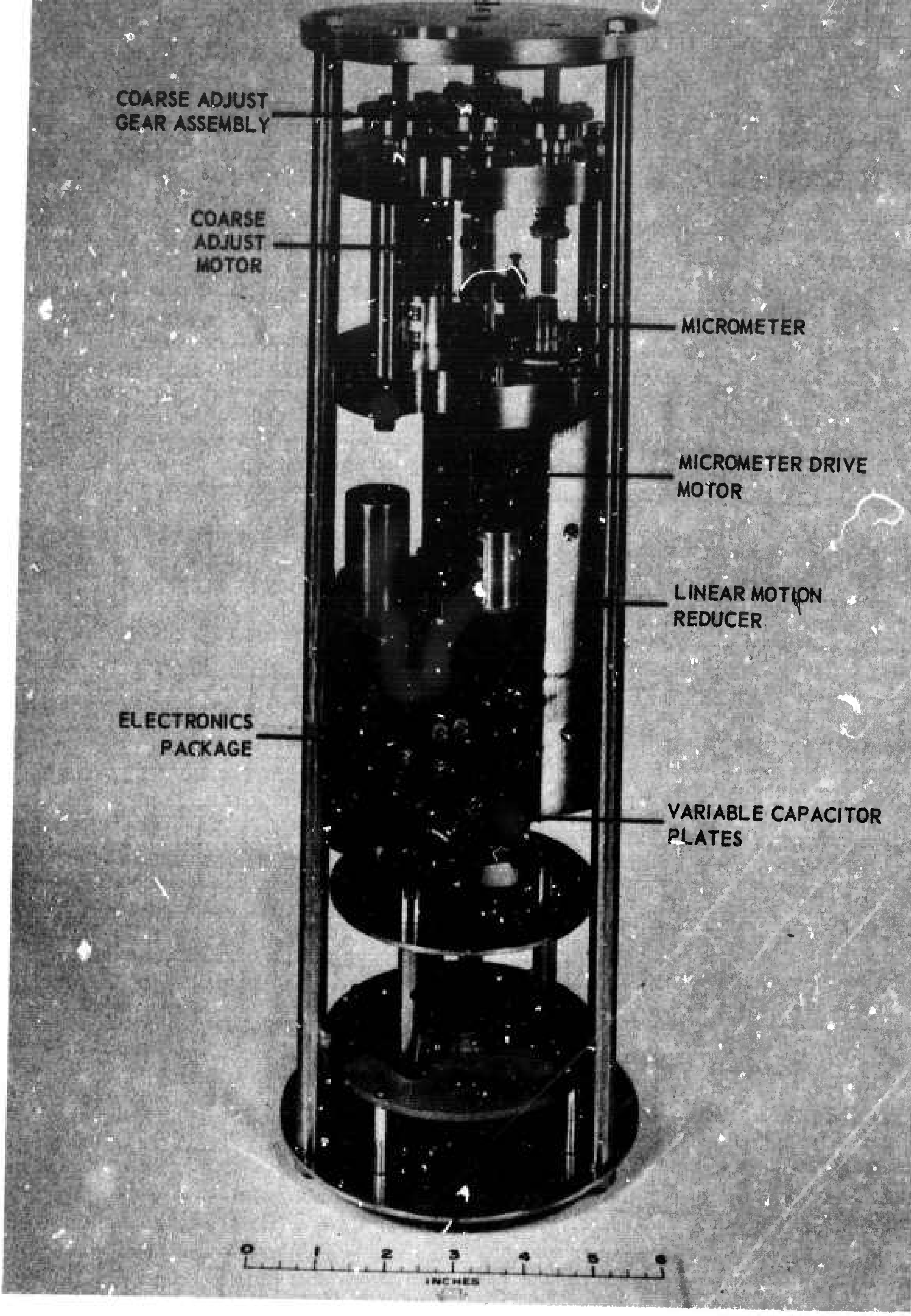

Figure 1. The variable-capacitance transducer for the vertical strain seismometer mounted in a test jig

G 3197

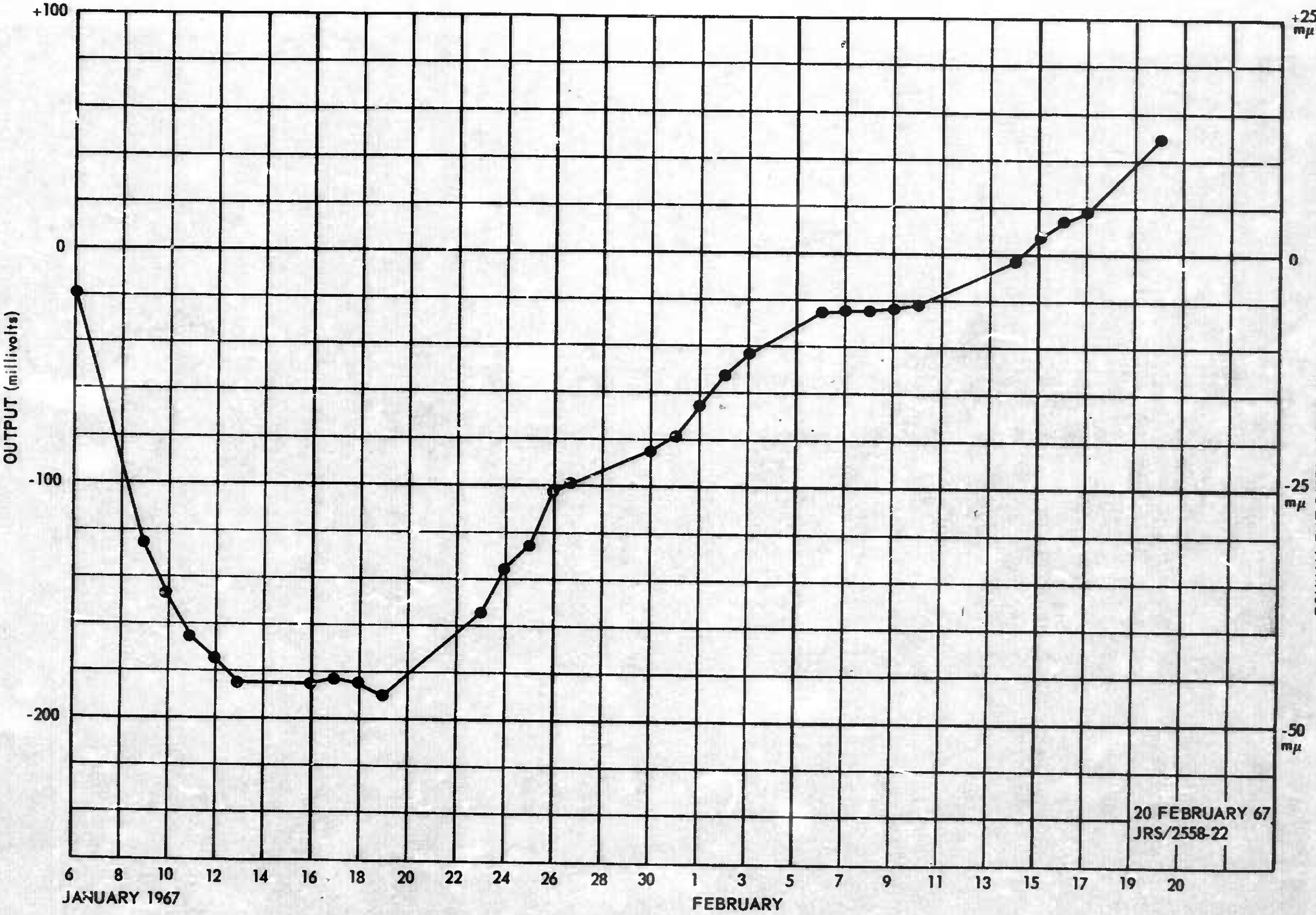

Figure 2. Drift of variable-capacitance transducer electronics package with fixed capacitor in both tank circuits. Package operated in borehole at depth of 8 meters

G 3198

readings during the test, this drift is believed to be caused by a small temperature rise in the borehole which caused changes in the oscillator crystal frequency, capacitance, and/or inductance.

2.1.2.2 Noise Level

Preliminary measurements of the combined electronic and mechanical noise levels of the VCT were obtained by operating the unit shown in figure 1 in a borehole at a depth of fifty feet. These measurements indicate that the noise level is approximately proportional to the period in the range from 1 to 100 seconds. The output noise level at 10 seconds is equivalent to about 0.05 to 0.1 millimicrons displacement at a sensitivity of 4 volts per micron.

Tests are planned in the near future to more accurately determine the VCT noise level. Both the horizontal and vertical versions will be operated under their normal environmental conditions in the clamped or "short rod" configuration. The noise will be recorded on tape and the spectra computed.

2.1.2.3 Phase Response

The phase response of the VCT was determined in the laboratory using a shake table. Figure 3 shows the phase shift of the unamplified transducer and of the transducer followed by an operational amplifier at a gain of X2.

2.1.2.4 Linearity and Dynamic Range

Laboratory tests were performed to determine the maximum linear output range of the VCT. Results indicate that the transducer is linear within ±2% from noise level to ±3.5 volts. This linear range is independent of sensitivity. Calculated dynamic range of the transducer is approximately 90 dB.

2.1.3 <u>Short-term Operation</u>

The VCT has proved very valuable under short-term operating conditions. Its most important use is in the determination of accurate calibration constants for the strain seismometers. It has also been of aid in studying seismometer phase discrepancies and in determining loss of calibration signals in the horizontal strain instruments.

2.1.4 <u>Long-term Operation</u>

The VCT in its present design is severely limited for use as a detector of routine seismic data. Two specific problem areas are instrument noise and environmental effects.

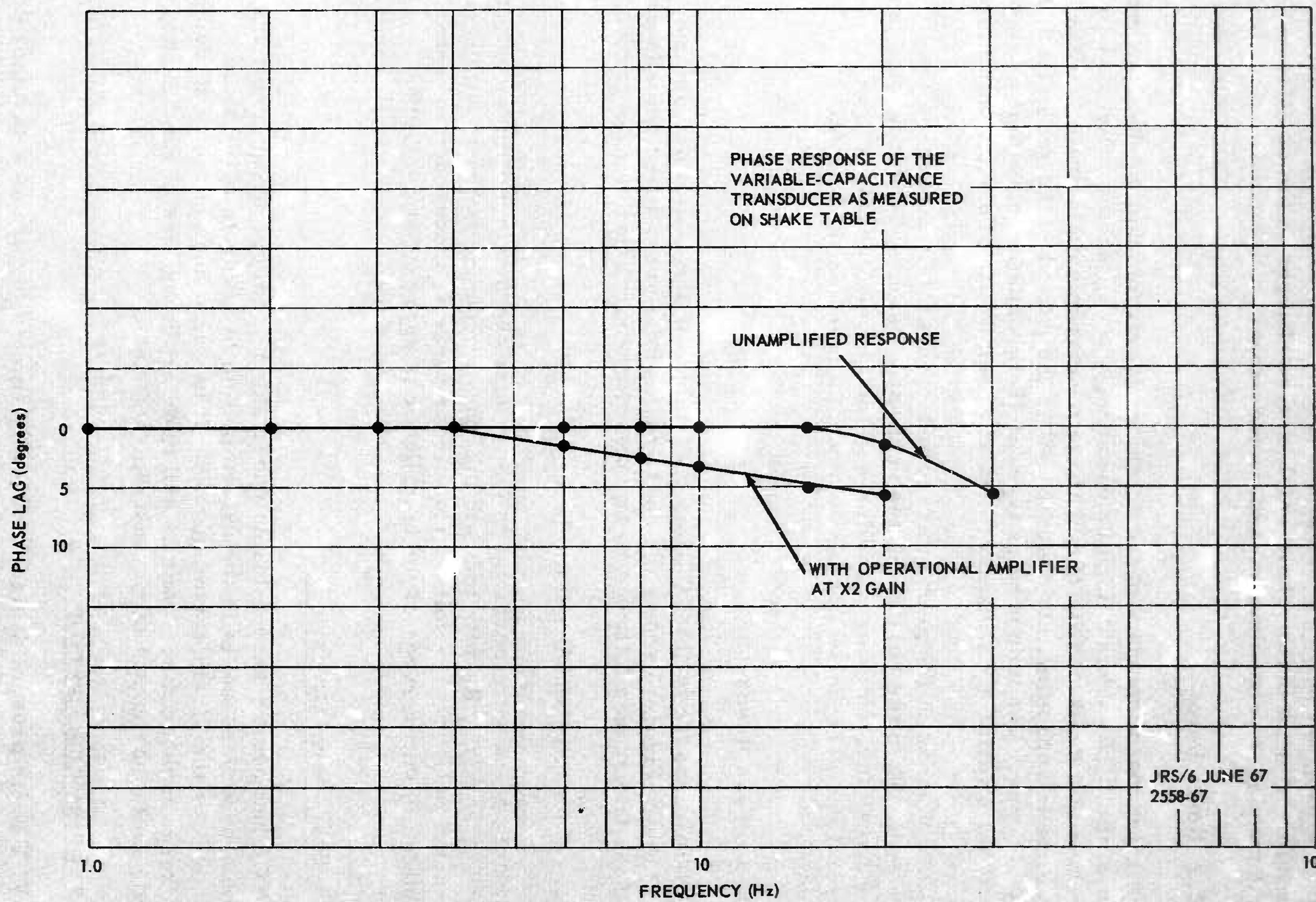

Figure 3. Phase response of an unamplified variable-capacitance transducer and a transducer followed by an operational amplifier at a gain of two

G 3199

2.1.4.1 Instrument Noise

By comparing transducer noise levels (paragraph 2.1.2.2 above) and the average spectrum of microseisms at WMSO, several preliminary conclusions can be drawn. In the case of the vertical strain seismograph, under optimum conditions, instrument noise amplitude exceeds the microseismic amplitude at all frequencies except for a narrow band from about 0.5 to 0.125 Hz.

Since horizontal strain motion is theoretically about three times greater than vertical strain motion, microseismic detection with the horizontal strain is not as limited as in the vertical case. Under favorable conditions, detection of microseisms is possible in the band between about 1.0 and 0.08 Hz. Beyond these frequencies, instrument noise again exceeds the microseismic level. More detailed information on the seismic detection capability of the VCT will be available after completion of tests described in paragraph 2.1.2.2 above.

2.1.4.2 Environmental Effects

Data recorded by the secular strain monitor during the last several months show long-term displacement between the fixed and transducer ends of the horizontal strain seismometers. As could be expected, the data indicate a cyclic character, coinciding with long-term temperature changes during the year. During those seasons when the rate of temperature change is greatest, displacements averaging 2.1 microns per day have been recorded. Displacements of this magnitude exceed the linear operating range of the VCT at maximum sensitivity.

A compensator has been built to eliminate this drift. Although preliminary tests indicate this approach to be feasible, the possibility of introducing more noise into the system should not be overlooked.

In general, environmental effects can be significantly reduced by operating any VCT well below the earth's surface. In the case of the vertical seismometer which is operated at a depth of about 18 meters, the drift is much smaller. However, drift remains serious because of the requirement for operating the vertical strain seismograph at higher magnification.

2.2 AMPLITUDE AND PHASE MEASUREMENTS AT THE FIXED AND FREE ENDS OF THE STRAIN SEISMOMETERS

Item 1c of the Statement of Work (appendix 1) requires the installation of a variable-capacitance transducer in the vertical strain seismometer No. 2 and on the NE horizontal strain seismometer in order to measure the amplitude and phase of the motion actually imparted to the fixed ends of the strain rods during electrical calibration. A discussion of test results follows.

Measurements, using a VCT were made of the displacement of the quartz tubing at the calibrator near the fixed end and at the data coil on the free end of the tube on the horizontal strain seismometer. An 80 percent loss of calibration signal between the fixed and free end was measured on the north strain seismometer (SN) as shown in the amplitude response curves of figure 4, and a 40 percent loss of calibration signal in the northeast seismometer (SNE) as shown in figure 5. Contrary to these results, both seismometers show only small phase differences between the fixed and free ends in the frequency band of interest (figures 6 and 7), and both show phase responses in close agreement with theory. In addition close matching of phase response between strain and inertial seismometers is achieved using calibrator motion. Additionally, studies using earthquake data show no discrepancies that would suggest large losses in motion.

It is possible that simulated earth motion induced by the calibrator is attenuated by the tube suspension during calibration, whereas the suspensions move with the earth when the seismometer is recording earth strain. It is also possible that the calibrator is producing a torque due to an imbalance in sensitivity of the two coils composing the calibrator.

Any loss of motion caused by calibrator torque may be resolved by measuring motion induced by displacement at the fixed end. This measurement would be made at both the fixed and free end. The next step would be to adapt the electromagnetic calibrator on the vertical strain seismometer for use on the horizontal seismometer. The necessary modification is quite simple.

Operation of a VCT to measure motion at the calibrator of the vertical strain seismometer has been postponed, particularly since the use of an electromagnetic (E-M) calibrator to replace the magnetostrictive calibrator has resolved existing phase discrepancies. There is no evidence of loss of motion between the fixed and free ends. On the contrary, measurements with a reliably calibrated VCT on the free end of the vertical strain seismometer yields a free-end displacement of 0.75 millimicrons per milliamp of calibrator current. This compares favorably with a theoretical value of 1.0 mμ per mA based on design constants. In addition, the amplitude and phase characteristics (figures 8 and 9) of the seismometer measured at the free-end in response to constant displacement of the E-M calibrator do not deviate appreciably from those of a linear system. Also, a comparison of earthquake data between vertical strain, summed orthogonal horizontal strain, and inertial seismograph outputs reveals no losses.

To reduce effects that could lead to improper operation of the vertical strain seismometer, plans exist for operating the seismometer with the VCT removed to simplify the moving-coil transducer package. Included will be testing of the seismometer with a shorter (10-meter) tube section to reduce problems such as bending of the tube, contact of tube with the borehole casing, and misalignment of the tube where it enters the transducer package.

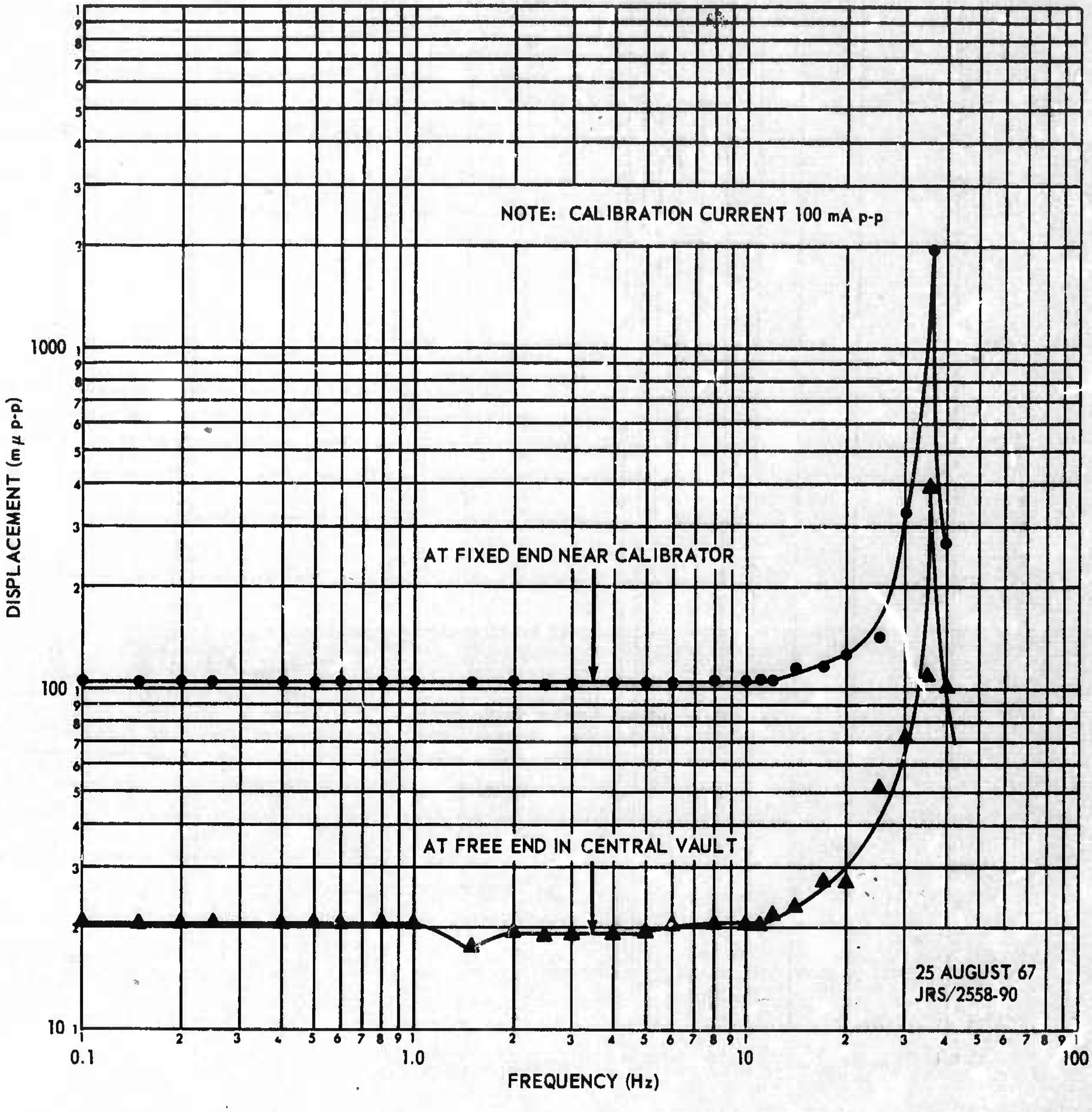

Figure 4. Amplitude response of north strain seismometer measured with a variable capacitance transducer at each end showing an apparent 80 percent loss in calibration motion between fixed and free ends

G 3200

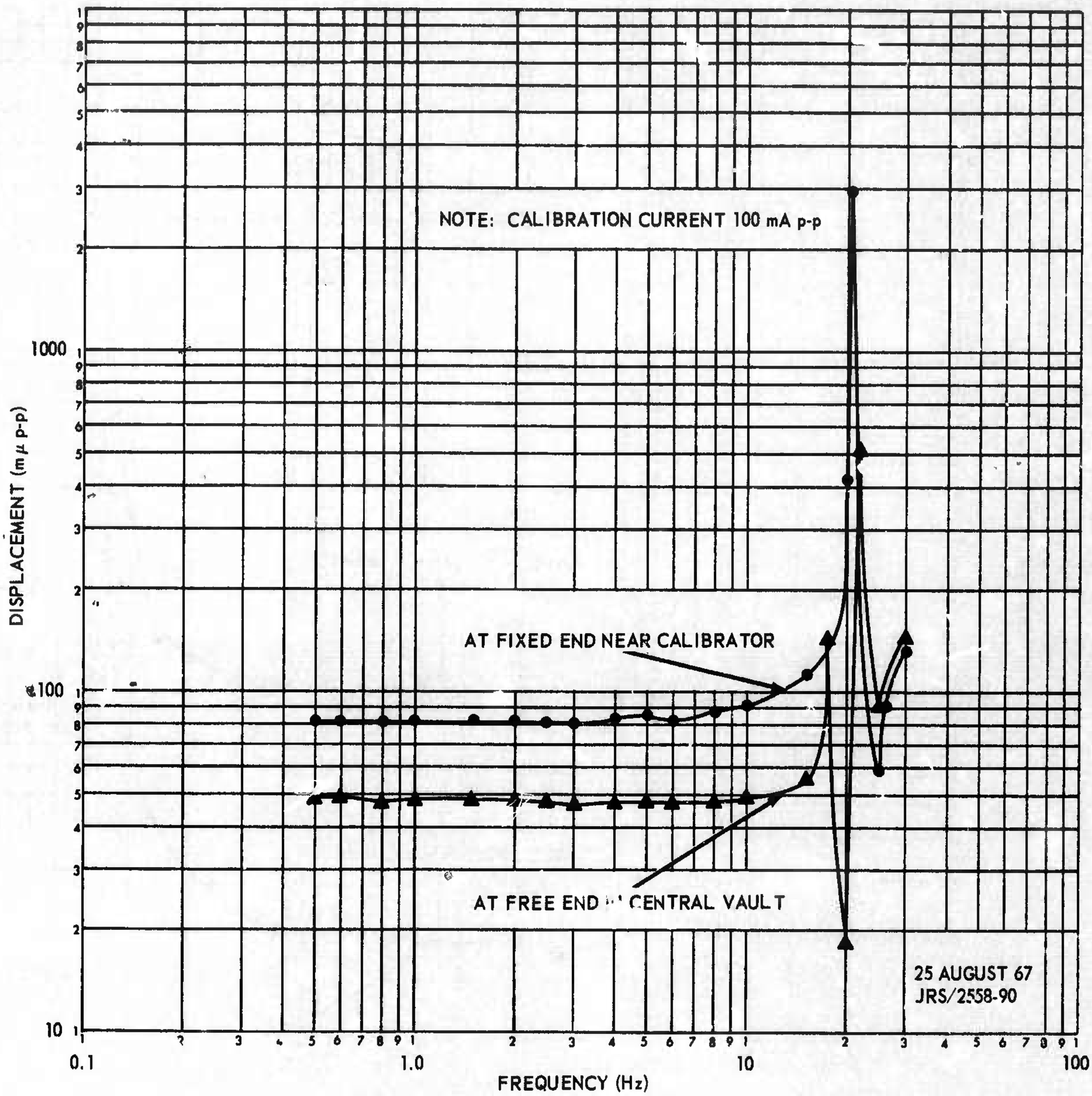

Figure 5. Amplitude response of northeast strain seismometer measured with a variable capacitance transducer at each end showing an apparent 40 percent loss in calibration motion between fixed and free ends

G 3201

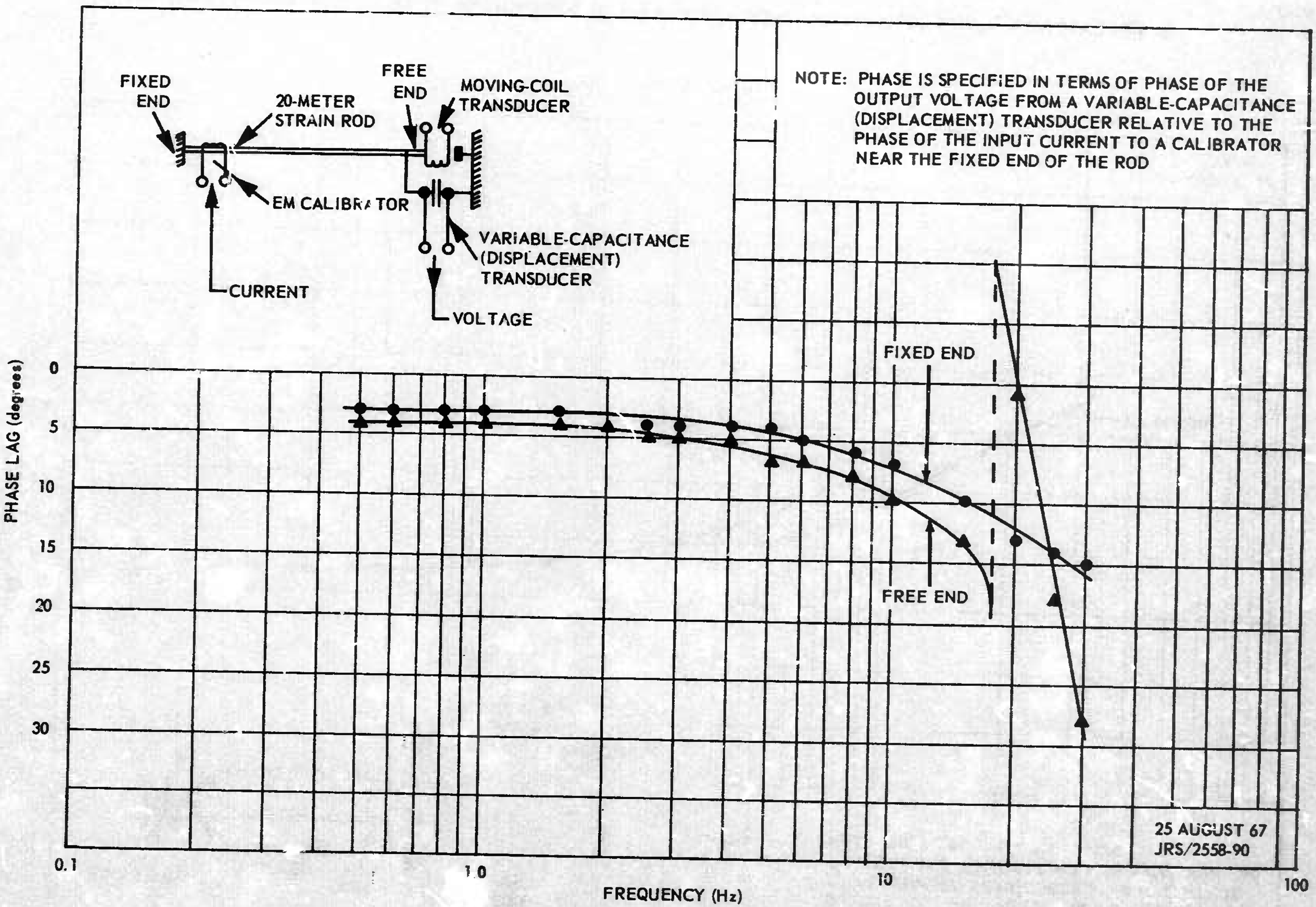

Figure 7. Phase response of northeast strain seismometer measured with a variable capacitance transducer showing minor phase lags in the band of interest (0.5 to 10 Hz) at both the fixed and free ends of the seismometer

G 3203

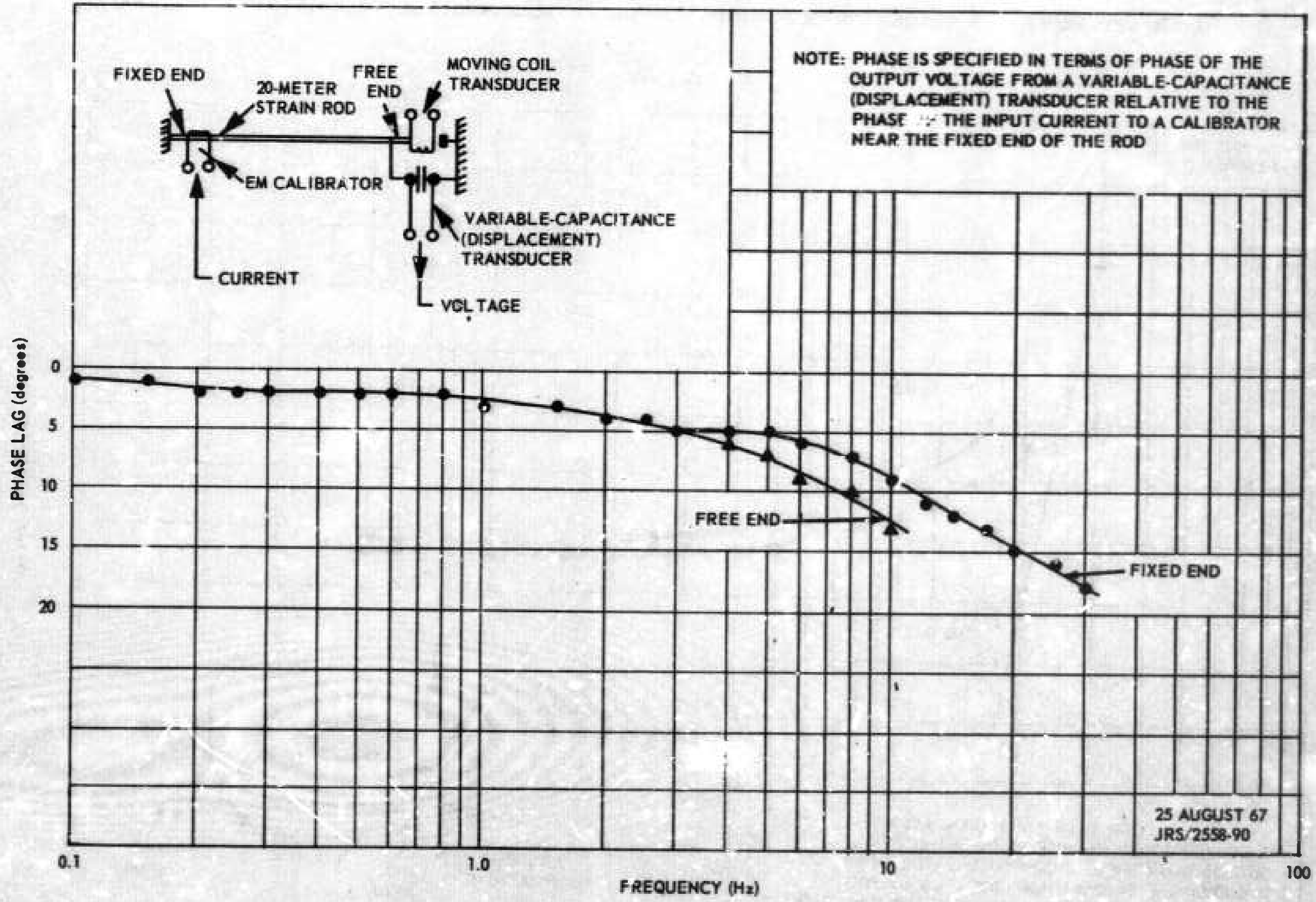

Figure 6. Phase response of north strain seismometer measured with a variable capacitance transducer showing minor phase lags at fixed and free ends of the seismometer

G 3202

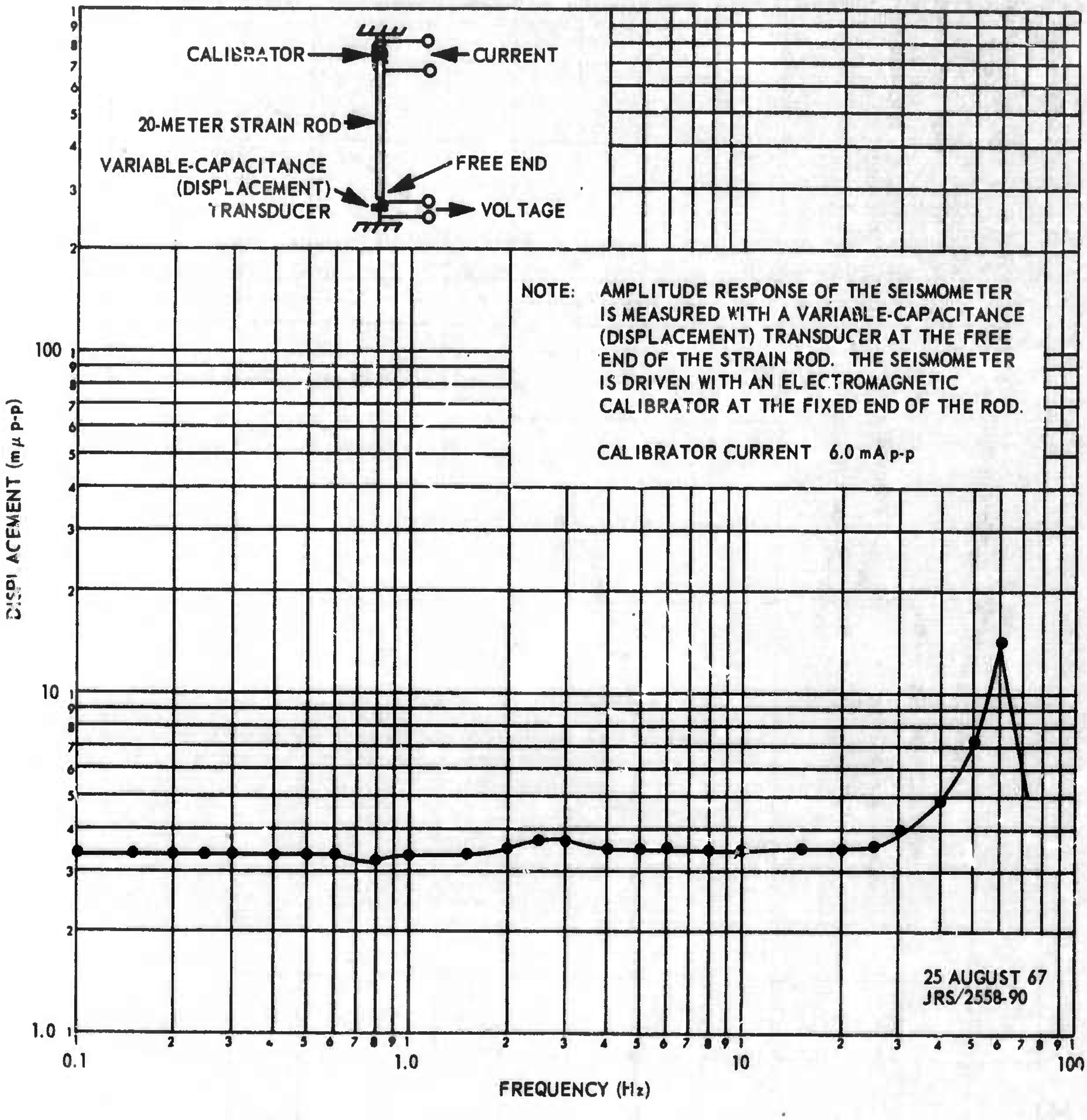

Figure 8. Amplitude response of the vertical strain seismometer in response to calibrator motion

G 3204

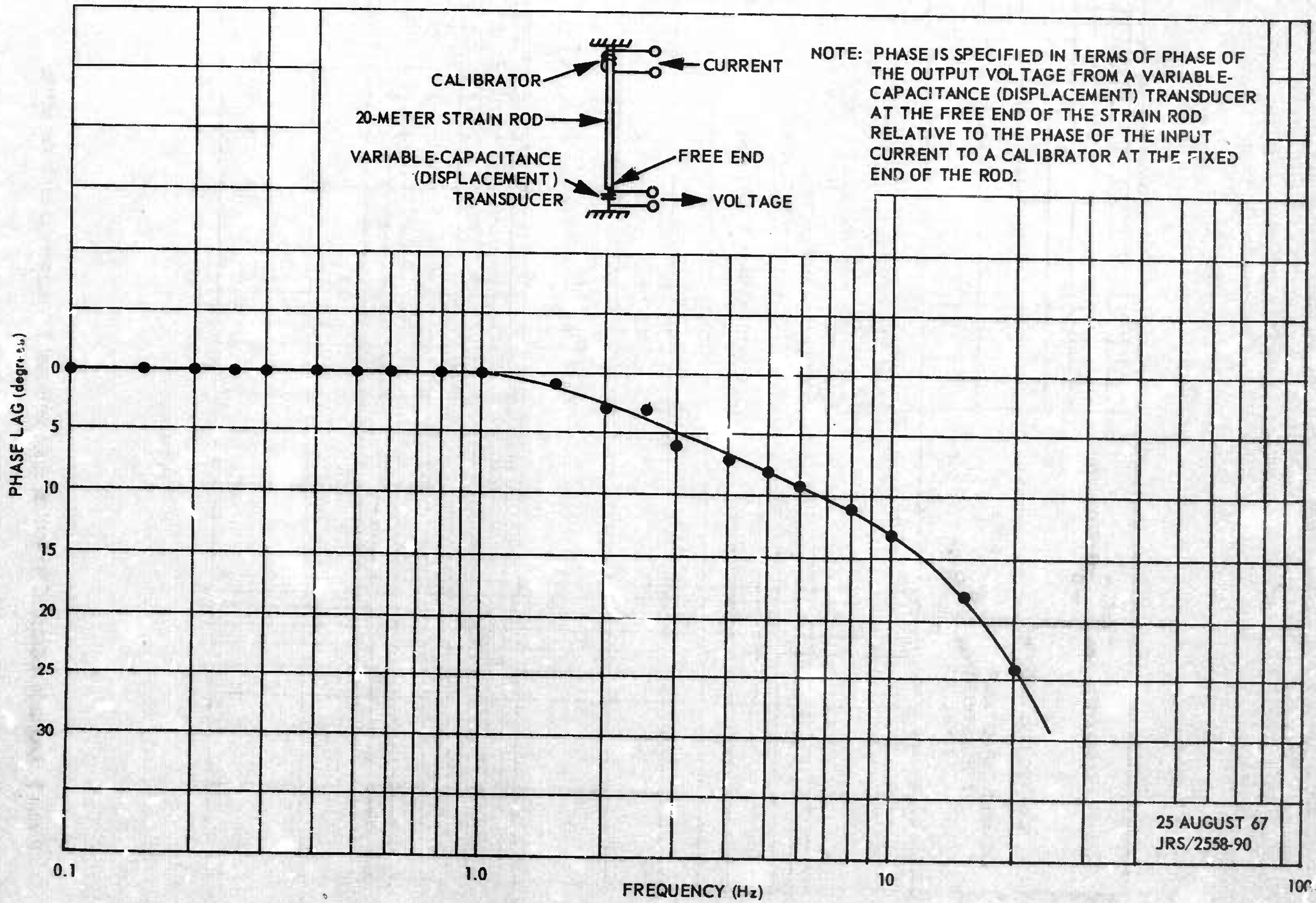

Figure 9. Phase response of the vertical strain seismometer in the plastic cased borehole

G 3205

2.3 SPECIFICATIONS OF THE MATCHING FILTER FOR THE SHORT-PERIOD STRAIN-INERTIAL SEISMOGRAPH COMBINATION

Successful matching of the amplitude and frequency response of the strain and inertial seismographs in the short-period range (0.1 - 10 Hz) has been accomplished with Narrow Bandpass Filter, Model 28900, designed specifically for that purpose. Six strain channels containing the filter have been in operation for eight months. Specifications for the filter were prepared and forwarded to the Project Office on 14 September 1967.

3. SEISMOGRAPH DEVELOPMENT

3.1 LONG-PERIOD HORIZONTAL STRAIN

3.1.1 Present Status

One of the most promising applications of strain seismometers is in the long-period band, 6-100 seconds, where seismic waves are less affected by crustal inhomogeneity. Three applications of long-period strain seismometers that are discussed later in Section 5 of this report and that justify a stronger research effort are:

a. The detection of surface waves from an earthquake from one direction in the presence of an earthquake from another, using a strain inertial combination of seismographs;

b. The enhancement of the initial arrival of the long-period body wave by cancelling Rayleigh microseisms using a combination of the summed outputs of orthogonal horizontal long-period strain seismographs and a vertical long-period inertial seismograph;

c. Identification of wave types and earthquake phases from a comparison of the amplitude and phase between strain and inertial seismographs.

The status of long-period strain instrumentation resulting from a relatively small development effort is discussed below. The improvement required to upgrade the instrumentation to permit full use in the above applications is also given.

At present, the long-period horizontal strain instrumentation at WMSO has been developed to a capability equivalent to that of the conventional long-period inertial seismograph of 1963. At that time, inertial systems were capable of operating at a system magnification of 5K to 10K at 25 seconds. Present advanced long-period inertial seismographs operate at gains of 50K to 100K.

Currently, the long-period north strain seismograph (SNL) in the surface installation at WMSO is operating in combination with a long-period north inertial seismograph (NLL) at a gain of 10-15K. A block diagram of the system is shown in figure 10. To obtain matched responses to ground motion, a filter is required in the strain circuit.

The amplitude responses (figure 11) of SNL and NLL measured early in the operation indicate a match within 10 percent in the period range of main interest. This match is considered sufficient for the purpose of evaluating the directional array capabilities of long-period strain. The phase response of SNL (figure 12) shows the close match between theoretical and empirical data. Figure 13 shows the close phase match between SNL and NLL.

Figure 14 is an analog playback of the long-period strain channel showing the relative levels of uncompensated tape noise; system electronic noise; seismic background and environmental noise; and a plot of wind velocity. Figure 15 is a playback of portions of a magnetic-tape recording of the SNL and NLL channels covering the period 1900Z on 10 July to 1515Z on 11 July 1967. This typical record contains microseismic background and seismic events. Portions of the record are contaminated with electrical pulses and wind noise. From figures 14 and 15 and similar recordings, it is estimated that the magnification of SNL is limited to an equivalent inertial magnification of about 15K at 25 seconds. The gain is limited by background noise, the source of which is not known. Figure 14 shows that tape noise and system electrical noise contribute little to the total noise observed. However, it is obvious that a high correlation exists between wind velocity and background noise. The effect of atmospheric pressure changes is not precluded, although the vault has been sealed to the point where air pressure changes recorded on a microbarograph in the vault appear to have low correlation with strain background. The relation between strain and wind velocity shown in figure 16 suggests that ground coupled air-pressure changes may be a major source of noise. Mechanical noise in the strain seismometer cannot be ruled out as a possible source of noise. Tests using a 1-meter strain interval to minimize ground-coupled air-pressure changes are being prepared to obtain a measure of possible thermal-mechanical noise in the moving-coil transducer.

Figure 17 contains plots of coherence and phase difference between NLL and SNL. Spectra of NLL and SNL at equivalent inertial magnifications are also shown. The relatively high strain amplitudes in the spectrum of SNL, and the low coherence between NLL and SNL at periods longer than 5 seconds indicate the the source of the noise on SNL is either environmental or in the instrument.

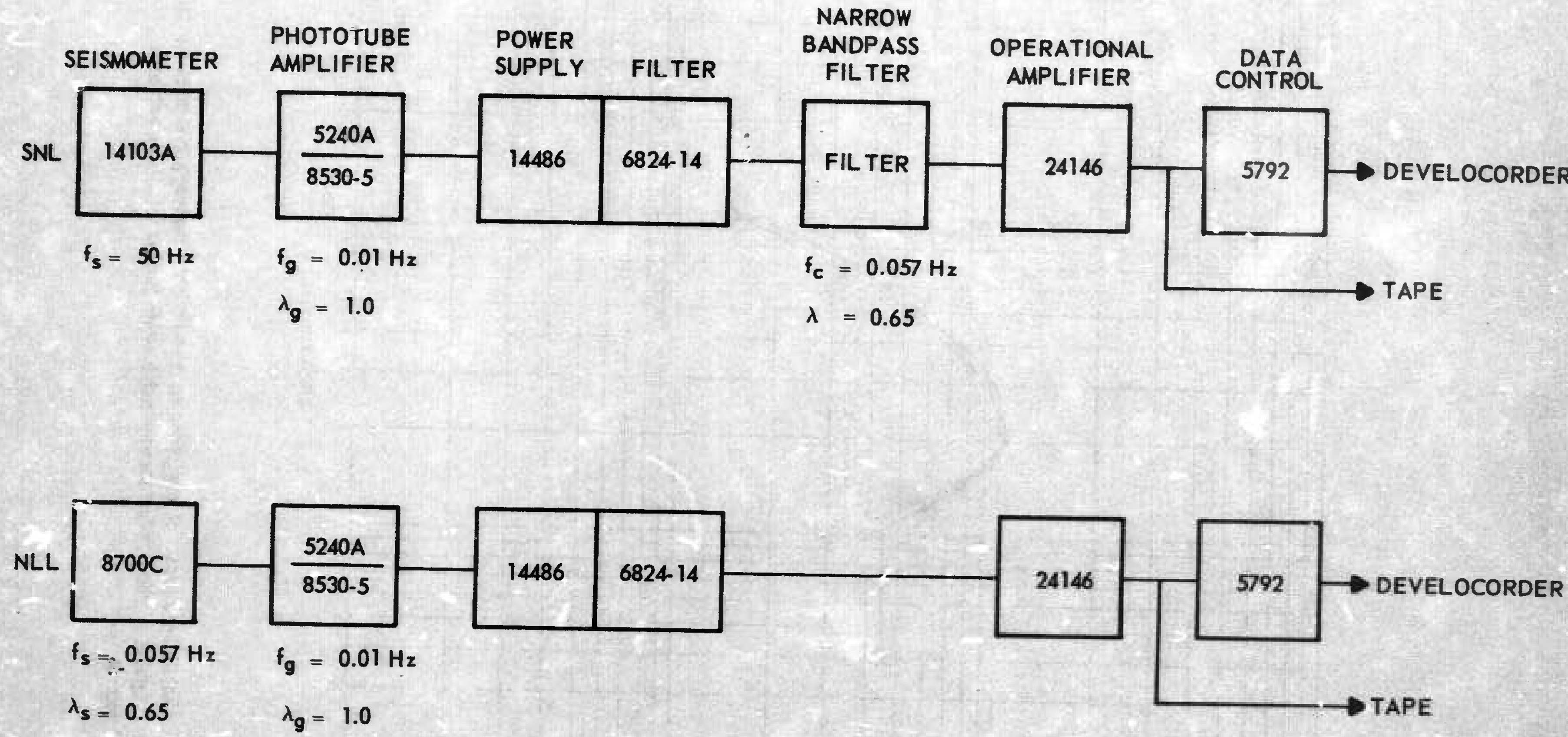

Figure 10. Block diagram of strain (SNL) and inertial (NLL) seismograph components in long-period directional array at WMSO

G 3206

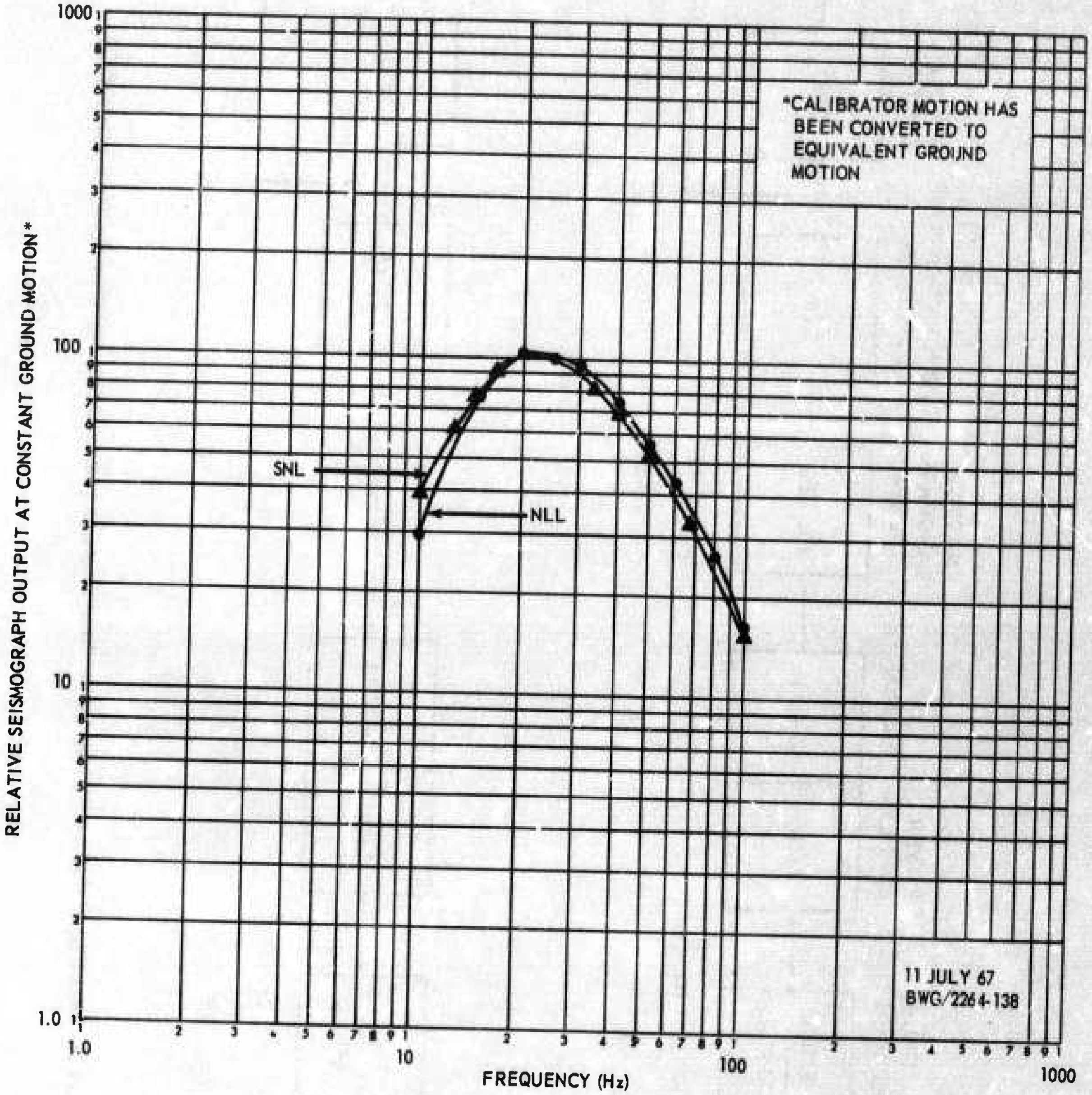

Figure 11. Amplitude responses of long-period north strain (SNL) and long-period north inertial (NLL) seismographs to ground motion showing match within 10 percent in the period range 13 to 100 seconds

G 3207

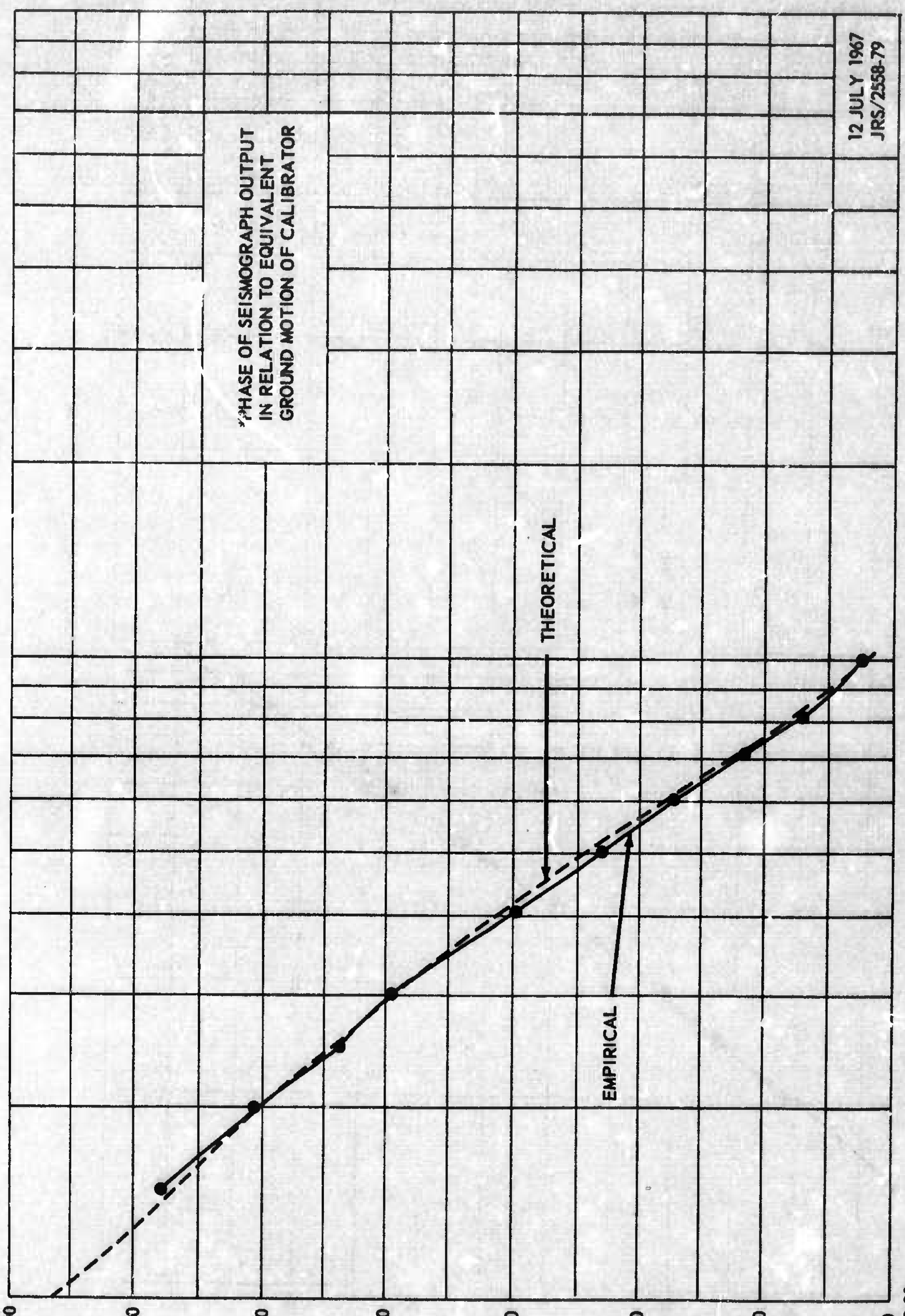

G 3208

Figure 12. Phase response of SNL to ground displacement showing close match with theoretical response

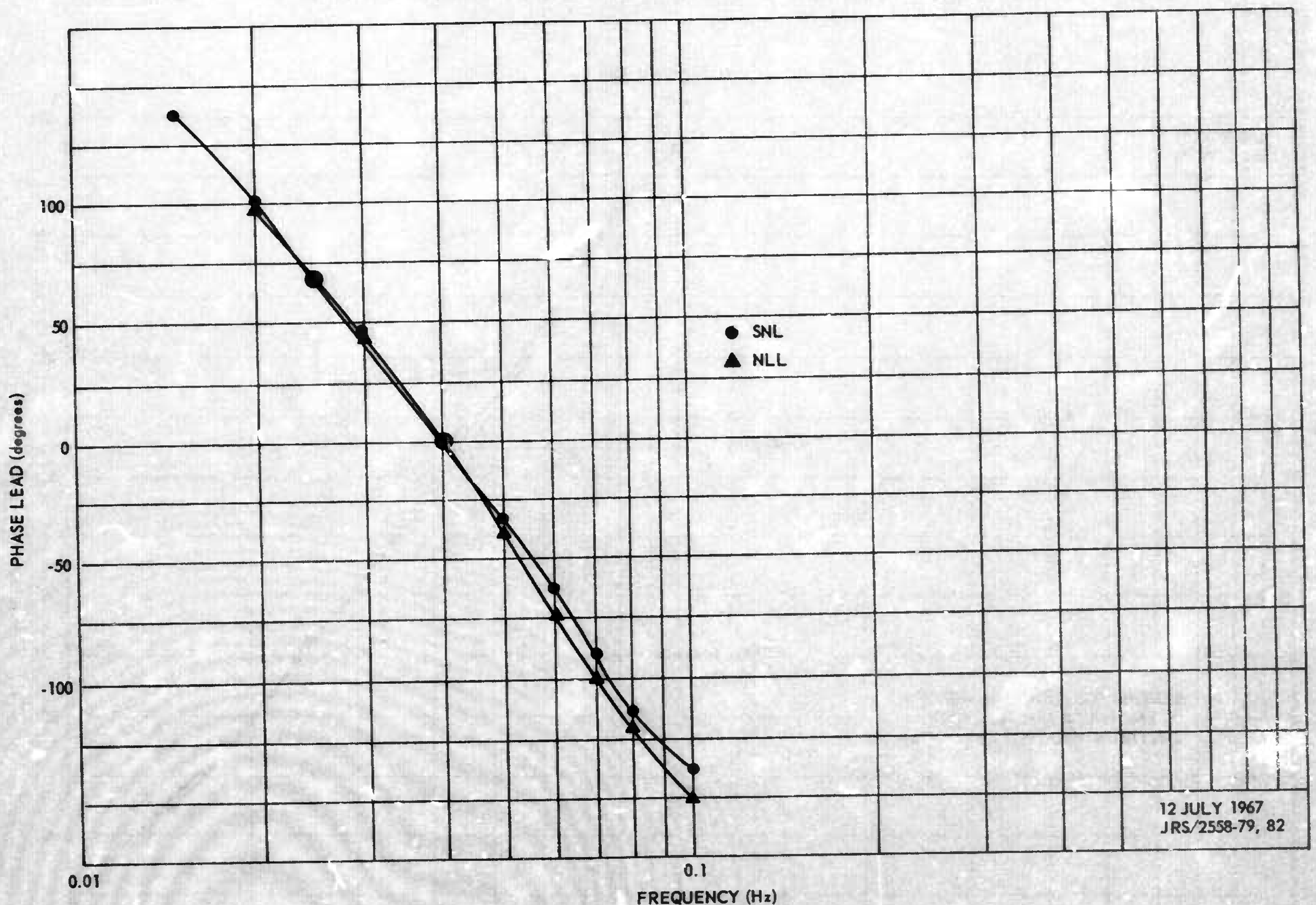

Figure 13. Phase responses of SNL and NLL showing close match

G 3209

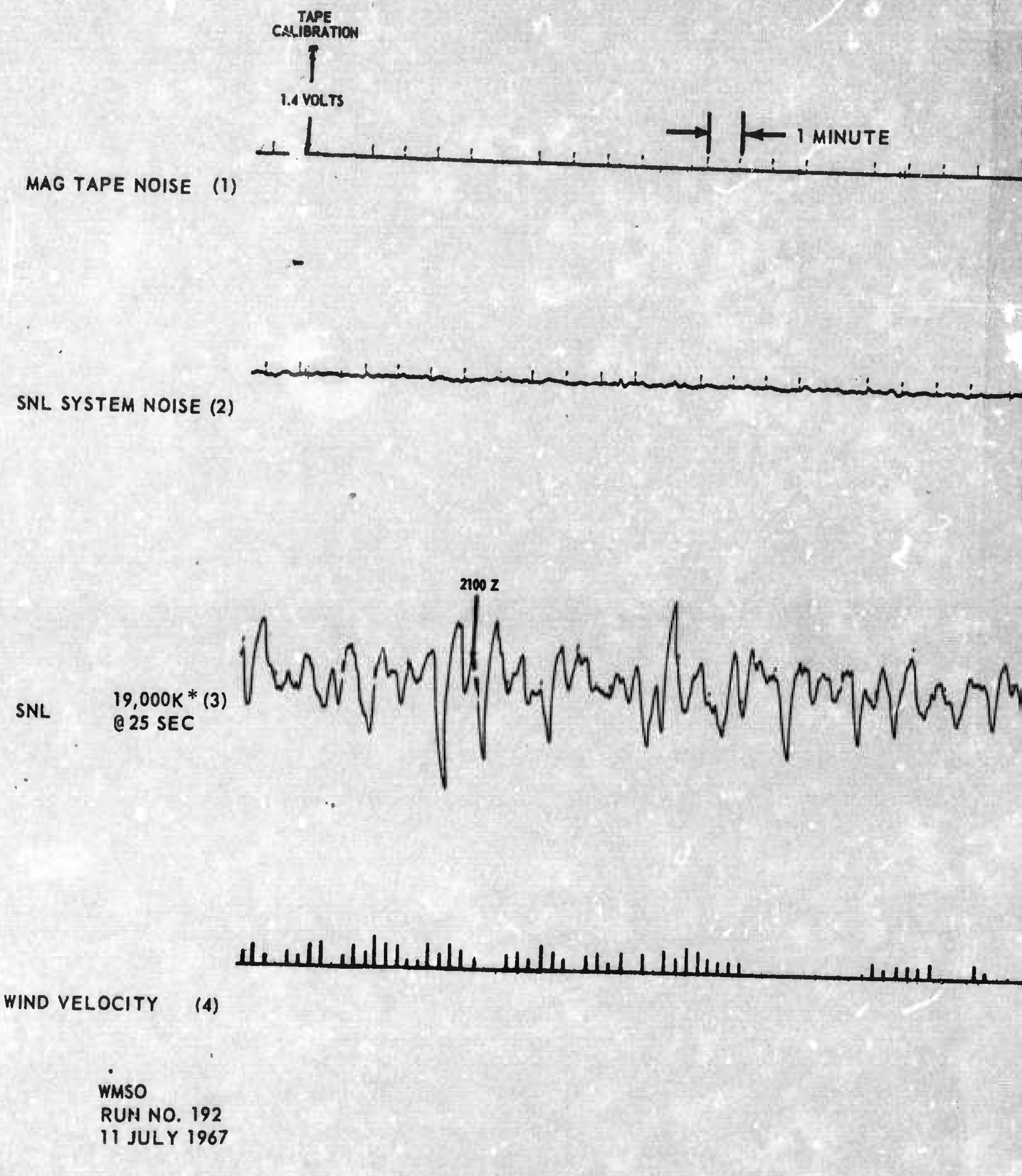
TAPE CALIBRATION
1.4 VOLTS
1 MINUTE
MAG TAPE NOISE (1)
SNL SYSTEM NOISE (2)
2100 Z
SNL
19,000K* (3)
@25 SEC
WIND VELOCITY (4)
WMSO
RUN NO. 192
11 JULY 1967

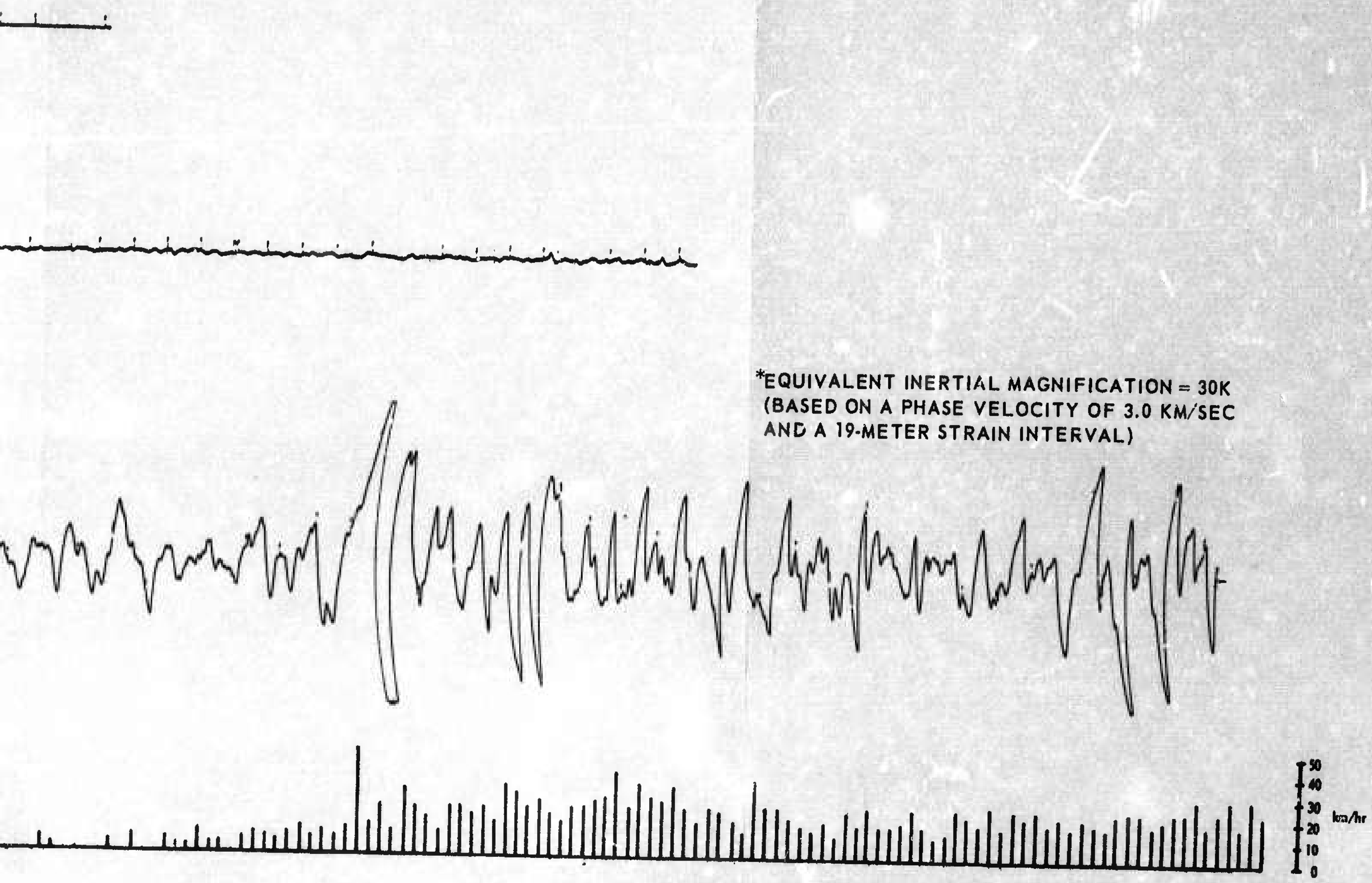

Figure 14. Analog playback of long-period strain north (SNL) channel showing (1) Dummy loaded magnetic-tape recorder output (uncompensated) (2) Dummy loaded PTA through tape recorder (3) Seismic background (4) Plot of wind velocity readings

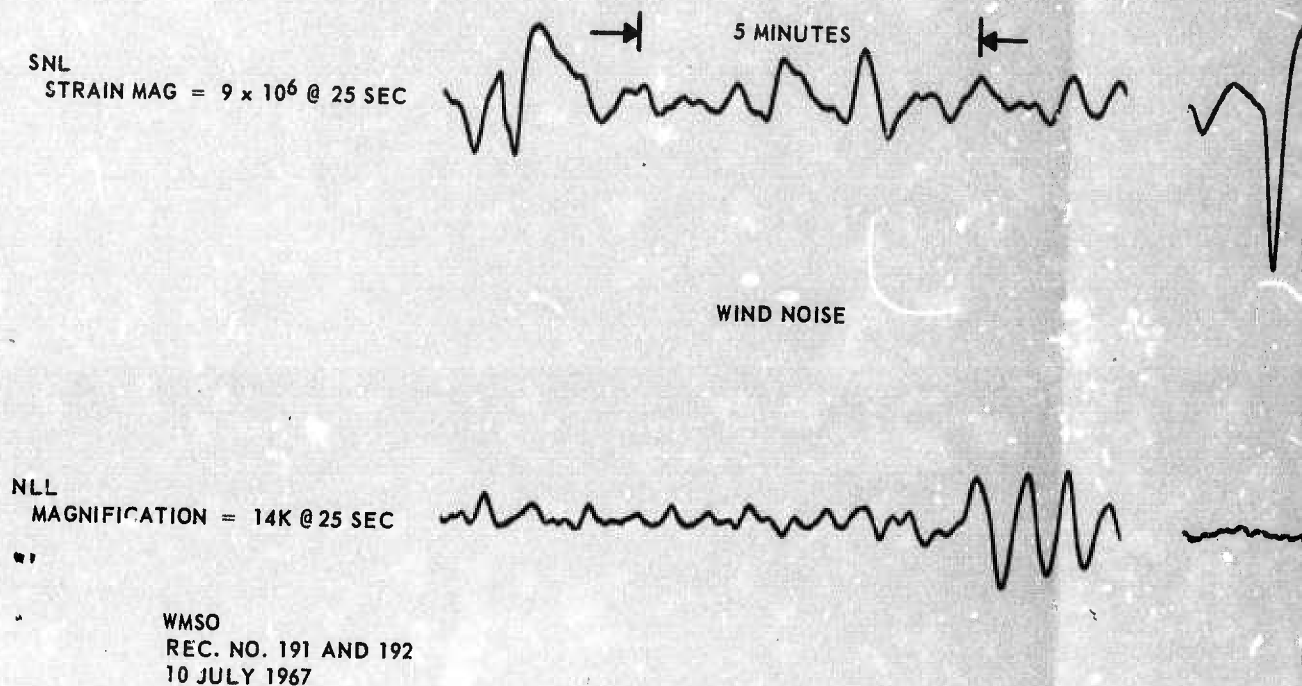
SNL
STRAIN MAG = 9×10^6 @ 25 SEC
5 MINUTES
WIND NOISE
NLL
MAGNIFICATION = 14K @ 25 SEC
WMSO
REC. NO. 191 AND 192
10 JULY 1967

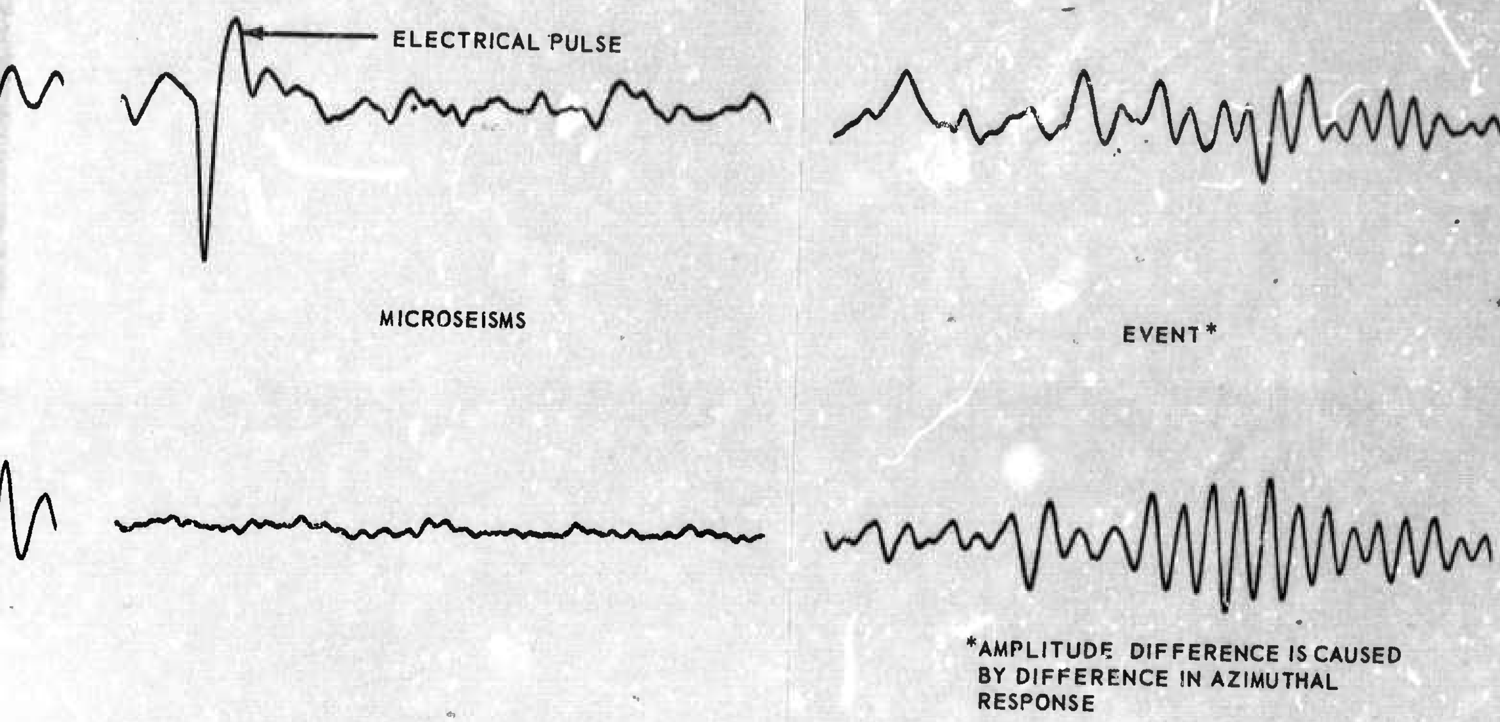

Figure 15 Long-period north strain and inertial playback from portions of magnetic tape recording showing microseisms and an event contaminated with wind noise and electrical pulses in the interval 1900Z on 10 July to 1515Z on 11 July 1967

G 3210

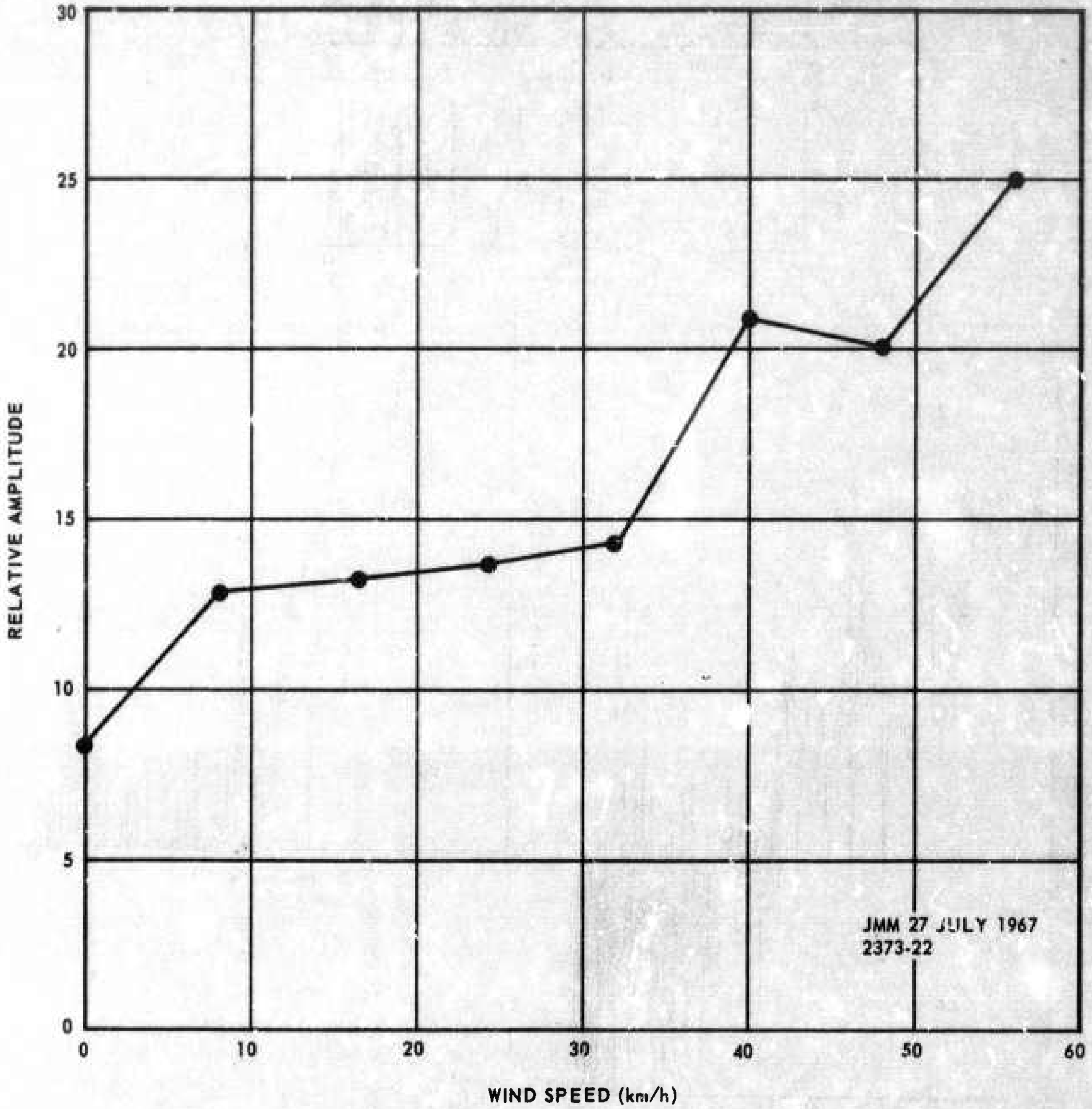

Figure 16. Wind noise as a function of wind speed measured on SNL seismograms in the period range 30-60 seconds

G 3211

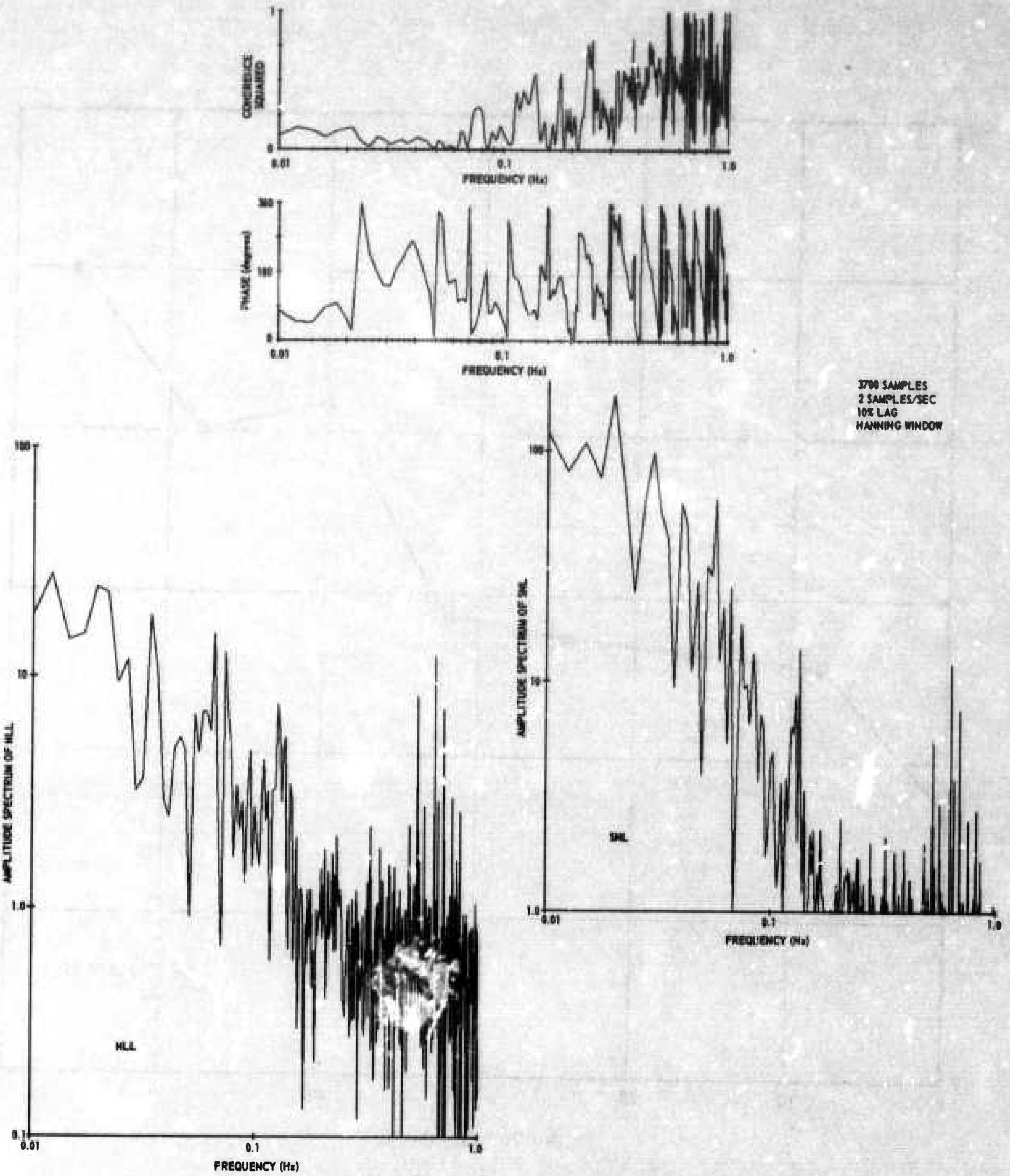

Figure 17. Coherence and phase difference between and spectra of the long-period north inertial (NLL) and the long-period north strain (SNL) seismograph recordings of seismic background noise. WMSO tape recorder No. 1, record No. 193, 2006Z - 2036Z

G 3212

The improved coherence and phase and the increased similarity in spectra of NLL and SNL during the occurrence of an earthquake is demonstrated in figure 18.

It is cautioned that although the low correlation in figure 17 is obviously caused by either environmental or instrumental noise, the coherence for microseismic background noise is expected to be low in both the short-period and long-period frequency range, 0.01-10 Hz. This is demonstrated for short-period microseisms in figure 19. Low coherence is attributed to the difference in directional responses of the two instruments and the complexity of the microseismic pattern as proved by the high coherence obtained for a regional event.

3.1.2 Required Improvements for Successful Application of Long-Period Strain

In order to improve the signal-to-noise ratio at long periods (15-40 seconds), the present strain magnification must be increased from its present maximum of about 15K to about 90K (equivalent inertial magnification) to match the present advanced long-period magnifications (50K-100K) and to cancel micro-seisms. In order to record Rayleigh particle motion of 40×10^{-9} meters at 20 seconds, and still be able to cancel these microseisms by at least 12 dB, we must reduce existing mechanical noise by a factor of four (x4) to the level of electrical noise, and then increase the sensitivity of the seismometer by a factor of 6. It is doubtful that environmental conditions in the 4-meter deep horizontal strain installation at WMSO will be sufficiently stable to fully accomplish this goal. A possible approach is to operate a single long-period horizontal strain seismograph in a mine near Tonto Forest Seismological Observatory (TFSO). This would be a particularly favorable location because it would permit comparing the strain directional array with the inertial long-period array at TFSO. Successful resolution of 20-second microseisms can be accomplished by eliminating what is believed to be mechanical noise in the suspension of the present transducer coil; by operating with an improved Alnico 9 magnet of smaller diameter and greater sensitivity; and using a seismometer 50 meters long.

4. EVALUATION

4.1 OPERATION AT VARIOUS DEPTHS IN THE BOREHOLE

Plans have been made and most of the necessary equipment obtained for operating the vertical strain seismometer at different depths in the 107-meter steel-cased borehole. The 19-meter seismometer will first be

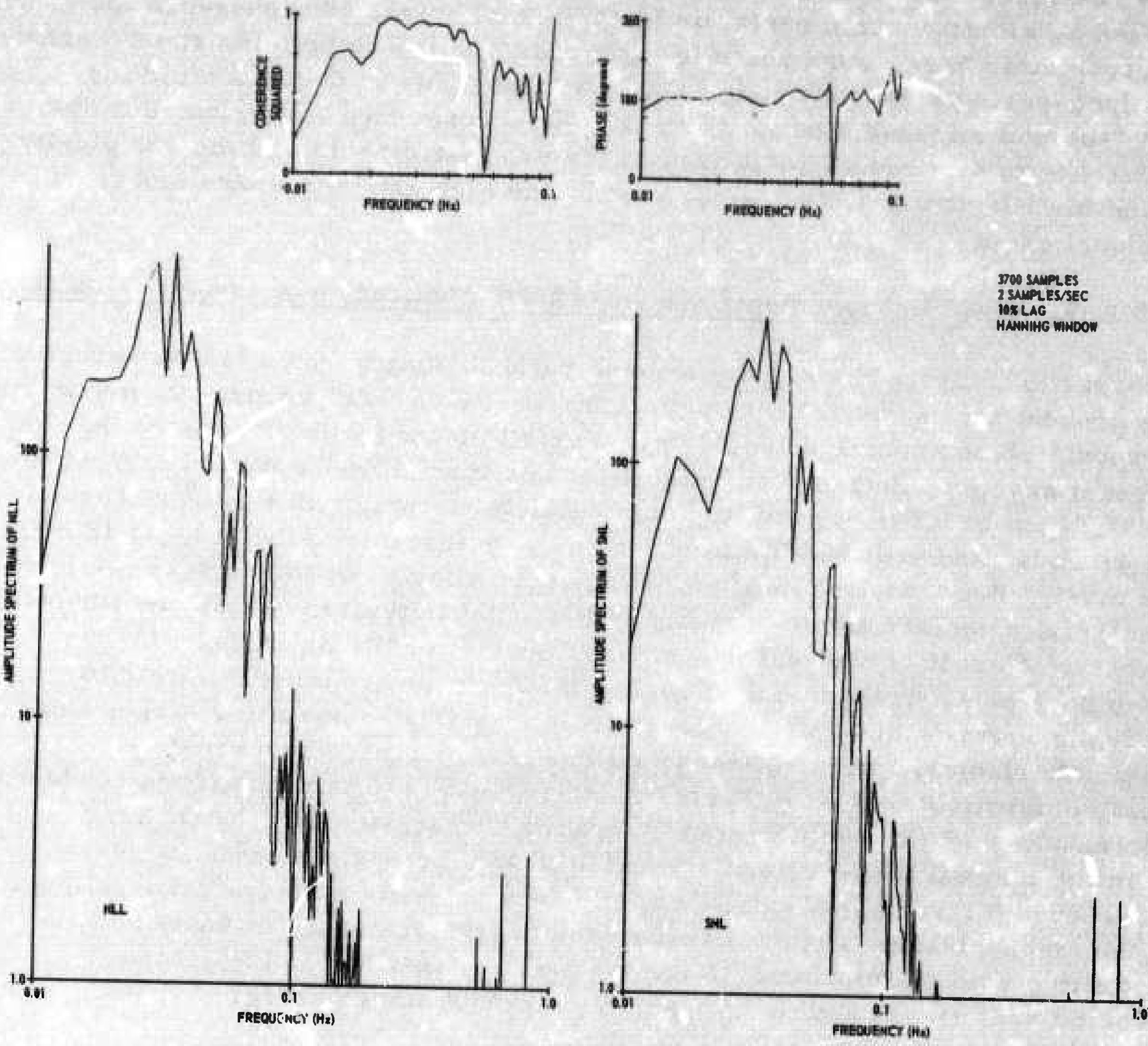

Figure 18. Coherence and phase difference between and spectra of the long-period north inertial (NLL) and the long-period north strain (SNL) seismograph recordings of a teleseism recorded at WMSO on 21 June 1967; origin time: 06:49:56.6Z; Peru-Ecuador Border; 2.2S; 77.6W; AZ = 153°; Δ = 42°; h = 49 km

G 3213

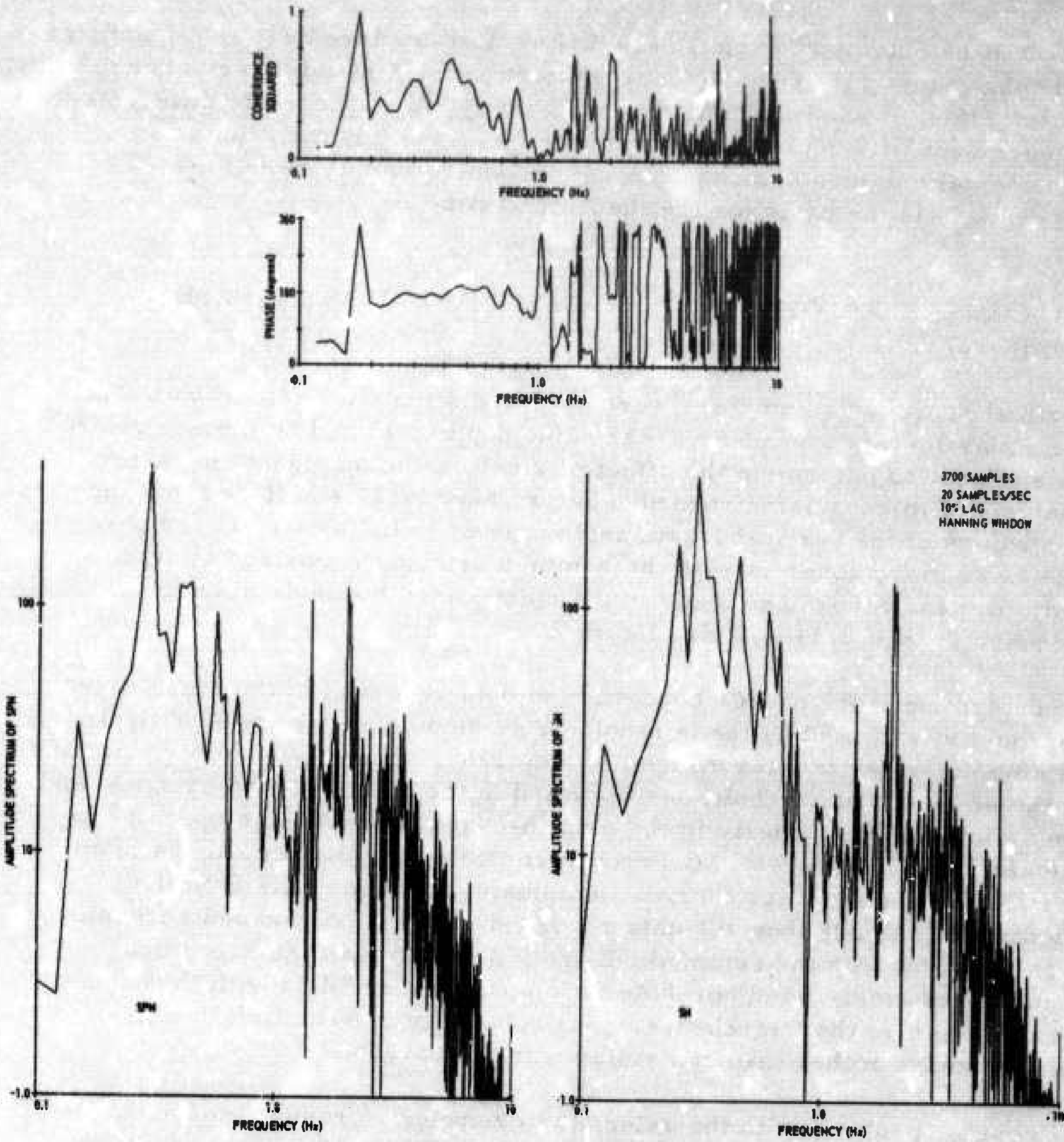

Figure 19. Coherence and phase difference between and spectra of the short-period north inertial (SPN) and short-period strain (SN) seismograph recordings of microseisms. WMSO tape recorder No. 3, record No. 171, 1521Z - 1524 Z

G 3214

operated 3 meters below the surface. Tests are scheduled for the first week in October 1967, following installation of new anchors on the seismometer in the plastic-cased borehole.

Data will be obtained on changes in differential displacement as a function of depth; change in coherency between vertical strain and other seismographs; and the effect of wind and temperature with depth. Changes in differential displacement with depth will be compared with theoretical values for fundamental and higher modes. A new seismic velocity model for WMSO (appendix 2) is the basis for the theoretical data.

4.2 COMPARISON OF THE STEEL-CASED AND PLASTIC-CASE BOREHOLES

Vertical strain seismometers were operated simultaneously in both a steel and a plastic-cased borehole at the same depths, 18 and 36 meters below the surface, to determine the effect of steel casing on signal character. Analysis of microseisms recorded before May 1967 established that the recordings of the vertical strain seismometer in the plastic-cased borehole were more coherent with the summed orthogonal horizontal strains than were the recordings made in the steel-cased borehole over the frequency range 0.14-1.0 Hz, figure 20.

To determine if the poorer coherence of data recorded in the steel-cased borehole was caused by the borehole or seismometer, the two vertical seismometers were interchanged in May 1967. The seismometer formerly in the steel-cased borehole was operated in the plastic-cased borehole and the seismometer formerly in the plastic-cased borehole was operated in the steel-cased borehole. Coherence computed for the recordings of an earthquake and the microseisms immediately preceding its P arrival (figures 21 and 22) show the data recorded in the plastic-cased borehole less coherent with the summed NE and NW strain than the recordings made in the steel-cased borehole. Comparing these data with those obtained before the interchange, poor coherence is seen to follow the seismometer rather than remaining with the borehole.

Although a problem with the seismometer appears present, some uncertainities also exist for this evaluation. From figures 23a through 23d measured vertical strain in the plastic-cased borehole is seen to compare most favorably with the sum of the north and east strains whereas the vertical strain in the steel-cased borehole compares most favorably with the sum of the northeast and northwest strains. Coherence between the recordings of the two vertical strains, however, is low (figure 23e). These results indicate that the recordings of the two pair of summed horizontal strains should also be relatively incoherent. Poor coherence however is not observed (figure 23f).

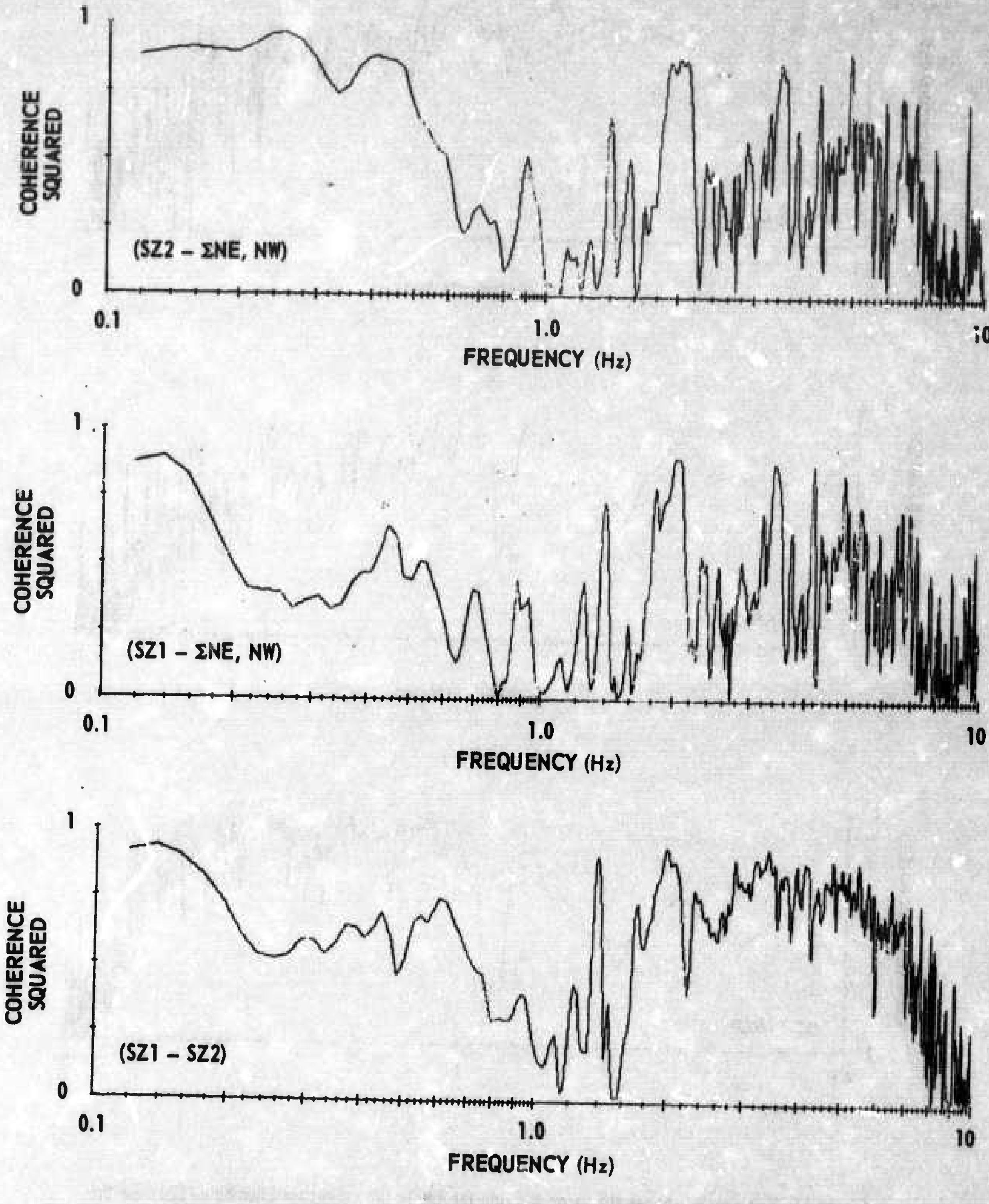

Figure 20. Coherence between the vertical strain located in the plastic-cased borehole (SZ2) and the crossed strains (ΣNE, NW), top, coherence between the vertical strain located in the steel-cased borehole (SZ1) and the crossed strains (ΣNE, NW), center, and coherence between the two vertical strains (SZ1-SZ2), bottom, illustrating poor coherence associated with SZ1. The recordings were made before the seismometers were interchanged in the boreholes and are of microseisms

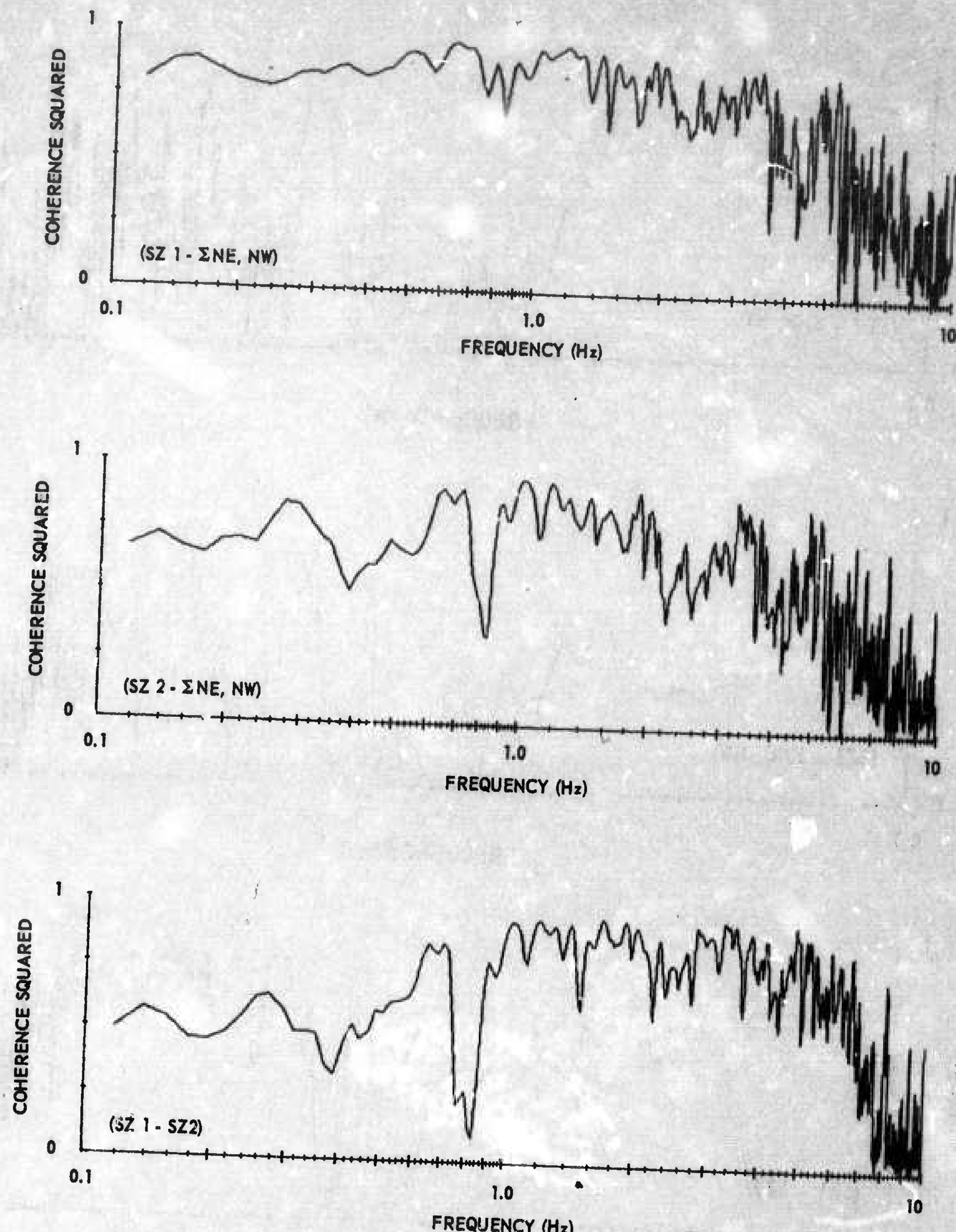

Figure 21. Coherence between the vertical strain located in the steel-cased borehole (SZ1) and the crossed strains (ΣNE, NW), top, coherence between the vertical strain located in the plastic-cased borehole (SZ2) and the crossed strains (ΣNE, NW), center, and coherence between the two vertical strains (SZ1 - SZ2), bottom, illustrating poor coherence associated with SZ2. The recordings were made after the seismometers were interchanged in the boreholes and are of an earthquake whose epicenter was near the coast of Nicaragua

G 3215

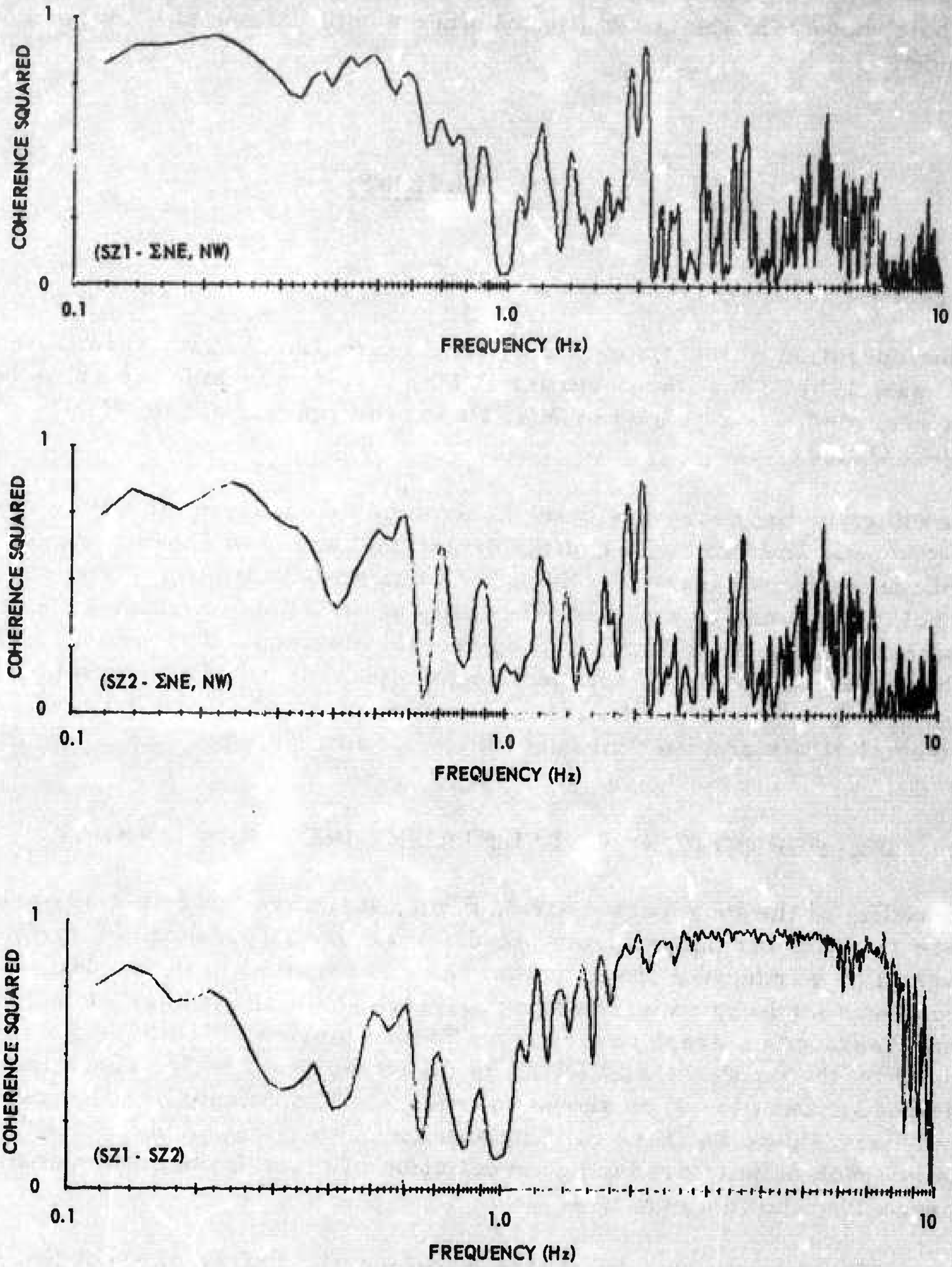

Figure 22. Coherence between the vertical strain located in the steel-cased borehole (SZ1) and the crossed strains (Σ NE, NW), top, coherence between the vertical strain located in the plastic-cased borehole (SZ2) and the crossed strains (Σ NE, NW), center, and coherence between the two vertical strains (SZ1 - SZ2), bottom, illustrating poor coherence associated with SZ2. The recordings were made before the seismometers were interchanged in the boreholes and are of microseisms

G 3216

From the data examined, poor coherence between vertical strain recordings appears to be caused by the seismometer which is in the plastic-cased borehole; however, the possibility of other complications has not been excluded.

5. APPLICATIONS

5.1 SHORT-PERIOD DIRECTIONAL ARRAY

Online operation of the short-period strain directional array terminated 11 August 1967. The Develocorder (WMSO No. 6) on which the array had been recorded was returned to WMSO upon the request of the WMSO Project Officer.

Recordings by the array are being assembled and analyzed to verify the effectiveness and limitations of the directional array to enhance signal. Earthquakes from essentially the same azimuth but different distances are being examined to evaluate the ability of the array to enhance P-waves by signal addition as a function of epicentral distance. The extent to which each element of the array will be able to reject microseisms is being examined as a function of frequency by computing coherence between horizontal strain and inertial recordings of microseisms.

5.2 LONG-PERIOD HORIZONTAL STRAIN DIRECTIONAL ARRAY

The ability of the long-period strain directional array to detect surface waves from an earthquake from one direction in the presence of surface waves of an earthquake from another is demonstrated in figure 24. This record was made by superimposing magnetic-tape recordings of an event from Alaska on an event record from South America. The Alaskan event (No. 1) on the north inertial (NLL) is displayed in trace 1. The South American event (No. 2) is shown on trace 2. The composite of traces 1 and 2 are shown as trace 3. The summation of strain and inertial seismograph outputs producing cancellation of trace 2 and enhancement of trace 1 is shown on trace 4.

Figure 25 shows the individual strain and inertial traces of event No. 1 and their summation (summed in phase to add signals from the north). Figure 26 shows the individual strain and inertial traces of event No. 2 and their summation (summed to cancel signals from the south).

System magnifications were set for maximum cancellation of Rayleigh waves. However, the marked differences in strain and inertial trace

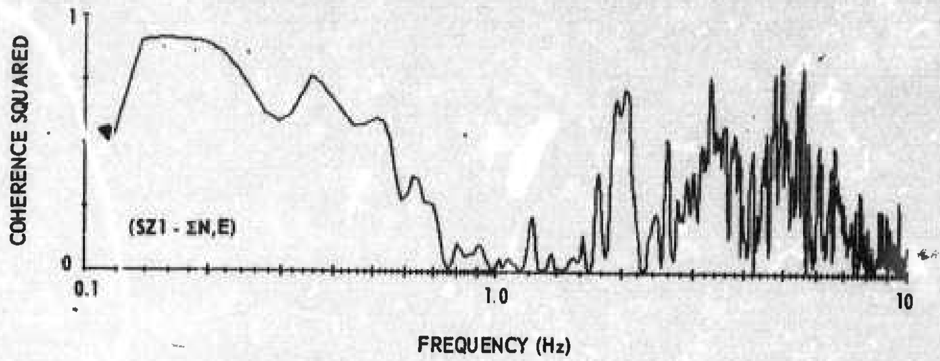

a. Coherence between the vertical strain in the steel-cased borehole and summation of the N and E strain recordings of microseisms

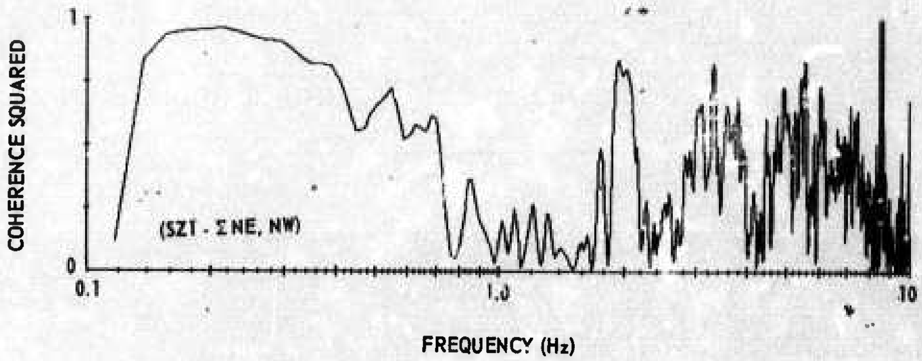

b. Coherence between the vertical strain in the plastic-cased borehole and summation of the N and E strain recordings of microseisms

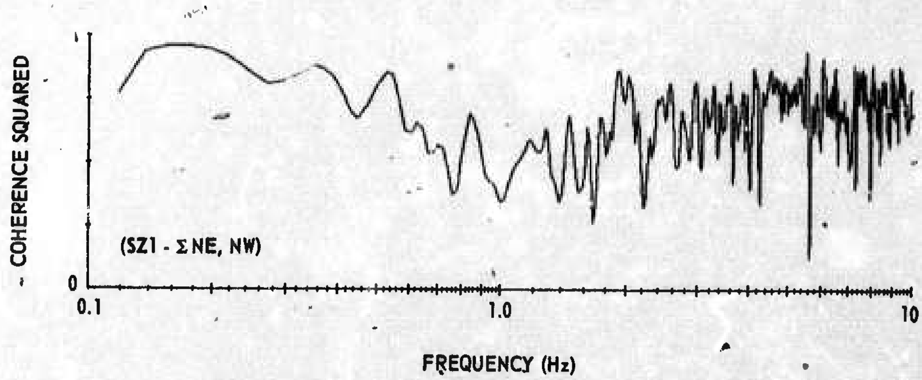

c. Coherence between the vertical strain in the steel-cased borehole and summation of the NE and NW strain recordings of microseisms

1

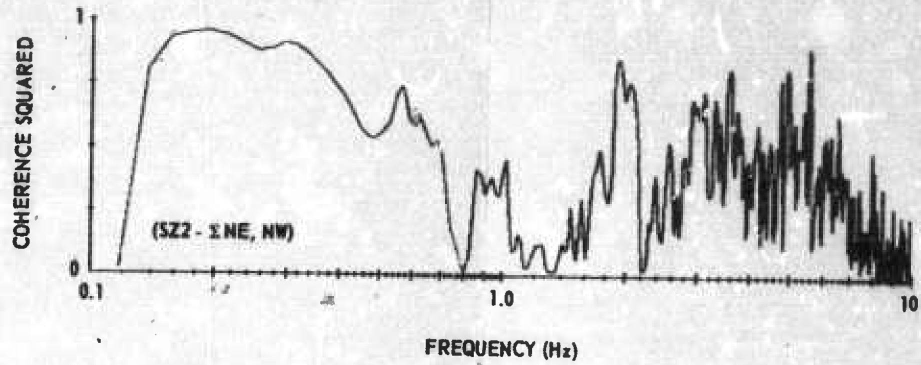

d. Coherence between the vertical strain in the plastic-cased borehole and summation of the NE and NW strain recordings of microseisms

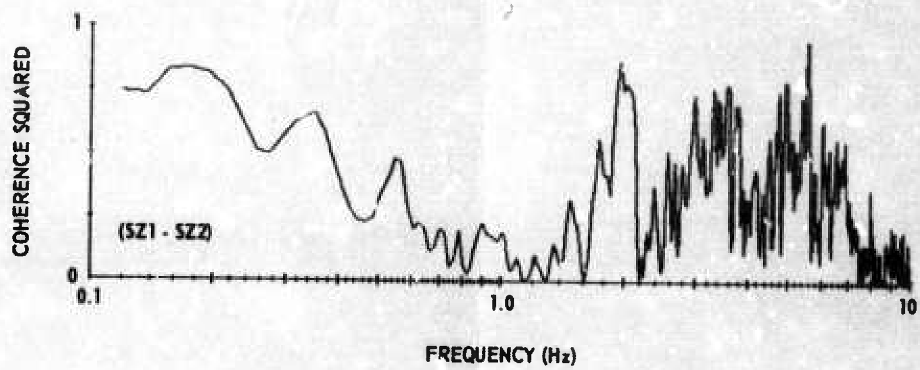

e. Coherence between the two vertical strain recordings of microseisms

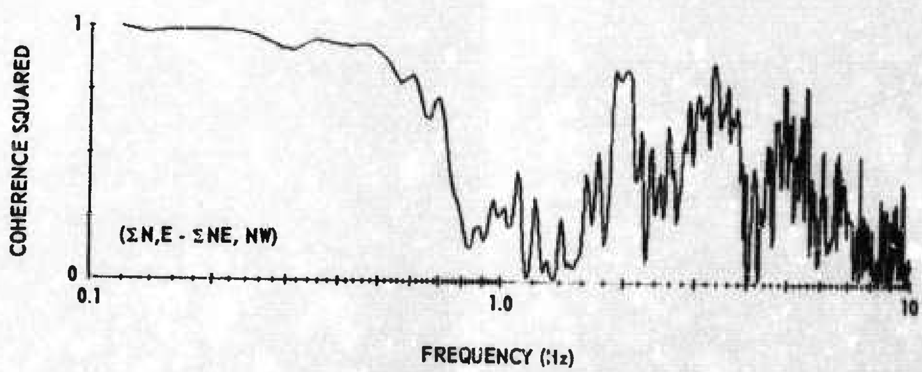

f. Coherence between the summation of the N and E strain and summation of the NE and NW strain recordings of microseisms

Figure 23. Coherence between vertical (SZ1 and SZ2) and crossed strains (ΣN, E and ΣNE, NW) showing that the vertical strain in the plastic-cased borehole compares most favorably with the sum of the north and east strains whereas the vertical strain in the steel-cased borehole compares most favorably with the sum of the northeast and northwest strains

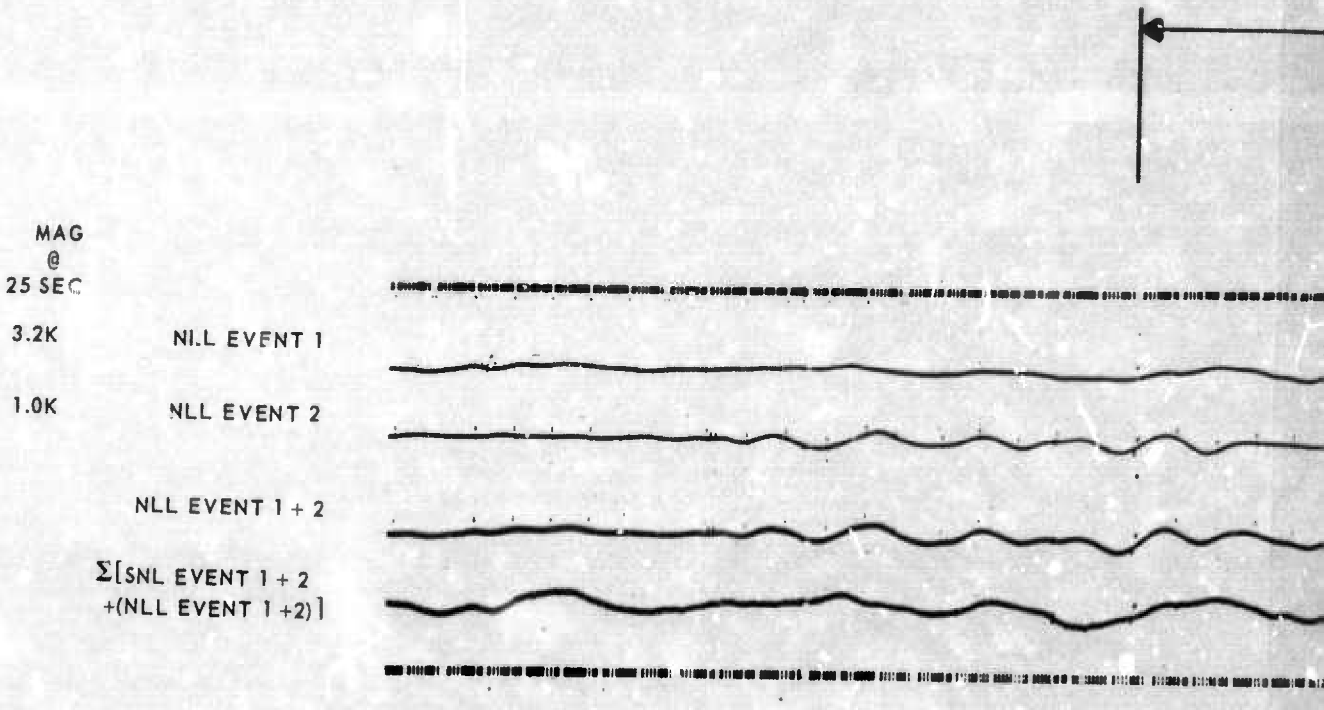

SNL - STRAIN, LONG-PERIOD NORTH

NLL - INERTIAL, LONG-PERIOD NORTH

WMSO
MAG TAPE NO. 1

EVENT 1

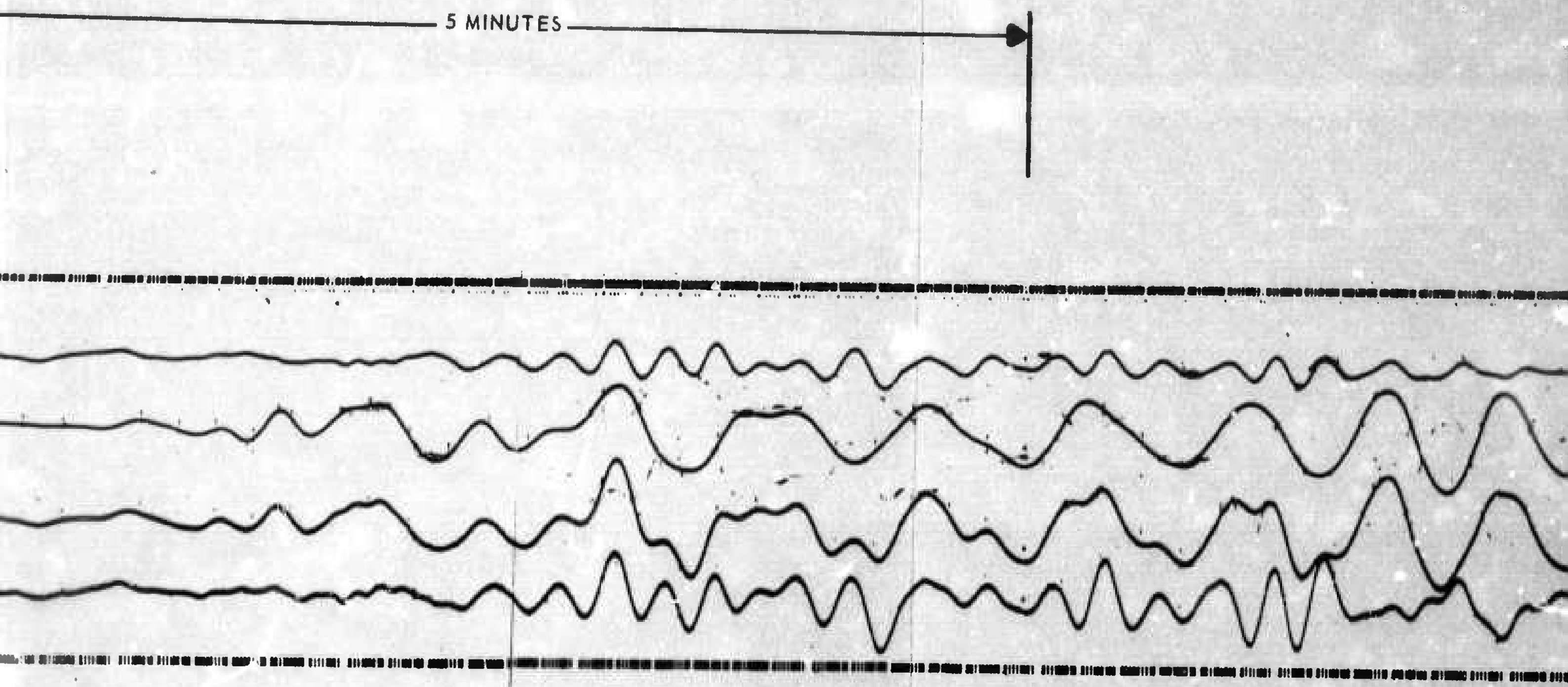

DATE: 23 JUNE 1967
ORIGIN TIME: 11:54:52.7Z
CENTRAL ALASKA
64.7 N, 148.7° W
AZ = 333°
Δ = 42°
MAG 4.6
h ≅ 30 KM

EVENT 2 - DATE: 21 JUNE 1967
ORIGIN TIME: 06:49:56.6Z
PERU-ECUADOR BORDER
2.2 S, 77.6 W
AZ = 153°
Δ = 42°
MAG 5.3
h = 49 KM

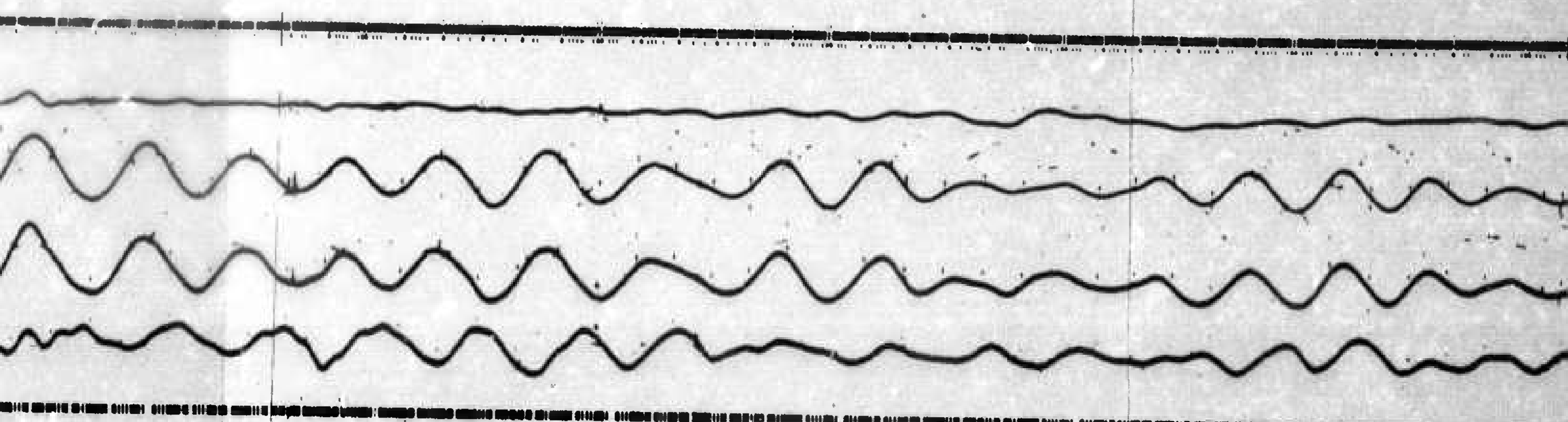

Figure 24. Superposition of magnetic rec
(Event No. 2) and an earthquake from Sou
the strain directional array
is suppressed

EVENT 2 - DATE: 21 JUNE 1967
ORIGIN TIME: 06:49:56.6Z
PERU-ECUADOR BORDER
2.2 S, 77.6 W
AZ = 153°
Δ = 42°
MAG 5.3
h = 49 KM

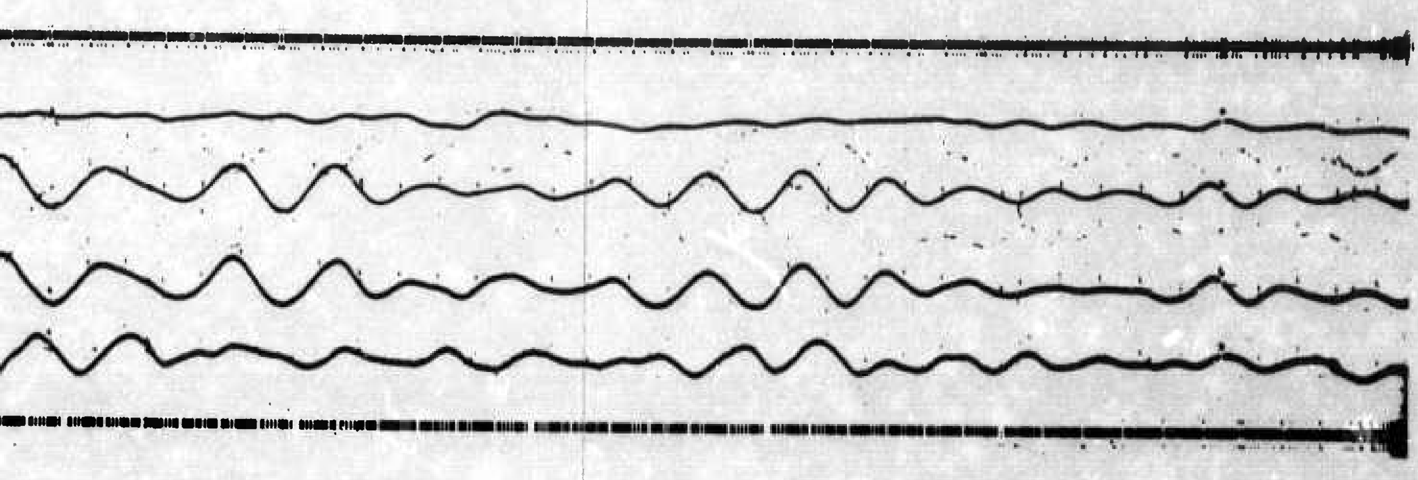

Figure 24. Superposition of magnetic recordings of an earthquake from Alaska (Event No. 1) and an earthquake from South America (Event No. 2) recorded on the strain directional array at WMSO. Event No. 1 is enhanced and Event No. 2 is suppressed

MAG
@
25 SEC

960K*	SNL	1
2.2K	NLL	2
	Σ	3

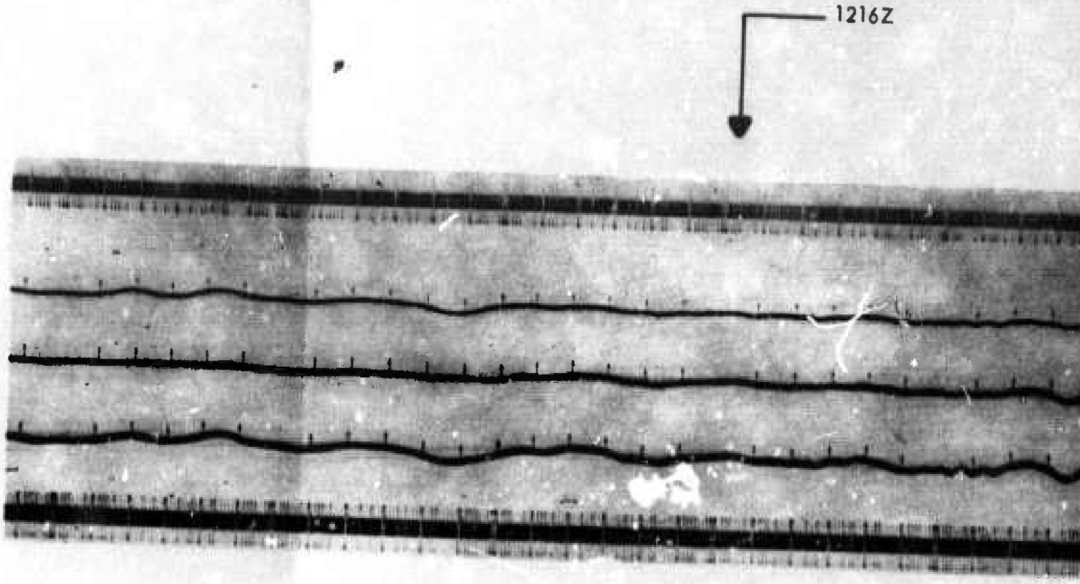

*EQUIVALENT INERTIAL MAGNIFICATION = 1.5K @ 25 SEC
(BASED ON A PHASE VELOCITY OF 3.0 KM/SEC AND A
19-METER STRAIN INTERVAL)

WMSO
MAG TAPE NO. 1
RUN NO. 174
23 JUNE 1967

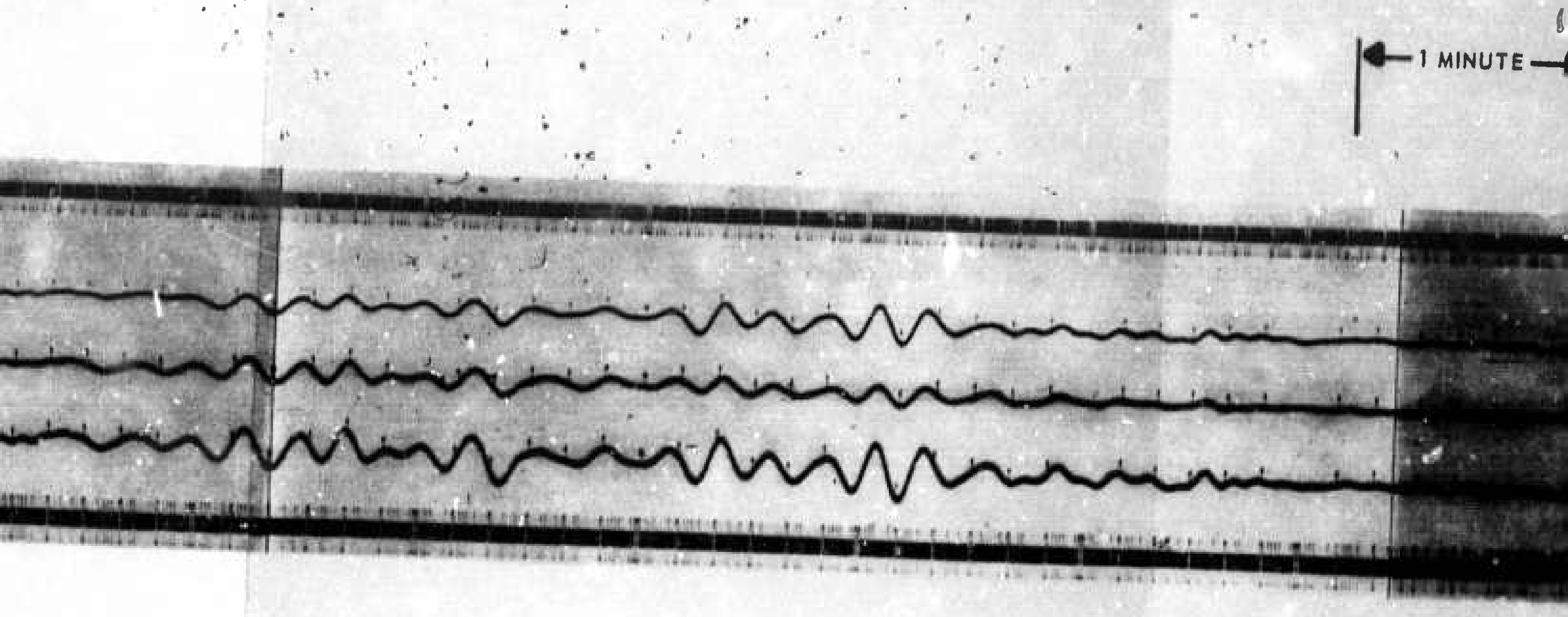
1 MINUTE

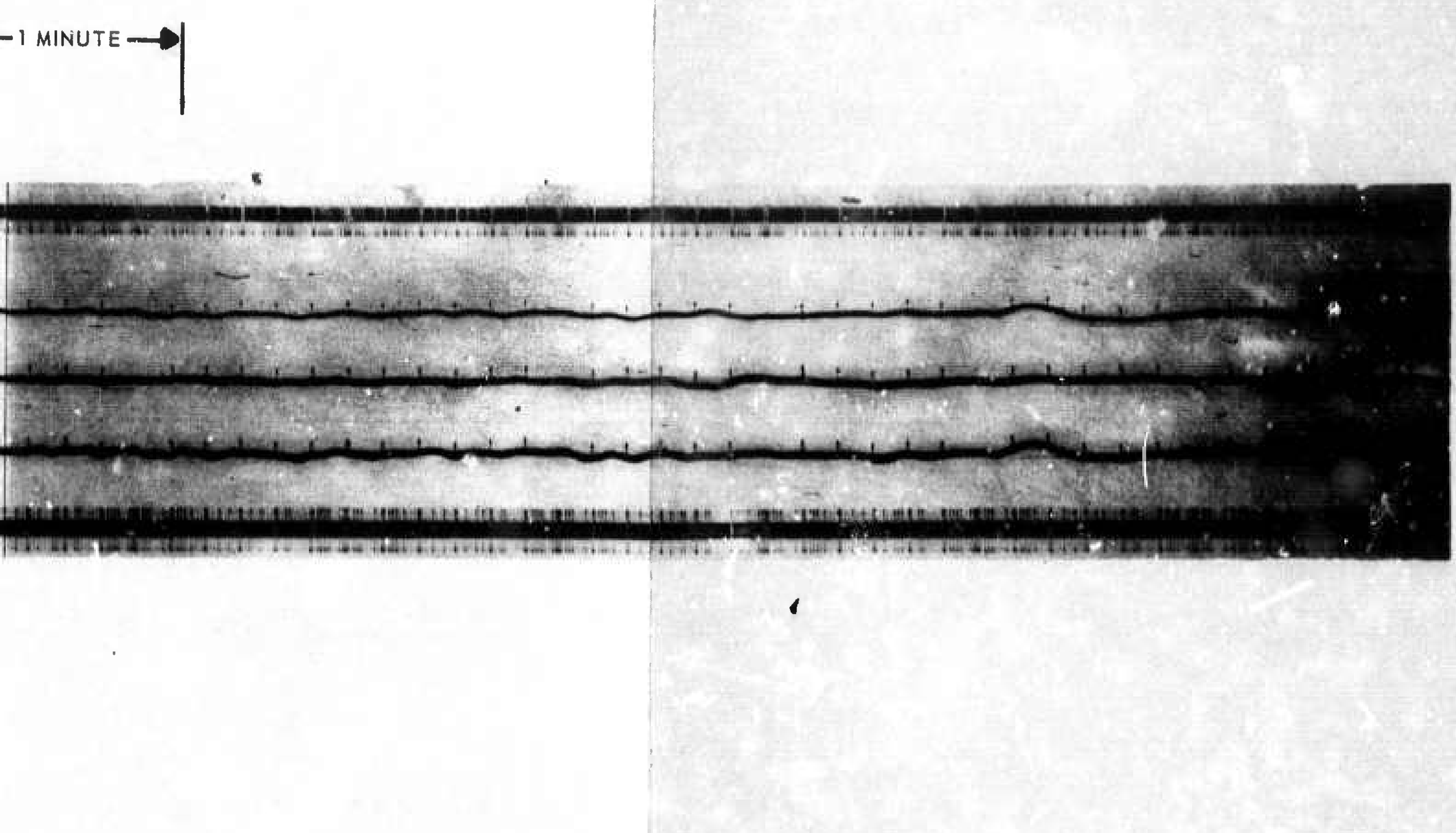

Figure 25. Tape playback of Event No. 1 (see figure 24) showing long-period north strain (SNL), long-period north inertial (NLL) and the sum of SNL and NLL

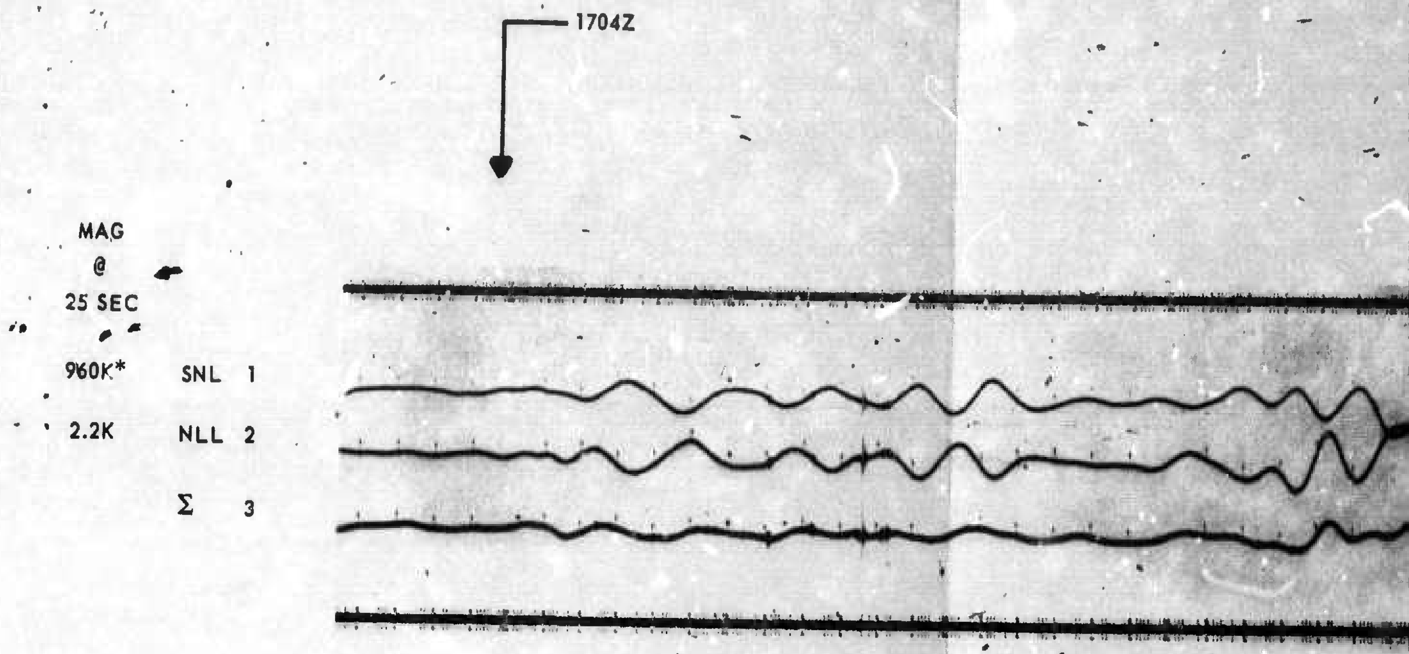

*EQUIVALENT INERTIAL MAG = 1.5K @ 25 SEC

WMSO
MAG TAPE NO. 1
RUN NO. 172
21 JUNE 1967

1

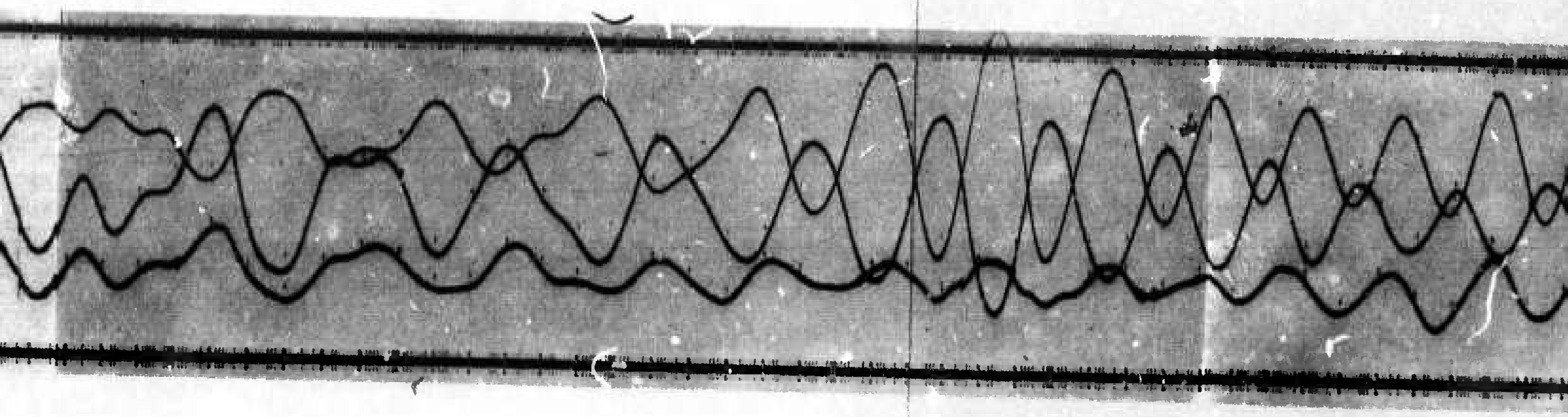

2

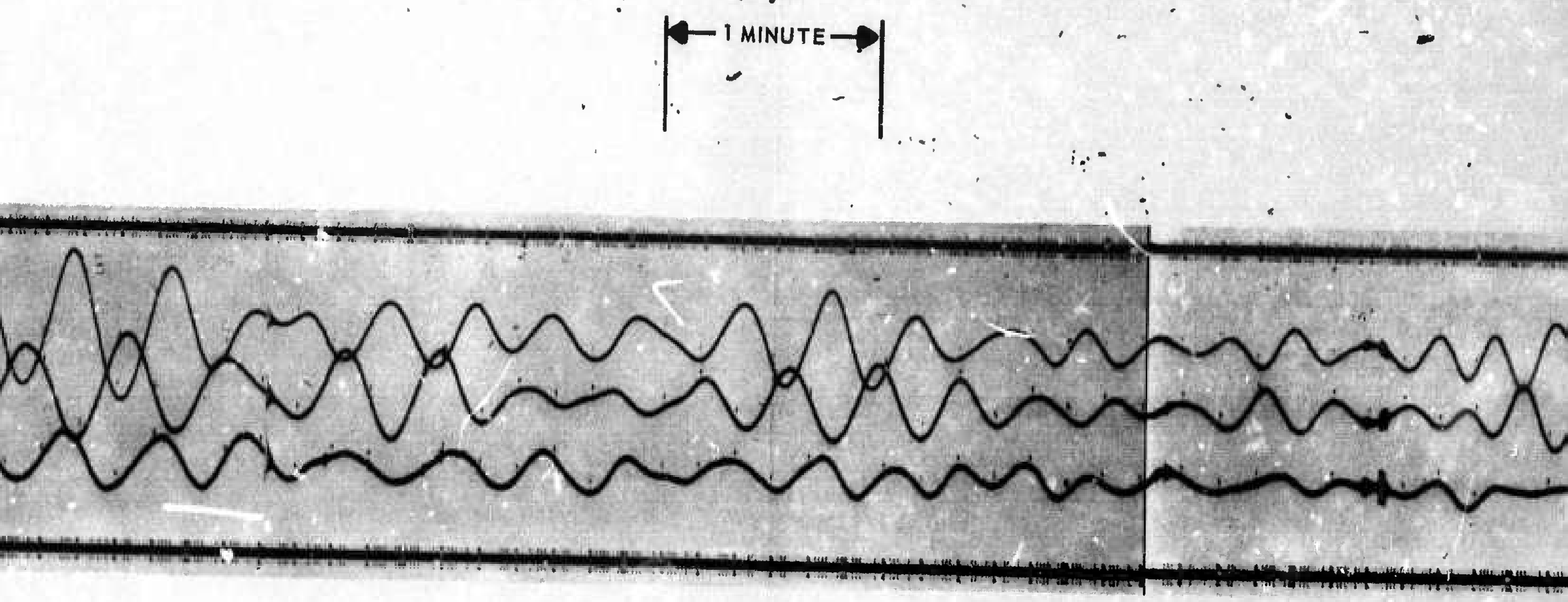

3

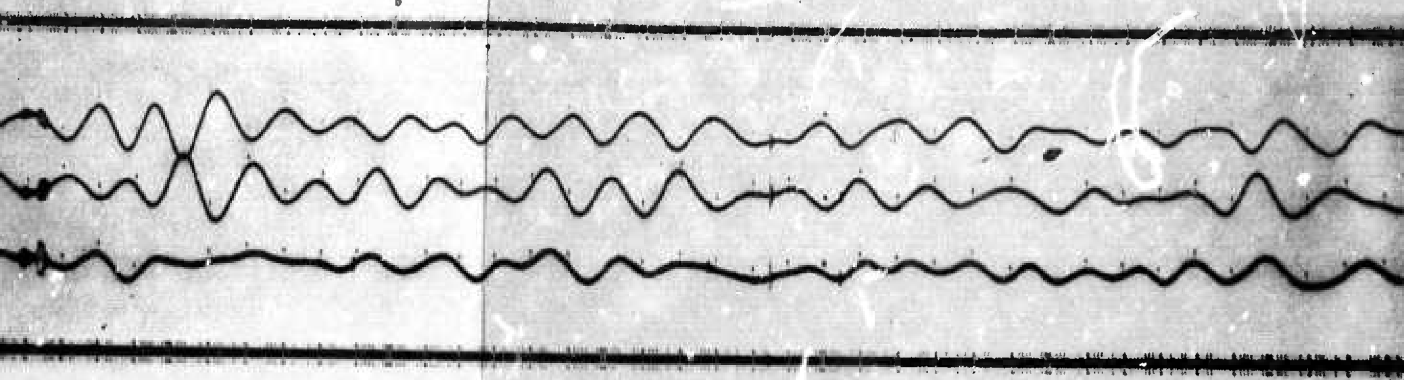

Figure 26. Tape playback of Event No. 2 (see figure 24) showing strain, inertial, and sum

4

A layered model for (WMSO) has been hypothesized and will be used in the theoretical study. This model was based upon a shallow velocity refraction survey, a sonic-velocity log in the 60 m (200 ft) deep shallow-buried array hole U6, published longitudinal and shear velocities for granite, a quarry blast study made jointly by Southern Methodist University and WMSO, a crustal study of Oklahoma made by the University of Tulsa, and WMSO, and Taggart's (1962) apparent P_n velocity distribution. The model is presented in detail in appendix 2.

5.4 SPECIAL RECORDING

5.4.1 Data for Multiple Coherence Studies

Magnetic tape and film records from 4 WMSO shallow-hole seismographs and 6 strain outputs covering Run Nos. 199 through 205 in July 1967 were forwarded to the Project Office for use in multicorrelation studies at Seismic Data Laboratories. Maximum bursts of microseisms were recorded at approximately 3 dB below the distortion point of the tape recorder to achieve a maximum signal-to-noise ratio.

Three additional Johnson-Matheson Seismometers, Model 4680, are available for operating in the strain vault if it is found that the space separation of the shallow-hole instruments causes excessive incoherence.

6. REFERENCES

Benioff, Hugo, 1935, A linear strain seismograph: Bull. Seism. Soc. Am. v. 25 (4), p. 283-309.

__________, 1962, The characteristics of strain and pendulum seismograph combinations: Proceedings of the Colloquium on Detection of Underground Nuclear Explosions, VESIAC Special Report 4410-36-X, Ann Arbor, Institute of Science and Technology, The University of Michigan, p. 442-455.

__________, and B. Gutenberg, 1952, The response of strain and pendulum seismographs to surface waves: Bull. Seism. Soc. Am., v. 42, p. 229-237.

Evernden, J.F., 1954, Direction of approach of Rayleigh waves and related problems, Bull. Seism. Soc. Am., 44, 159-184.

amplitudes that cannot be explained by velocity differences occur in several groups of Rayleigh waves. The hypothesis by Evernden (1954) suggesting the possibility of arrival of surface waves by other than great circle paths could explain the variation in strain-inertial amplitude ratio.

A study of these variations leading to a characterization of the pattern could be useful for establishing a program for automatic equalization of the ratios for maximum cancellation.

5.3 USE OF STRAIN AND PENDULUM SEISMOGRAPHS FOR WAVE IDENTIFICATION

Comparisons of strain seismographs to pendulum seismographs have been made by Benioff (1935), Benioff and Gutenberg (1952), Benioff (1962), Romney (1964), Major, Sutton, Oliver and Metsger (1964), Mikumo and Aki (1964), Gupta (1966, a, b), Shopland (1966), and Huang (1967). All of these investigators have used either the basic theory from Benioff's original paper in 1935 and/or have dealt with an isotropic elastic half-space. All have considered strain for wave lengths that are long compared to the length of the strain rod. Gupta and Huang considered body waves at various angles of incidence at the surface of a half-space and calculated the strain response as a function of the angle of incidence. Gupta (1966b) also determined that the effect of a finite depth and a finite length of the vertical strain instrument had a significant effect on the response to P and SV waves. Girard, Kirklin, Sherwin, and Shopland (1967) also extended Huang's results to plot horizontal and vertical differential displacement for SV waves as a function of the angle of incidence. Benioff and Gutenberg and Mikumo and Aki demonstrated that the response of a strain sesimograph compared with that of a pendulum seismograph from different earthquake phases can provide valuable phase identification criteria not available with either type of seismograph by itself.

A combined theoretical and empirical study starting with the above references is being undertaken to devise techniques for the use of strain and pendulum seismographs for wave identification. The empirical study will be made initially, using earthquakes producing clearly defined phases on the seismograms. The response of individual and combined strain instruments to the basic wave types will be determined and compared with that of the pendulum instruments and to the theoretically predicted response. In the theoretical study differential displacements will be predicted from a layered model primarily using the Thompson-Haskell matrix formulation and existing computer programs. It is believed that use of the calculated response of the layered model will assist in interpreting relationships between the vertical strain and the vertical pendulum, and provide information for establishing wave identification techniques.

A layered model for (WMSO) has been hypothesized and will be used in the theoretical study. This model was based upon a shallow velocity refraction survey, a sonic-velocity log in the 60 m (200 ft) deep shallow-buried array hole U6, published longitudinal and shear velocities for granite, a quarry blast study made jointly by Southern Methodist University and WMSO, a crustal study of Oklahoma made by the University of Tulsa, and WMSO, and Taggart's (1962) apparent P_n velocity distribution. The model is presented in detail in appendix 2.

5.4 SPECIAL RECORDING

5.4.1 Data for Multiple Coherence Studies

Magnetic tape and film records from 4 WMSO shallow-hole seismographs and 6 strain outputs covering Run Nos. 199 through 205 in July 1967 were forwarded to the Project Office for use in multicorrelation studies at Seismic Data Laboratories. Maximum bursts of microseisms were recorded at approximately 3 dB below the distortion point of the tape recorder to achieve a maximum signal-to-noise ratio.

Three additional Johnson-Matheson Seismometers, Model 4680, are available for operating in the strain vault if it is found that the space separation of the shallow-hole instruments causes excessive incoherence.

6. REFERENCES

Benioff, Hugo, 1935, A linear strain seismograph: Bull. Seism. Soc. Am. v. 25 (4), p. 283-309.

__________, 1962, The characteristics of strain and pendulum seismograph combinations: Proceedings of the Colloquium on Detection of Underground Nuclear Explosions, VESIAC Special Report 4410-36-X, Ann Arbor, Institute of Science and Technology, The University of Michigan, p. 442-455.

__________, and B. Gutenberg, 1952, The response of strain and pendulum seismographs to surface waves: Bull. Seism. Soc. Am., v. 42, p. 229-237.

Evernden, J.F., 1954, Direction of approach of Rayleigh waves and related problems, Bull. Seism. Soc. Am., 44, 159-184.

Girard, B.W., R.H. Kirklin, J.R. Sherwin, and R.C. Shopland, 1967, Multicomponent strain seismograph, quarterly report No. 6, Project VT/5081, 1 October to 31 December 1966: Geotech, A Teledyne Company, Technical Report No. 67-2, p. 22.

Gupta, Indra N., 1966a, Body wave radiation patterns from force applied within a half space: Bull. Seism. Soc. Am., v. 56 (1), p. 173-183.

__________, 1966b, Response of a vertical strain seismometer to body waves: Bull. Seism. Soc. Am., v. 56 (4), p. 785-791.

Herrin, Eugene and James Taggart, 1962, Regional variations in P_n velocity and their effect on the location of epicenters: Bull. Seism. Soc. Am., v. 52, p. 1037-1046.

Huang, Y.T., 1967, Effect of an elastically restrained boundary on SV-wave radiation patterns: Teledyne Industries, Geotech Division, Technical Report No. 66-111, p. 40.

Major, Maurice W., George H. Sutton, Jack Oliver, and Robert Metsger, 1964, On elastic strain of the earth in the period range 5 seconds to 100 hours: Bull. Seism. Soc. Am., v. 54 (1), p. 295-346.

Mikumo, Takeski and Keiiti Aki, 1964, Determination of local phase velocity by intercomparison of seismograms from strain and pendulum instruments: J. Geophys. Res., v. 69 (4), p. 721-731.

Romney, Carl, 1964, Combinations of strain and pendulum seismographs for increasing the detectability of P: Bull. Seism. Soc. Am., v. 54 (6), p. 2165-2174.

Shopland, Robert C., 1966, Shallow strain seismograph installation at the Wichita Mountains Seismological Observatory: Bull. Seism. Soc. Am., v. 56, p. 337-360.

APPENDIX 1 to TECHNICAL REPORT NO. 67-59

STATEMENT OF WORK TO BE DONE
AFTAC PROJECT AUTHORIZATION NO. VELA T/5081

EXHIBIT "A"

STATEMENT OF WORK TO BE DONE

AFTAC Project Authorization No. VELA T/5081

1. Instrumentation Development

a. Complete the development of the variable-capacitance transducer to extend the strain seismograph response to longer periods.

b. Complete the modification and testing of the seismometer transducers, amplifiers, filters, and associated circuitry to insure a consistent phase relationship between pendulum and strain seismographs.

c. Designand install secular strain monitors to improve the horizontal strain seismograph operation.

d. Improve the stability of the seismograph circuitry by installing a separate phototube amplifier shelter.

e. Install a variable-capacitance transducer on vertical strain seismometer No. 2 and on the NE horizontal strain seismometer in order to measure the amplitude and phase of the motion actually imparted to the fixed ends of the strain rods during electrical calibration.

2. Seismograph Development

a. Vertical Strain Seismograph

(1) Complete this design of the vertical strain seismograph by improving the anchor design, reshaping the instrument sections, and improving the mechanical reliability relative to installation, position locking, and removal.

(2) Improve the operation of the vertical strain seismograph by incorporating the developments listed in paragraphs 1a, 1b, and 2a(1).

b. Horizontal Strain Seismographs

(1) Improve the design of the horizontal strain seismographs by the addition of secular strain controls and seismograph housing modifications.

(2) Improve the operation of the horizontal strain seismographs by incorporating the developments listed in paragraphs 1a, 1b, 1c, 1d, and 2b(1).

3. Evaluation

a. Vertical Strain Seismograph. Test and evaluate the operation of the improved vertical strain seismograph in a new uncased borehole to be located adjacent to the present cased borehole. The uncased borehole is to be oil-filled and may contain the following features:

(1) Steel casing sections may be used for instrument anchor locations if the sections are decoupled from each other so that longitudinal casing rigidity is less than that of the surrounding rock formation.

(2) A continuous plastic casing may be used to maintain wall smoothness and hole integrity provided that the plastic is more compliant than the surrounding rock formation.

(3) Combinations of (1) and (2) may be used. In all instances where instrument anchors must lock against a borehole liner, the liner must be rigidly bonded to the borehole wall.

To facilitate the positioning of the instrument in the borehole, a permanent anchor may be used in the cased and uncased holes. This fixed depth operation might help to avoid the anchor malfunctioning which has been experienced.

b. Horizontal Strain Seismographs. Test and evaluate the operation of the improved horizontal strain seismographs in their improved housing.

c. Study the effect of the depth of the vertical strain seismometer on the coherence between outputs of the vertical strain seismograph and a pair of horizontal strain seismographs.

4. Applications

a. Record seismic data at Wichita Mountains Seismological Observatory on magnetic tape and 16 mm film; process magnetic tape data at the Geotechnical Corporation's central data processing facility and elsewhere as required; and determine spectra, phase, and coherency among the vertical strain, horizontal strain, and several pendulum seismometer control signals.

b. Experimentally corroborate the vertical strain seismograph performance relative to the 2 crossed-horizontal strain seismographs to verify that true earth strains are faithfully recorded by the vertical strain instrument.

c. Develop a thorough understanding and evaluation of the phase and amplitude performance of the strain seismographs and related pendulum systems.

d. Determine the usefulness of strain seismographs when used singularly and in combination with inertial instruments for wave identification, signal enhancement, detection of long-period signals, and rejection of noise arriving from selected azimuths. Determine the usefulness of strain seismographs in distinguishing between earthquakes and explosions. Schedule the program so as to provide preliminary results on the P-wave enhancement portion of the program not later than 30 Sept 65.

e. Investigate the extent of actual noise suppression and signal enhancement possible through various combinations of the strain and pendulum seismographs at WMSO and compare the results with signal-to-noise improvements predicted by theory.

(1) Collect data from the strain-seismograph system at WMSO and the companion pendulum seismographs.

(2) Analyze the collected data to determine the similarities and differences in character and composition of signals and noise measured by the strain and pendulum instruments.

(3) Ascertain theoretically and demonstrate experimentally the improvement in P-wave detection, enhancement, and identification possible using strain and pendulum seismographs in various combinations.

(4) Analyze a limited number of strain data from at least one other location for comparison with WMSO data.

f. Establish and provide the operation and analysis procedures necessary to operate comparable multicomponent strain seismograph facilities at other locations.

*5. Drawings

Provide drawings and specifications on items specified in paragraphs 2a(1), 2a(2), 2b(1), 2b(2), and the uncased borehole as outlined in paragraph 3 according to Data Items E-23-11.0, E-2-11.0, E-4-11.0, E-5-11.0, E-7-11.0, and T-13-28.0 contained in AFSCM 310-1. These drawings shall conform to the instructions contained in Attachment 2. Wherever Data Items conflict with Attachment 2, the latter will take precedence. Reproduction shall be accomplished in accordance with Data Item E-4-11.0, paragraphs 1b, 1f, 7, 9, 10, 11 and 12c(3), microfilm on aperture cards and non-reproducible paper copies. Index card keypunch format may vary from specifications as approved by AFTAC through the Project Officer. Aperture cards should be furnished in 2 copies, 1 positive and 1 negative.

6. Reports

Provide monthly, quarterly, final, milestone, and special progress reports in accordance with Data Item S-17-12.0, first sentence of paragraph 1. Wherever the Data Item conflicts with Attachment 1, the latter will take precedence. All reports under this project will be forwarded to HQ USAF (AFTAC/VELA Seismological Center), Wash., D.C. 20333.

---

*For the purposes of this contract, the provisions of paragraph 5 of this Exhibit "A" are hereby waived. In lieu thereof, the following provisions shall apply.

"5. Drawings. Drawings shall be furnished in accordance with the provisions of line item 7 of the DD Form 1423 and attachments thereto."

APPENDIX 2 to TECHNICAL REPORT NO. 67-59

SEISMIC VELOCITY MODEL FOR THE WICHITA MOUNTAINS SEISMOLOGICAL OBSERVATORY

NOTE: This appendix is a reproduction without modification of a memorandum submitted to the Project Office on 5 September 1967. It is here provided in support of statements made in Section 5.3 of the preceding text.

MEMORANDUM

22 August 1967

FROM: James E. Fix

SUBJECT: Seismic Velocity Model for the Wichita Mountains Seismological Observatory

---

1. INTRODUCTION

This memorandum reviews the published seismic velocities, the geology, the gravity, and the magnetic field of the Wichita Mountains of southwestern Oklahoma. A model is hypothesized for the longitudinal wave velocity (V_p) and the shear wave velocity (V_s) from the surface to below the Mohorovicic discontinuity (Moho). Because of numerous igneous intrusions, the model will not be exact for the entire area but it will estimate average values of the velocity structure in the Wichita Mountain horst. The model assumes that layering and major joints visible on the surface are limited to a 500 m depth. Sources for the data are cited and the assumptions made in arriving at the model are discussed. Section 2 presents the model and discusses the data from which it is derived. Section 3 briefly describes the regional geology, section 4 discusses possible additional refinement of the model, and section 5 lists precautions in using the model. References are given.

2. SEISMIC VELOCITY MODEL

2.1 The Model - Figures 1 and 2 present the seismic velocity model hypothesized. Table 1 lists the velocities corresponding to the curves. Table 1a lists a layered approximation to the velocity curves for use in computer programs that calculate dispersion curves and amplitude vs depth. (All figures and tables 1 and 1a are at the end of the memorandum.)

2.2 Data Contributing to the Model - The longitudinal seismic velocity (V_p) model is based upon a shallow velocity refraction survey at the Wichita Mountains Seismological Observatory (WMSO) with an 8 lb sledge hammer and a Dyna Metric Seismic Timer, a sonic-velocity log taken to the full 200 ft (60 m) depth of the shallow-buried array hole U 6 (at WMSO), published velocities for Woodbury granite, a sonic-velocity log made in an exploratory granite hole of 10,000 ft depth in Wyoming, a quarry blast study made jointly by SMU and Geotech about WMSO, a crustal study of Oklahoma made by the University of Tulsa, and Herrin and Taggart's apparent P_n velocity distribution. The shear velocity (V_s) model is based upon the theoretical relationship to V_p and published values of shear velocities. In general all data agree and none of the data positively contradict the other sources. The major difference is between the quarry blast study which yielded two layers above the Moho and the crustal study of Oklahoma which yielded three layers. Details of the various studies are summarized below. In the following sections longitudinal velocity V_p will be intended wherever the word velocity is used without a modifier.

2.2.1 Shallow Refraction Survey - The shallow refraction survey is reported by Kim and Tiroff (1964). An 8 lb sledge hammer provided an input to a Seismic Timer, Dyna Metric Model 117. Data were taken in the vicinity of nine seismometer vaults at WMSO. Results of the survey show a thin low velocity layer underlain by a higher velocity layer. Values varied from vault to vault. The average values and range of values are given in table 2. Figure 2 of part 4, TR 64-1 (Kim and Tiroff) summarizing the results is attached.

Table 2. Apparent surface velocities (V_p) at WMSO

	Average of 9 values	High	Low
Thickness of top layer	1.5 m (4.9 ft)	9.3 ft	2.1 ft
Apparent V_p first layer	472 m/sec	677 m/sec	290 m/sec
Apparent V_p second layer	2.96 km/sec	4.57 km/sec	1.71 km/sec

The average values for the surface layer are included in the model. The velocity of the second layer is quite variable and is low for that expected for granite. It is suspected that this low velocity is the result of weathering and severe jointing and layering in the area as discussed in section 2.2.4. The velocity of the second layer in the model is taken as the average of values determined during the shallow refraction survey. As shown in the survey, the results vary considerably from one vault to another; therefore, the model will only be an approximation to true conditions. The thickness of the second layer in the model is taken as 3 m (10 ft). This thickness was taken because (1) the sonic-velocity log described in section 2.2.2 shows a higher velocity below a depth of 15 ft and (2) the shallow refraction survey data do not have sufficient resolution to rule out the higher velocity at this depth. If the model is correct in the thickness of the top two layers and in their velocities along with the velocity under the second layer, the refraction survey would indicate the third layer at a traverse distance of about 45 ft. Most of the traverses were 70 ft which includes this distance. However, the 1 millisecond resolution of seismic timer could introduce errors that would not clearly show a third velocity with only the two or three data points available beyond 45 ft.

2.2.2 Velocity Log of WMSO Hole U 6 - Brown (1966) presents a sonic-velocity log from one of thirteen holes drilled to a depth of 200 ft for a shallow-buried array at WMSO. Figure 3 from his report (TR 66-95) showing this log is attached. The log shows at least seven low velocity "spikes" that are probably due to joints and layers in the rock. A bulk density log was also obtained. The density determined by the log is 2.60 ±0.05 g/cm^2 which is lower than the 2.62-2.69 range for granites summarized by Press in Clark (1966). The low density indicates the possibility of some porosity. The layering indicated by the low velocity "spikes," the visible major joints observed on the surface, and the low density all lead to the assumption that a low velocity should be observed for the granite composition rock below the weathered layer throughout the Wichita province. Velocity for depths between 4.5 m (15 ft) and 61 m (200 ft) for the model is taken from this log as 56.5×10^{-6} sec/ft = 17,700 ft/sec = 5.39 km/sec. The log also indicates a low velocity layer from a depth of 12.5 m (41 ft) to a depth of 15 m (50 ft) that is not included in the model. The average velocity of this layer is estimated at 85×10^{-6} sec/ft = 11,770 ft/sec = 3.59 km/sec. This low velocity layer is not included in the model because it could be caused by severe jointing localized near this specific hole.

2.2.3 Velocity Log of Perdasofpy No. 1 - Data are available from a sonic-velocity log of the Perdasofpy No. 1 well about 15 miles from WMSO and northeast of the major fault separating the Wichita igneous province from the adjacent sedmimentary basin (see section 3 on regional geology). It is felt that these data do not apply to the WMSO model and they have not been included in the model. Igneous rocks at depth are overlain by limestones at Perdasofpy but the densities of the limestones are somewhat comparable to "granites" and the pressures at depth should be reasonably close to those from a continuous column of granite. Therefore, the observed velocities could be typical of what might be expected if the granites and rhyolites in the WMSO area were as layered with alternating instrusions, extrusions, and tuff extrusions as illustrated by Ham from the Stanolind cores from the Perdasofpy well. Based on the regional geology, Ham (1963) and Ham et al (1964) interpret the immediate vicinity of WMSO as having a surface layer of undetermined thickness of the Wichita granites and Carlton rhyolites underlain by the Raggedy Mountain gabbro. Consequently, the actual structure is probably more competent near WMSO than at Perdasofpy; thus the Perdasofpy velocities have not been used in the model. Figure 5 from Geotech report TR 64-33 with the sonic-velocities is attached for reference.

2.2.4 Published Seismic Velocities for Granite - Press in Clark (1966) summarizes V_p and V_s for many rock types. The measurements listed are primarily from Birch (1960, 1961) and Simmons (1964 a, 1964 b). Most of Birch's measurements were actually made by Herrin and Simmons.

The Wichita granite is in reality a granodiorite and the Carlton rhyolite is the extrusive counterpart with the same chemical composition. Thus both should exhibit about the same velocity characteristics. Simmons (1967) has collected rock samples from the Wichita province and at some future date is going to measure the velocities at several pressures. He expects that at low pressures the rhyolite will have higher velocities than the granite because of a finer grain structure. At higher pressures, he expects both to have the same velocities.

Birch and Simmons' granite from Rockport, Massachusetts, when modified for temperature effects would match Herrin and Richmond's (1960) granite model taken from Hughes and Maurette's (1957) Woodbury granite. These velocities are lower than many "granites" but fit the observed data fairly well. A lower velocity granite is substantiated by the average value of 5.6 km/sec for the upper layer measured in the quarry blast study and the average value of 5.96 km/sec for the upper layer measured in the crustal study.

Herrin and Richmond's granite model for both V_p and V_s in table 3 is adopted as the asymptote for the WMSO model. The WMSO velocity model approaches Herrin and Richmond's model at a 0.5 km depth.

Values for V_s for the two thin surface layers and the 200 ft depth are all calculated from V_p using Hughes and Maurette's value of 0.263 for Poisson's ratio at a 2 km depth. Because of other greater uncertainties, 0.263 was used as a constant at all depths.

Table 3. Herrin and Richmond " Hughes Model" Woodbury Granite

Depth	P velocity km/sec	S velocity km/sec
0	5.59	3.19
1	5.90	3.34
2	6.05	3.43
3	6.11	3.48
4	6.14	3.52
5	6.15	3.54
6	6.15	3.56
7	6.15	3.57
8	6.15	3.59
9	6.16	3.60
10	6.16	3.60
11	6.16	3.61
12	6.16	3.62

2.2.5 Velocity Log for Cased Exploratory Hole "A" - An exploratory hole was drilled to 10,000 ft depth in granite in the Wind River Uplift in west central Wyoming. The geology is entirely different from the Wichita province in that the entire section of the Wind River Uplift was essentially the result of a single episode and is generally free from the layering of the Wichita province which has been subjected to many episodes of extrusion of rhyolite and intrusion of granite laid over the underlying gabbro. The sonic-velocity log of the Wyoming hole (figure 2 TR 65-76 attached) corresponds very well with Herrin and Richmond's model with a velocity below the weathered zone of about 5.5 km/sec and a velocity at a depth of 3 km of about 6.1 km/sec. The low velocity layers are probably caused by high temperature in regions of higher radioactivity content found in the hole.

2.2.6 Quarry Blast Study - A study of the crustal structure in the vicinity of WMSO was made in 1964 jointly by SMU and Geotech using primarily nonreversed profiles from two major quarries. Results of the study (Geotech TR 64-118, 1964) indicate an upper layer 19.7 km thick with an average velocity of V_p = 5.6 km/sec and a lower layer, still above the Moho, of undetermined thickness with an average velocity V_p = 7.3 km/sec. The single velocity of 5.6 km/sec is taken to be the result of an average velocity derived from fitting a straight line to the data rather than a curved line that is indicated by the variation of velocity with depth as pressure and temperature increase. Thus, it is believed not to contradict the granite model.

The WMSO model uses the 19.7 km depth to the bottom of the granite and the 7.3 km/sec velocity of the lower layer. At this depth the pressure is about 5 kbar. The 7.3 km/sec is a high velocity for a gabbro composition so the underlying layer is probably more basic than gabbro and is probably an olivine rich gabbro. A velocity ratio from Birch and Simmons for a dunite from Webster, North Carolina, has been used to calculate V_s = 4.13 km/sec for the model.

2.2.7 Crustal Study of Oklahoma - In 1964 the University of Tulsa (Qualls 1965) in cooperation with the University of Wisconsin, Jersey Production Research Company and Seismograph Service Corporation made a reversed profile refraction study of the crustal structure of Oklahoma from a point southwest of WMSO to a point northeast of Tulsa. Qualls' MS Thesis (1965) describes the work in detail, and Tryggvason and Qualls (1967) summarized the results in the most recent JGR as follows:

a. 0-0.54 km depth sediments V_p = 4.0 km/sec;

b. 0.54 - 13.7 km depth V_p = 5.96 ±0.01 km/sec;

c. 13.7 - 29.6 km depth V_p = 6.66 ±0.01 km/sec;

d. 29.6 - 50.9 km depth $V_p = 7.20 \pm 0.02$ km/sec:

e. 50.9 km depth Moho $V_p = 8.32 \pm 0.02$ km/sec;

f. All layers essentially horizontal.

The crustal study included a major portion of the State of Oklahoma, whereas, the quarry blast study described above remained closer to WMSO. Because the quarry blast study revealed only two layers above the Moho, and because two layers are hypothesized from the regional geology, only a two layer model is considered in the WMSO model. Qualls upper layer velocity of 5.96 km/sec is not significantly different from the quarry blast study upper layer velocity of 5.6 km/sec. It also would fit the low granitic velocities well. Qualls lower layer velocity of 7.20 km/sec is close to the quarry blast study lower layer velocity of 7.3 km/sec. In the WMSO model, Qualls average depth to the Moho of 50.9 km is adopted although it might be another 1.2 km deeper in the WMSO vicinity. The model adopts Qualls value for $V_p = 8.32$ km/sec below the Moho.

The Moho velocity is higher than normal but is in excellent agreement with Herrin and Taggart (1962). The quarry blast study used data from WMSO and the Perdasofpy site (APOK), and estimated a Moho velocity of 8.4 km/sec for a Gulf of California earthquake and a velocity of 8.5 km/sec for an accidental explosion in San Antonio, Texas.

Both models adopt $V_s = 4.63$ km/sec below the Moho. This velocity was calculated from V_p using Poisson's ratio calculated from Bullen's velocities in the mantle (Bullen, 1963).

3. REGIONAL GEOLOGY

The regional geology of the WMSO region is described in detail in Ham (1963) and Ham, Dension, and Merritt (1964). Geotech (1964, TR 64-103 Rev) and Phelan (1965) report on a gravity and magnetic survey of the Wichita Mountains on a regional basis and of WMSO on a detailed basis. Figure 9 of TR 64-103 (attached) shows Ham's interpretation of the geology. Figure VI from Qualls (1965) gives a larger scale cross section.

Surface outcrops and well control indicate two major periods both with repeated igneous activity. There are five major basement rock groups in the Wichita Province. The oldest is the Tillman Metasedimentary Group which is at least 15,000 ft thick but is not thought to underlie WMSO. The intermediate age rocks which probably underlay WMSO are the Navajoe Mountain Basalt - Spilite Group and its intrusive equivalent, the Raggedy Mountain gabbro. The Navajoe Mountain Group consists of basalt, spilite, andesite, and tuff. The total thickness is probably several thousand feet. The Raggedy Mountain gabbro consists of diallage and olivine gabbro, anorthosite, and diorite. It is a layered intrusion in excess of 10,000 ft thick and was injected as an elongate lens into the Tillman metasediments. One of the youngest rocks of the Wichita Province is the extrusive Carlton rhyolite which flowed onto a land surface and represents an extensive volcanic field at least 4500 ft thick. The other young rock is the Wichita granite which was emplaced as sills intruding the lower part of the Carlton rhyolite and in part occuring as irregular plutons and sills cutting all other rocks of the Wichita province.

As indicated in figure 9 of TR 64-103 and figure VI of Qualls, the Wichita Mountains are a horst raised above sedimentary basins on both sides by repeated faults. The major faults at the contact with the igneous uplift are about 36 miles (57.9 km) apart.

The regional gravity data substantiate the geologic evidence for a higher density material underlying the rhyolite and granite. Phelan in his Thesis (1965) and the Geotech report (TR 64-103) has approximated the observed residual gravity anomaly by a gabbro body approximately 36 miles (57.9 km) wide, less than 2.1 miles (3.4 km) beneath the surface, less than 4.8 miles (7.7 km) thick, with two roots extending downward 6 to 8 miles (9-1/2 to 13 km). As in all gravity work, this solution is not unique, but it provides a close match between observed and theoretical gravity. The depths and thicknesses hypothesized by Phelan do not agree with the seismic velocity model.

4. POSSIBLE ADDITIONAL REFINEMENT

The model presented here is based on the expected geologic structure and some longitudinal wave velocity measurements. Additional refinements can be made by detailed analysis of wave transmissions in the WMSO vicinity by comparison of theoretical and observed velocities. To date a study of this type has not been made.

5. PRECAUTIONS IN USE OF MODEL

The hypothesized model should be representative of the seismic velocities in the WMSO area. However, it should be remembered that the Wichita Mountains are an igneous horst about 36 miles (57.9 km wide) lying between two sedimentary basins. Surface waves or apparent surface waves with wave lengths short compared to this width will be controlled by the velocity profile of the Wichita province. Surface waves with longer wave lengths will be affected some by the velocity structure of the sedimentary basins, and as wave length increases, to an increasing extent by the deeper structure. Qualls' model given in 2.2.7 is suitable for the sedimentary basins. Since Qualls' model contains high velocities for sedimentary basins, his velocities are close to those of the WMSO igneous model; therefore, extreme changes in wave character are probably not to be expected. However, Herrin and Taggart (1965) have experienced about a 17 degree shift in apparent azimuth of approach at WMSO for signals from the Nevada Test Site. Consequently, some major refractions are taking place for short epicentral distances, probably at the major faults at the limits of the horst.

6. REFERENCES

Birch, Francis, 1960, The velocity of compressional waves in rocks to 10 kilobars, part 1: Jour. of Geop. Res., 65 (4), p. 1083-1102

Birch, Francis, 1961, The velocity of compressional waves in rocks to 10 kilobars, part 2: Jour. of Geop. Res., 66 (7), p. 2199-2224

Brown, T. G., 1966, Technical Report No. 66-95, Cased hole installation for shallow-buried array at WMSO: Garland, Texas, Teledyne Industries, Geotech Division, 9 p.

Bullen, K. E., 1963, An introduction to the theory of seismology: Cambridge, Cambridge Univ. Press, p. 223

Clark, Jr., Sydney P., Ed., 1966, Frank Press, Seismic velocities, section 9 in Handbook of Physical Constants, Rev. Ed., Memoir 97: New York, The Geological Society of America, Inc., 587 p.

Geotechnical Corp., 1964, Technical Report No. 64-33, Deep well site report Perdasofpy No. 1 well, Comanche County, Oklahoma: Garland, Texas, 38 p.

________________, 1964, Technical Report No. 64-103 Rev, Gravity and magnetic survey of the area within and surrounding the Wichita Mountains Seismological Observatory array: Garland, Texas, 25 p.

________________, 1964, Technical Report No. 64-118, Final report of the operation of the Wichita Mountains Seismological Observatory, 1 March 1963 through 30 June 1964; and Semiannual Report No. 8, Project VT/036, 1 January through 30 June 1964: Garland, Texas, p. 90-100

Ham, W., 1963, Basement rocks and structural evolution of southern Oklahoma: Ardmore, Oklahoma, Ardmore Geological Society Field Conference Guidebook

Ham, W., Denison, R. E., and Merritt, C. A., 1964, Basement rocks and structural evaluation of southern Oklahoma: Oklahoma Geological Survey Bulletin 95, Norman, Oklahoma, University of Oklahoma

Herrin, Eugene, and Taggart, James, 1962, Regional variations in P_n velocity and their effect on the location of epicenters: Bul. Seis. Soc. Amer., 52, p. 1037-1046

Herrin, Eugene and Taggart, James, 1965, personal communication

Herrin, Eugene and Richmond, Jean, 1960, On the propagation of the Lg phase: Bul. Seis. Soc. Amer. 50 (2), p. 197-210

Hughes, Darrell S. and Maurette, Christian, 1957, Variation of elastic wave velocities in basic igneous rocks with pressure and temperature: Geophysics, 22 (1), p. 23-31

Kim, Won H. and Tiroff, Kenneth P., 1964, Part 4 to Technical Report No. 64-1, Shallow refraction study of seismometer installations in J. W. Guyton's Technical Report No. 64-1, Study of short-period seismic noise semi-annual technical summary report No. 3, 1 July 1963 to 31 December 1963: Carland, Texas, The Geotechnical Corp., 7 p.

Phelan, Michall Joseph, 1965, Gravity and magnetic survey of the Wichita Mountains, Oklahoma: St. Louis, Missouri, MA Thesis, Washington University, 47 p.

Qualls, Bob Ralph, 1965, Crustal study of Oklahoma: Tulsa, Oklahoma, MS Thesis, The University of Tulsa, 82 p.

Simmons, Gene, 1964 a, Velocity of compressional waves in various mineral at pressures to 10 kilobars: Jour. Geop. Res., 69 (6), p. 1117-1121

Simmons, Gene, 1964 b, Velocity of shear waves in rocks to 10 kilobars 1: Jour. Geop. Res., 69 (6), p. 1123-1130

Simmons, Gene, 1967, personal communication

Teledyne Industries, Geotech Division, 1965, Technical Report No. 65-76, Deep hole site report cased exploratory hole "A" (u) (confidential): Garland, Texas

Tryggvason, E. and Qualls, B. R., 1967, Seismic refraction measurements of crustal structure in Oklahoma: Jour. Geop. Res., 72 (14), p. 3738-3740

7. ATTACHMENTS

Table 1, this memorandum
Table 1a, this memorandum
Figure 1, this memorandum
Figure 2, this memorandum
TR 64-1, Part 4, figure 2
TR 66-95, figure 3
TR 64-33, figure 5
TR 65-76, figure 2
TR 64-103 Rev., figure 9
Qualls (1965) figure VI

Table Seismic velocity model for WMSO

Depth km	V_p km/sec	V_s km/sec
0-0.0015	0.472	0.268
0.0015-0.0045	2.96	1.68
0.0045-0.061	5.39	3.07
0.500	5.78	3.26
1	5.90	3.34
1.5	5.98	3.40
2	6.05	3.43
3	6.11	3.48
4	6.14	3.52
5	6.15	3.54
10	6.16	3.60
19.7-	6.16	3.62
19.7+	7.30	4.13
50.9-	7.30	4.13
50.9+	8.32	4.63

NOTE

The model is based upon Wichita granite and/or Carlton rhyolite to a depth of 19.7 km, then olivine gabbro of Raggedy Mountain group to the Moho at a depth of 50.9 km.

Table 1a. Layered approximation to seismic velocity model for WMSO for use with computer programs

Layer No.	Depth km	Thickness km	V_p km/sec	V_s km/sec	Density gm/cm^3
1	0-0.0015	0.0015	0.472	0.268	2.50
2	0.0015-0.0045	0.003	2.96	1.68	2.55
3a	0.0045-0.018288	0.013788	5.39	3.07	2.60
3b	0.018288-0.037597	0.019309[a]	5.39	3.07	2.60
3c	0.037597-0.061	0.0234	5.39	3.07	2.60
4	0.061-0.1	0.039	5.43	3.09	2.60
5	0.1-0.2	0.1	5.50	3.14	2.61
6	0.2-0.3	0.1	5.61	3.18	2.62
7	0.3-0.5	0.2	5.72	3.24	2.62
8	0.5-1.0	0.5	5.84	3.30	2.63
9	1.0-1.5	0.5	5.94	3.36	2.63
10	1.5-2.0	0.5	6.01	3.41	2.63
11	2.0-3.0	1.0	6.08	3.46	2.63
12	3.0-4.0	1.0	6.12	3.50	2.63
13	4.0-5.0	1.0	6.15	3.53	2.63
14	5.0-10.0	5.0	6.16	3.57	2.63
15	10.0-19.7	9.7	6.16	3.61	2.63
16	19.7-50.9	31.2	7.30	4.13	3.25
17	50.9-	-	8.32	4.63	3.32

[a] Length of vertical strain seismometer

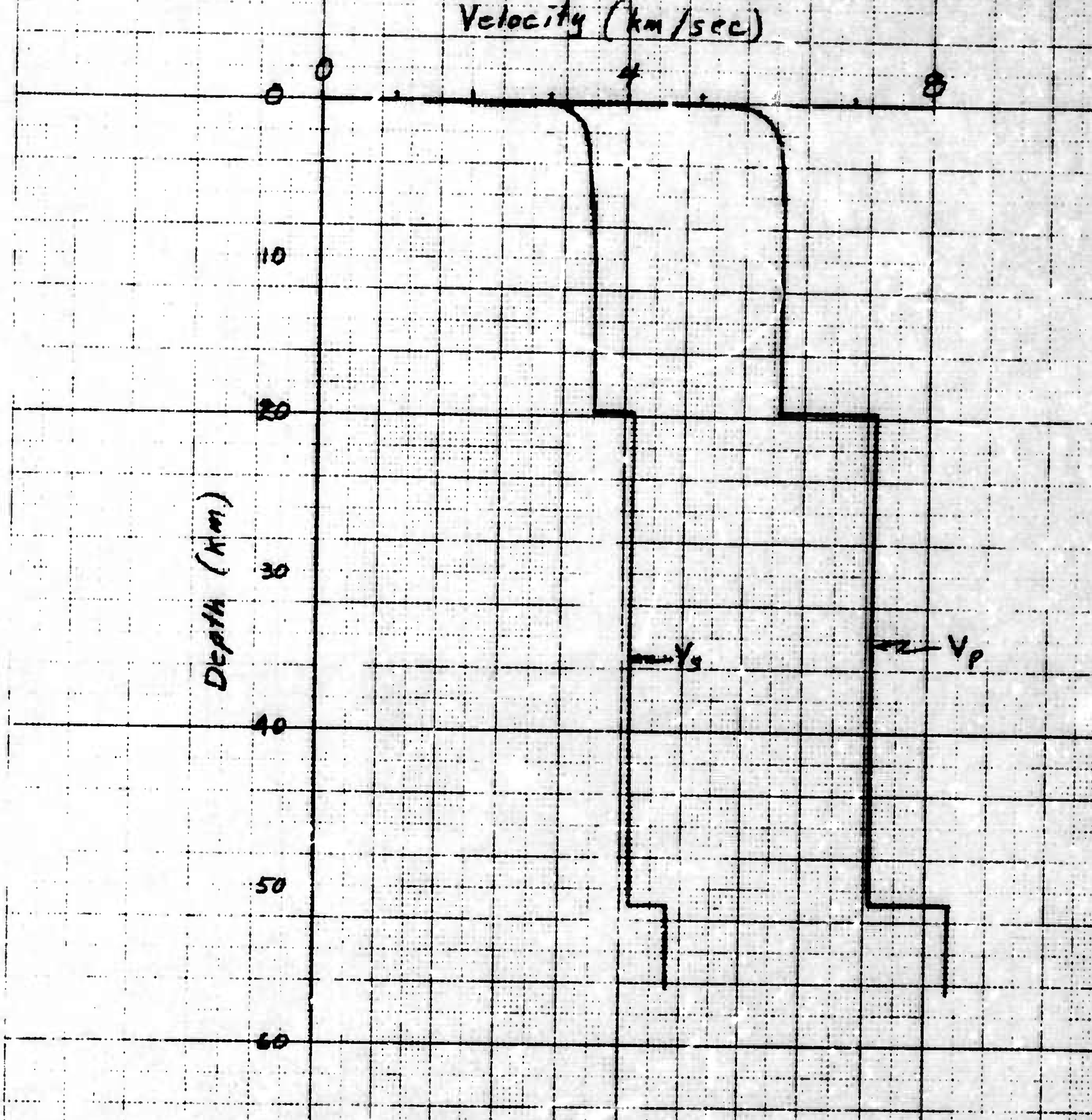

Figure 1. Seismic Velocity Models for WMSO

JEF
11 Aug 67

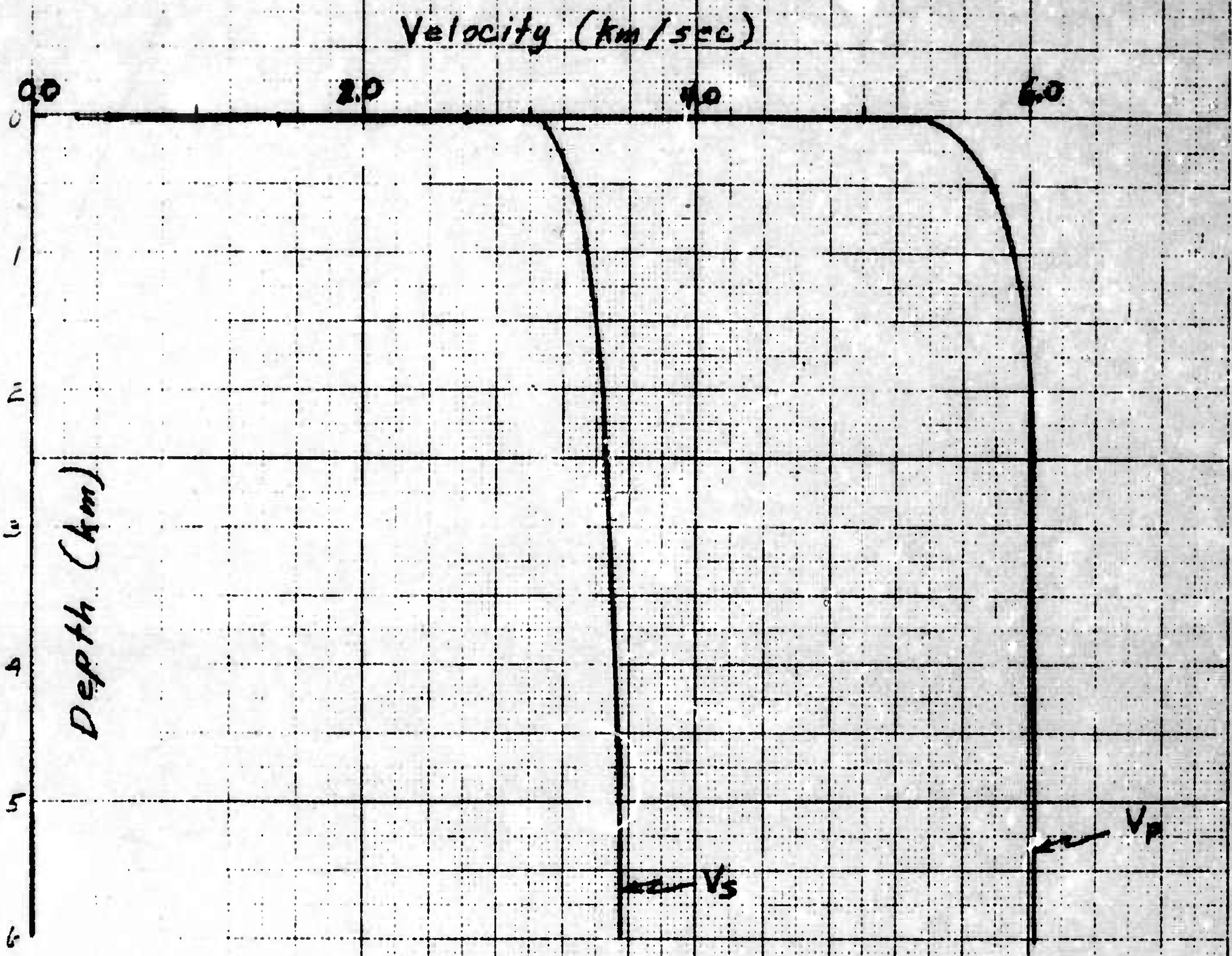

Figure 2. Seismic Velocity Models for WMSO

JEF
11 Aug 67

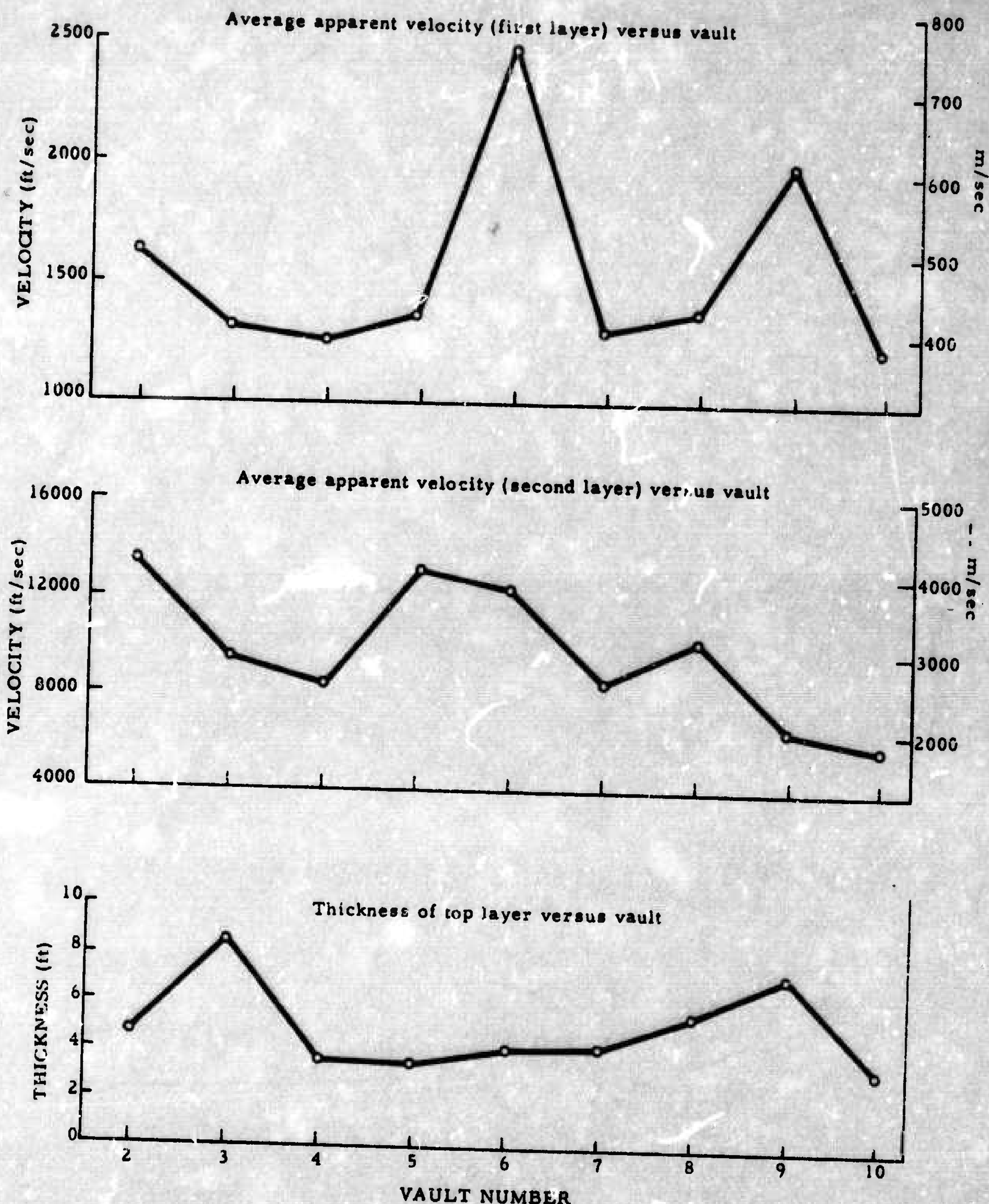

Figure 2. Velocities of the first layer, velocities of the second layer, and thickness of the first layer, near nine seismometer vaults at WMSO

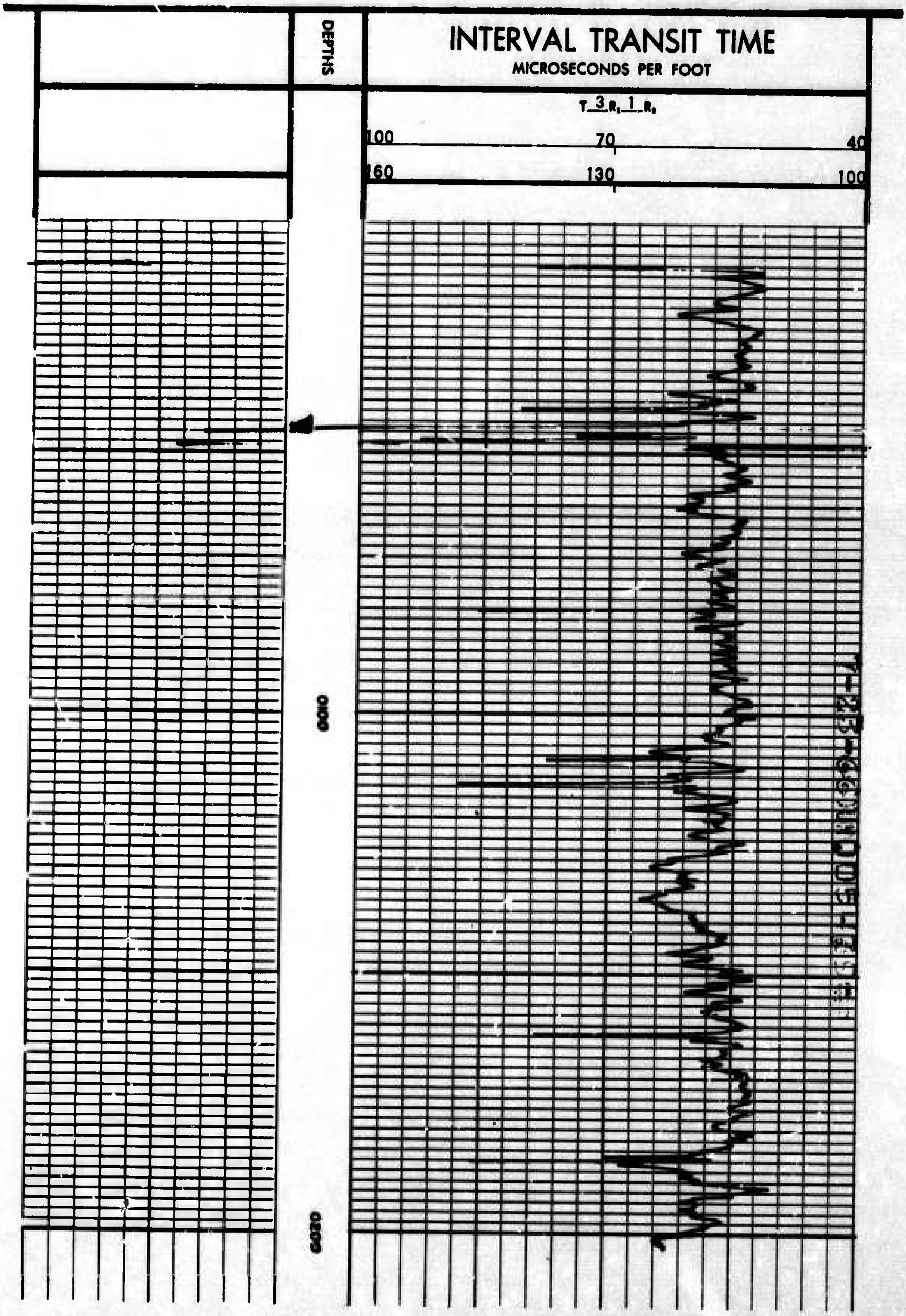
DEPTHS
INTERVAL TRANSIT TIME
MICROSECONDS PER FOOT
T 3 R1 1 R2
100
70
40
160
130
100
0100
0200
7-23-66

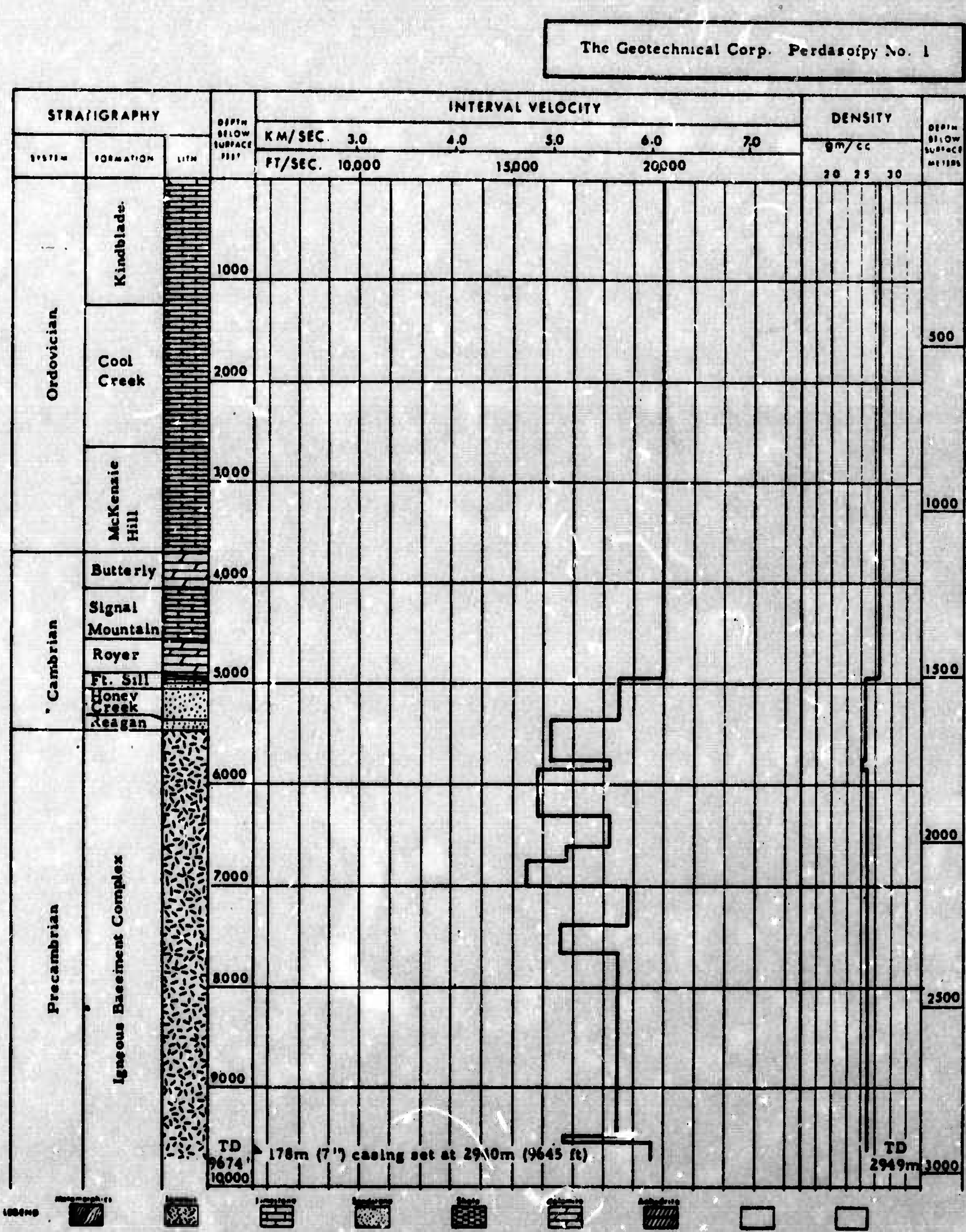

The Geotechnical Corp. Perdasofpy No. 1
STRATIGRAPHY
SYSTEM
FORMATION
LITH
DEPTH BELOW SURFACE FEET
INTERVAL VELOCITY
KM/SEC. 3.0 4.0 5.0 6.0 7.0
FT/SEC. 10,000 15,000 20,000
DENSITY
gm/cc
2.0 2.5 3.0
DEPTH BELOW SURFACE METERS
Ordovician
Kindblade
Cool Creek
McKenzie Hill
Cambrian
Butterly
Signal Mountain
Royer
Ft. Sill
Honey Creek
Reagan
Precambrian
Igneous Basement Complex
1000
2000
3000
4000
5000
6000
7000
8000
9000
10000
500
1000
1500
2000
2500
3000
TD 9674'
178m (7") casing set at 2940m (9645 ft)
TD 2949m
LEGEND

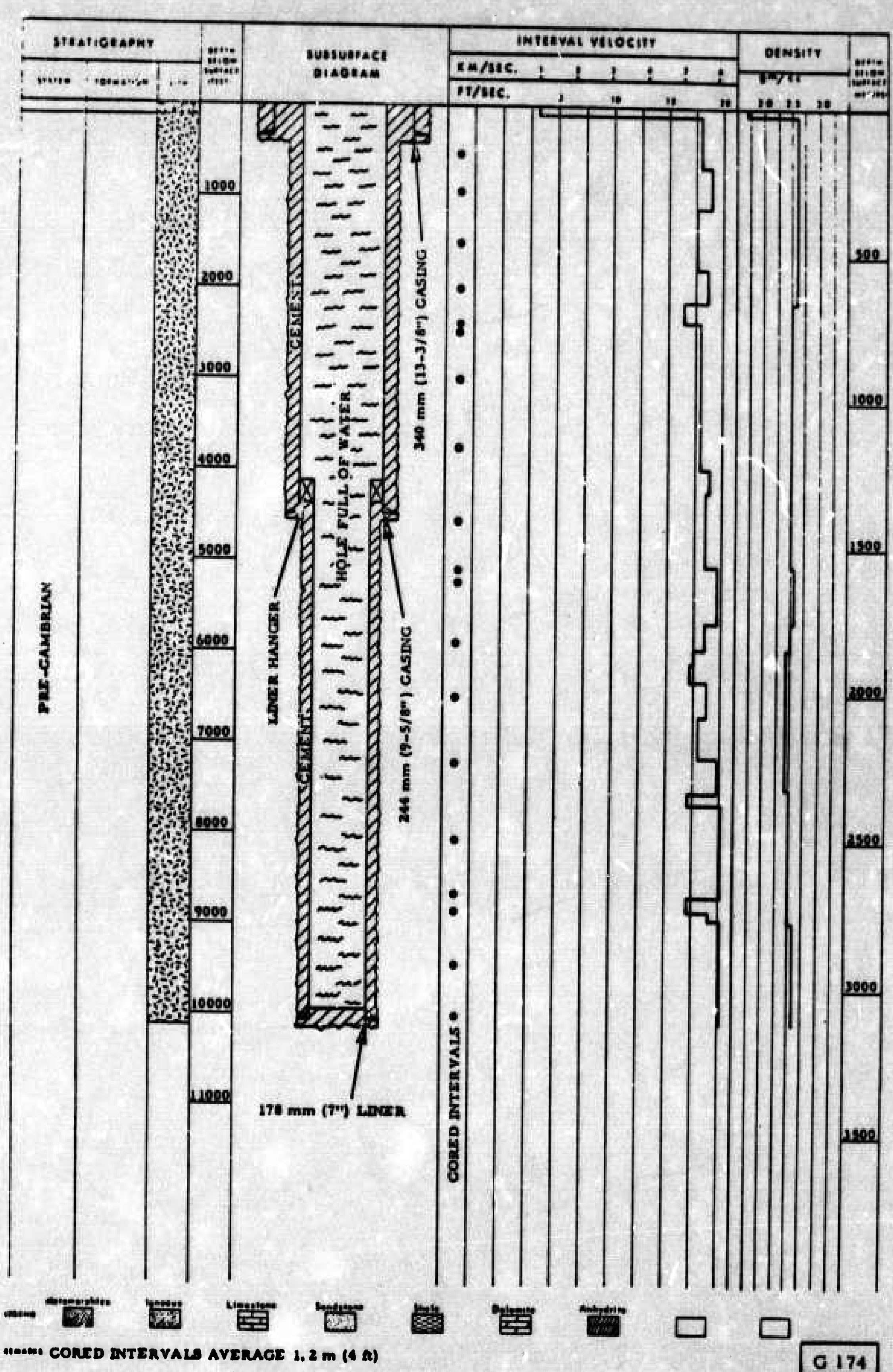

Figure 2. Subsurface diagram, cased exploratory hole "A"

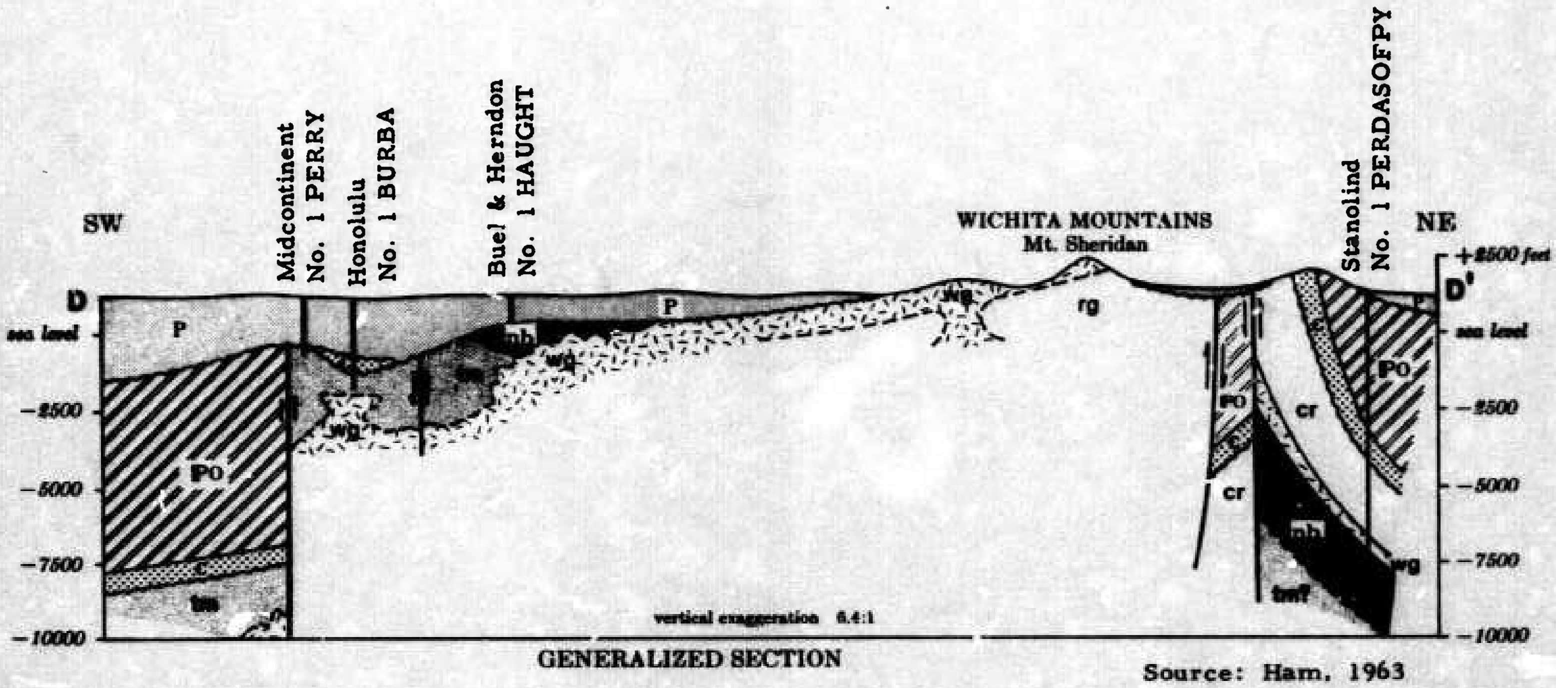

P - Permian
PO - Late Pennsylvanian and early Ordovician
c - Cambrian

cr - Carlton rhyolites
wg - Wichita granites
nb - Navajoe Mountain basalt-spilite

tm - Tillman metasediments
rg - Raggedy Mountain gabbro

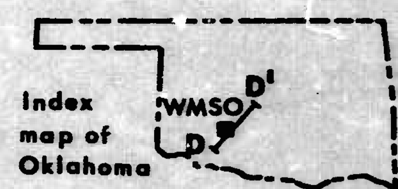

Figure 9. Cross section through Wichita Mountains showing Perdasofpy No. 1

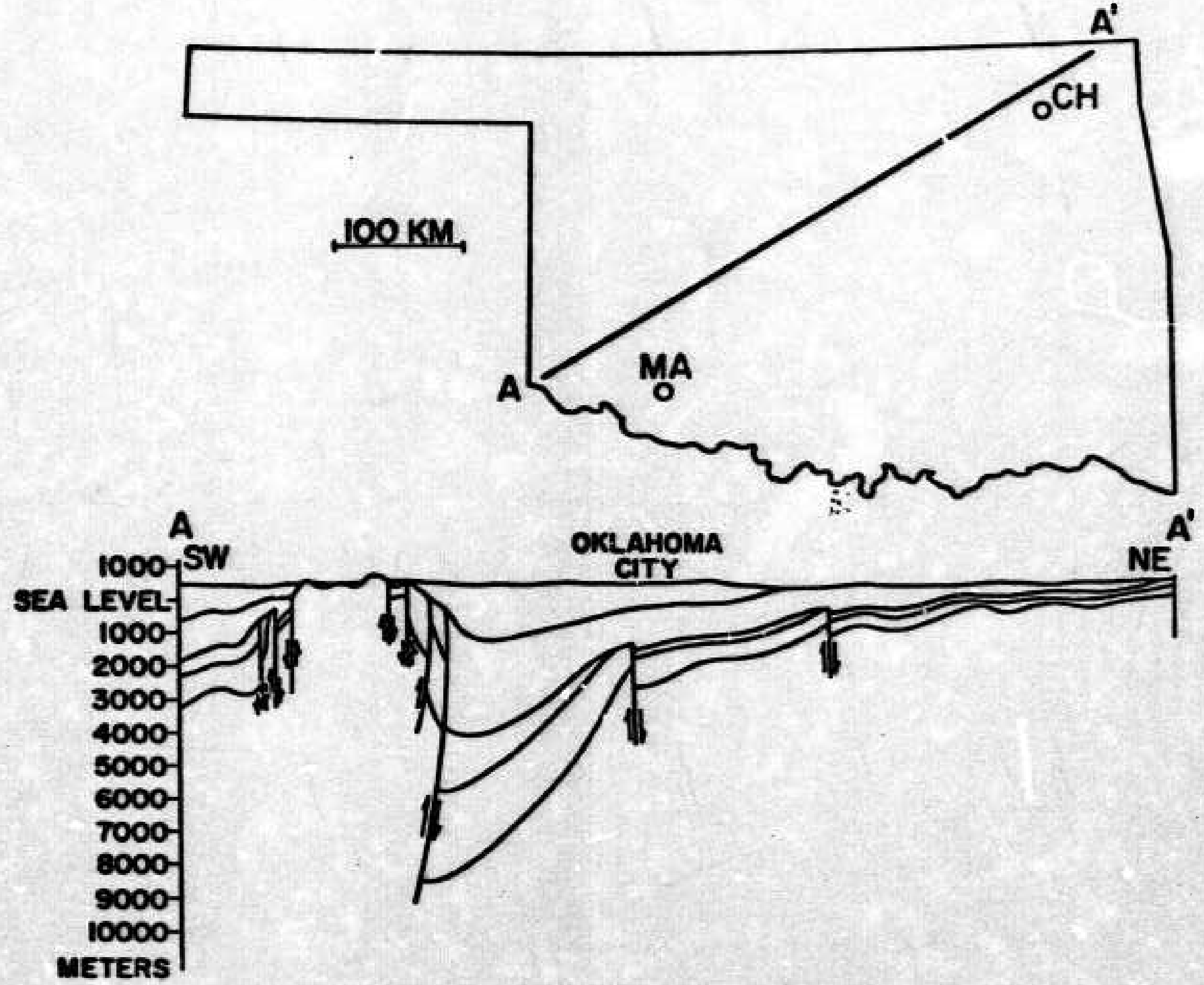

FIGURE VI. GEOLOGIC CROSS SECTION PARALLELING REFRACTION PROFILE

(Modified from Jordan, 1964)

UNCLASSIFIED

Security Classification

DOCUMENT CONTROL DATA - R & D

(Security classification of title, body of abstract and indexing annotation must be entered when the overall report is classified)

1. ORIGINATING ACTIVITY (Corporate author) Geotech A Teledyne Company 3401 Shiloh Road, Garland, Texas 75040	2a. REPORT SECURITY CLASSIFICATION UNCLASSIFIED 2b. GROUP

3. REPORT TITLE

Quarterly Report No. 9, Project VT/5081
Multicomponent Strain Seismograph

4. DESCRIPTIVE NOTES (Type of report and inclusive dates)

Quarterly Report, 1 July - 30 September 1967

5. AUTHOR(S) (First name, middle initial, last name)

Shopland, Robert C.
Kirklin, Richard H.
Sherwin, John R.
Fix, James E.

6. REPORT DATE 12 October 1967	7a. TOTAL NO. OF PAGES 75	7b. NO. OF REFS 13
8a. CONTRACT OR GRANT NO. AF 33(657)-15288 b. PROJECT NO. VELA T/5081 c. d.	9a. ORIGINATOR'S REPORT NUMBER(S) Technical Report No. 67-59 9b. OTHER REPORT NO(S) (Any other numbers that may be assigned this report)	

10. DISTRIBUTION STATEMENT

Qualified requestors may obtain copies of this report from DDC

11. SUPPLEMENTARY NOTES	12. SPONSORING MILITARY ACTIVITY HQ USAF (AFTAC/VELA Seismological Center) Washington, D.C. 20333

13. ABSTRACT

Earthquake data and phase and amplitude responses measured at both the fixed and free ends of the horizontal strain seismometer show no discrepancies that would explain the apparent loss of motion between the ends during calibration. The capability of the long-period horizontal strain and inertial seismographs to operate as a matched pair has been demonstrated. The ability of the long-period strain directional array to discriminate between surface waves arriving simultaneously from different epicenters was also successfully demonstrated. A comparison of data from vertical strain seismometers interchanged in the steel-cased and plastic-cased boreholes indicates the problem of low coherence of strain signals between the two boreholes is caused by one of the strain instruments rather than differences in the boreholes. A seismic model for Wichita Mountains Seismological Observatory (WMSO) was hypothesized for the longitudinal wave velocity and for the shear wave velocity from the surface to below the Mohorovicic discontinuity. An evaluation is given of the variable-capacitance transducer as a calibration monitor and as a transducer for recording seismic data.

DD FORM 1 NOV 65 1473

UNCLASSIFIED

Security Classification